CHEMICAL REVIEWS

MARCH 26, 2014 VOLUME 114 NUMBER 6 pubs.acs.org/CR

SINGLE MOLECULE IMAGING AND MECHANICS: SEEING AND TOUCHING MOLECULES ONE AT A TIME

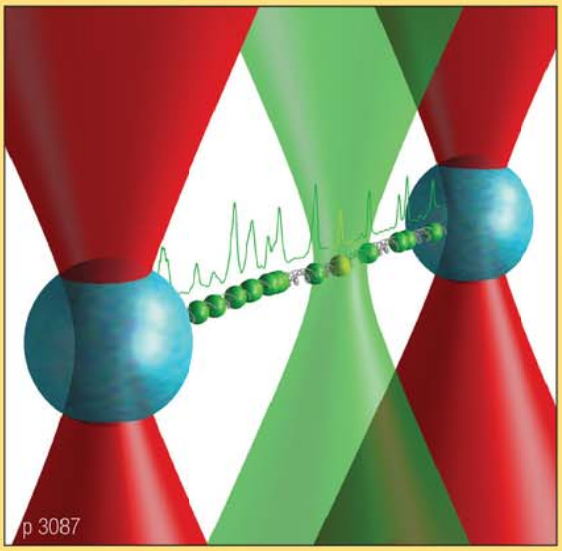

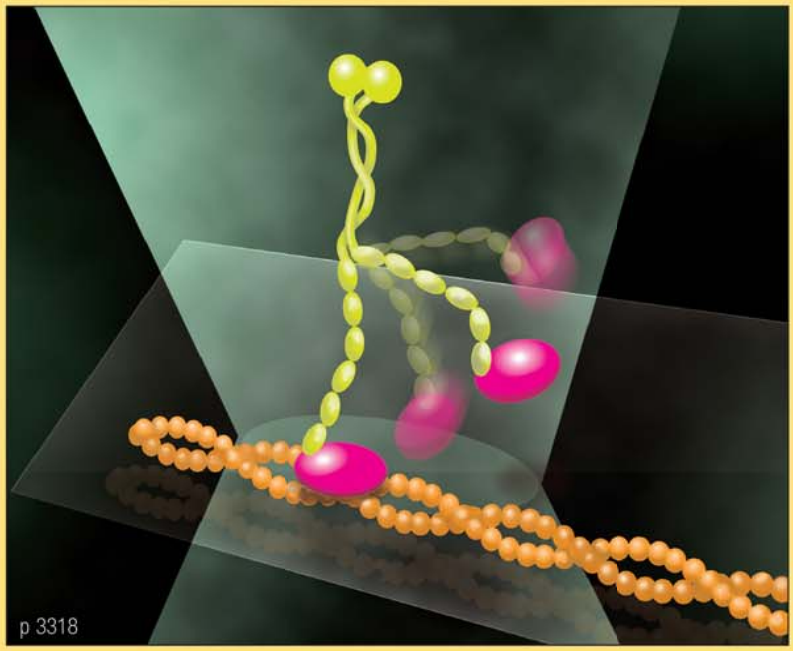

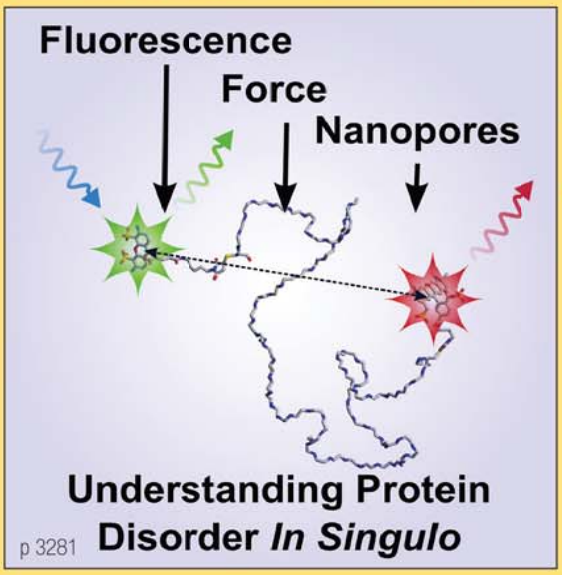

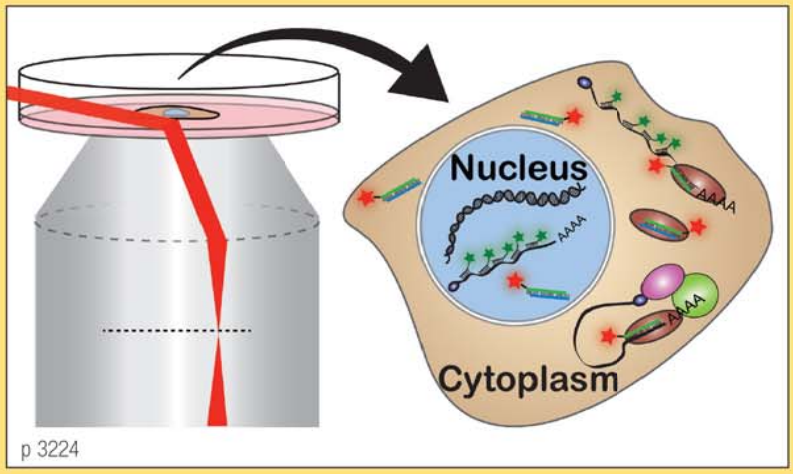

ACS Publications
MOST TRUSTED. MOST CITED. MOST READ.
www.acs.org

CHEMICAL REVIEWS

Review

pubs.acs.org/CR

Single Molecule Fluorescence Approaches Shed Light on Intracellular RNAs

Sethuramasundaram Pitchiaya,[†,‡,∥] Laurie A. Heinicke,[‡,∥] Thomas C. Custer,[§,∥] and Nils G. Walter*[,†,‡]

[†]Single Molecule Analysis in Real-Time (SMART) Center, [‡]Single Molecule Analysis Group, Department of Chemistry, and [§]Program in Chemical Biology, University of Michigan, Ann Arbor, Michigan 48109-1055, United States

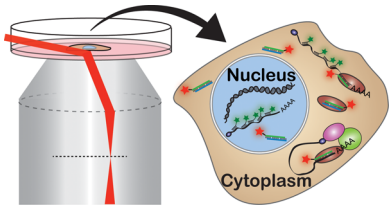

CONTENTS

1. INTRODUCTION

The eukaryotic cell is highly complex. Ever since Robert Hooke discovered "cells" in 1665 when training his comparably primitive microscope on a sliver of cork, scientists have aimed to identify and characterize all functional components of the cell. Around the turn of the millennium, the Human Genome Project laid open our entire cellular catalogue, but shockingly discovered that less than 21 000 protein-coding genes, just ∼5-times the number of a bacterium such as *Escherichia coli*, span only ∼1.2% of the over 3 billion base pairs of the human genome.[1−4] This lack of proteomic inventory initially perplexed the scientific community but then spurred debates of possible underlying RNA contributions to cellular complexity.[5,6] The Encyclopedia Of DNA Elements (ENCODE) project, an international collaborative research effort, was initiated to provide a comprehensive picture of all

Special Issue: 2014 Single Molecule Mechanisms and Imaging

Received: September 9, 2013
Published: January 8, 2014

   dx.doi.org/10.1021/cr400496q | *Chem. Rev.* 2014, 114, 3224−3265

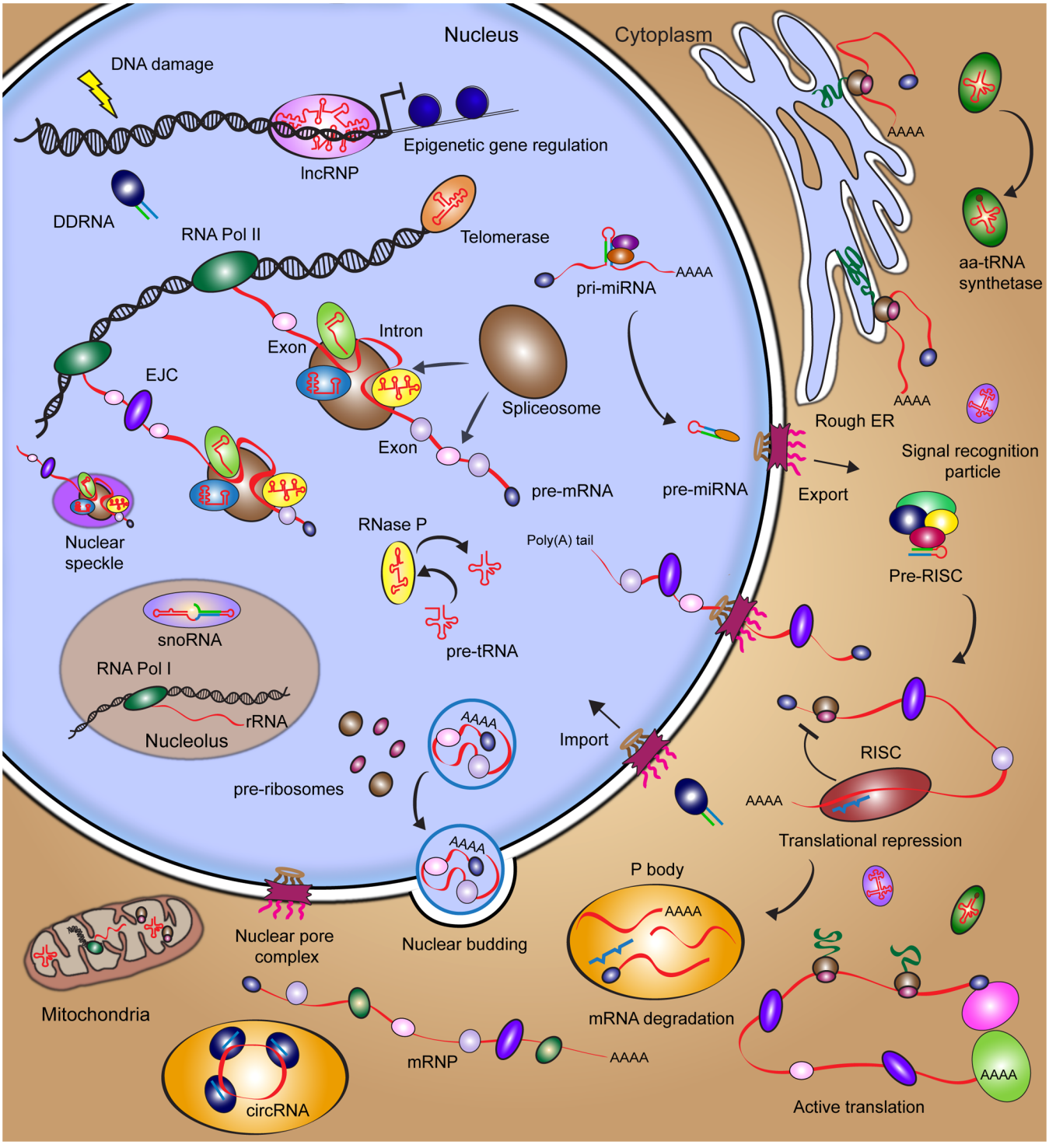

Figure 1. Survey of the RNA biology in a eukaryotic cell. Detailed descriptions of RNA and RNP complexes are provided in section 2.

functional elements within the human genome through unbiased, transcriptome-wide coverage by RNA deep-sequencing (RNA-seq).[7] Particularly striking are the discoveries that at least 75% of the genome is transcribed and that by far most of these transcripts do not code for proteins, but rather "non-coding" RNAs (ncRNAs), many of which are still uncharacterized in terms of their structure and function.[7,8] Currently, more than 80 000 distinct ncRNAs have been identified in human cells, which reveals an unexpected and exciting RNA landscape in our body (with excerpts highlighted in Figure 1).[9]

Many RNA elements have been found to originate from overlapping loci, suggesting that similar RNA sequences can be distinctly generated or processed to perform different biological functions.[10,11] In an effort to understand the complex functional networks these RNAs are involved in, systems biology approaches are beginning to be implemented. Abetting such holistic approaches are single molecule methods that promise to provide quantitative mechanistic details for individual biomolecules within living cells.

dx.doi.org/10.1021/cr400496q | Chem. Rev. 2014, 114, 3224−3265

Table 1. Representative Classes of RNAs Found in a Eukaryotic Cell

category	name	RNA length (nts)	function	refs[a]	databases	single molecule refs[a]
coding RNA	messenger RNA (mRNA)	variable	protein coding	15,41	470,471	225,233,268,270,278,292,307,315,345,400,423,430,434
	ribosomal RNA (rRNA)	~120−5,000	translation	472−474	475	
	signal recognition particle RNA	300	translation	107	476	
housekeeping noncoding RNA	transfer RNA (tRNA)	70−100	translation	100	477,478	
	small nuclear RNA (snRNA)	60−450	splicing	43		343
	small nucleolar (snoRNA)	60−300	RNA editing	92	479	
	RNase P RNA	~500	tRNA maturation	105	480	
	telomerase RNA	~400−1,300	chromosome extension	199,200	481	
	hepatitis delta virus (HDV) ribozyme	~84	unknown	69,71,482		
	hammerhead ribozyme	~100	unknown	67,68		
	microRNA (miRNA)	20−24	post-transcriptional gene silencing	139,143,148,149	483−485	135,454,455
small noncoding RNA (<200 nts)	small interfering RNA (siRNA)	20−24	post-transcriptional gene silencing	143	481,485	
	DNA-damage response RNA (DDRNA)	20−35	DNA repair	123,124,177		
	PIWI-interacting RNA (piRNA)	24−31	germline gene silencing	121,486	487	
	circular RNA (circRNA)	variable	miRNA sponge	159,160		
	primal RNA (priRNA)	22−23	heterochromatin assembly	174		
midsized ncRNA <1 kb	promoter-associated RNAs (PARs)	variable	epigenetic gene regulation	187	481	
long noncoding RNA (>200 nts)	long noncoding RNA (lncRNA)	>200	epigenetic gene regulation	179	484,488,489	188,416−418
	5′-UTR	~150	mRNA regulatory element	78	490	
cis-acting ncRNA	3′-UTR	~300	mRNA regulatory element	78,118	490	
	introns	variable (up to thousands)	mRNA regulatory element	491	492	

[a]Representative references. Please refer to the text for a comprehensive list.

dx.doi.org/10.1021/cr400496q | Chem. Rev. 2014, 114, 3224−3265

While RNA-seq has proven powerful for discovering novel cellular RNAs, the approach is limited by the ensemble averaging and loss of spatiotemporal information caused by the isolation of cellular RNA. It thus remains unclear whether, for example, functionally important ncRNAs are expressed in low quantities across all cells of a sample or selectively expressed only in a few cells, which feigns low expression by dilution within the averaged measurement. Single molecule approaches have emerged as an unparalleled means to resolve complex cellular processes that are otherwise masked by such ensemble averaging. The recent implementation of single molecule fluorescence tools to characterize mRNA expression rates and levels, mRNA and microRNA localization, and ribonucleoprotein complex (RNP) association in living cells, together with the emergence of super-resolution imaging techniques such as PALM and STORM,[12] endows single molecule techniques with the potential to broadly dissect the functions and mechanisms of ncRNAs.

In this review, we begin with an overview of the different classes of RNAs in eukaryotic cells, in terms of their biogenesis, function, and localization (Figure 1 and Table 1). Given the extraordinary amount of literature on these subjects, where appropriate we guide the reader to pertinent reviews for further detail. Next, we summarize recent technical achievements of single molecule fluorescence microscopy in visualizing RNA and RNA−protein complexes in vivo. Finally, we highlight some applications of single molecule tools over the last 15 years that investigate RNA function within cells. Throughout the text, we will promote a vision of uniquely resolving the still shrouded multitude of functional mechanisms of RNAs, especially ncRNAs, through single molecule approaches.

2. CELL BIOLOGY OF RNA

2.1. Life Cycle of mRNA

2.1.1. Transcription and Splicing of Pre-mRNA. The best-characterized RNAs of the cell are protein-coding mRNAs and the ncRNAs involved in their processing. Over the last 50 years, biochemical, structural, and biophysical studies have provided a wealth of information on mRNA biogenesis, function, and localization. It is well-known that mRNA does not function as a naked biomolecule but rather as part of larger RNP complexes.[13−15] RNA-seq technologies coupled with RNA−protein cross-linking have been successful in mapping RNA target binding sites of RNA-binding proteins on a genomic scale.[16−19] These data have revealed extensive, sometimes unexpected RNP networks within the cell that are summarized in a recent review.[20] Not surprisingly, single molecule studies have been employed most extensively to study mRNA transcriptional kinetics, expression levels, processing, and localization (see section 4), motivated by the stochasticity and cell-to-cell variability associated with such processes.[21] Here, we survey the numerous mRNA−protein (mRNP) complexes formed during biogenesis and processing of precursor-mRNAs (pre-mRNAs) into mature transcripts (Figure 1) and what role each processing event plays in the ultimate fate of an mRNA. Within this section, we also provide descriptions of the housekeeping ncRNAs that are involved in each step of mRNA maturation.

Pre-mRNAs are predominantly transcribed by RNA polymerase (Pol) II and typically contain three distinguishable elements: protein-coding exons, flanking untranslated regions (5′- and 3′-UTRs), and (long) noncoding introns.[22] By the act of splicing, introns are excised from the pre-mRNA, ultimately resulting in a processed mRNA with joined, contiguous exons.[23,24] This process is catalyzed by the spliceosome, an RNP of large size, based on certain features on the pre-mRNA splice site: usually an intronic GU 5′-end splice site, an internal A-branch site, and AG 3′-end splice site. In humans and other complex metazoans, pre-mRNA is cotranscriptionally bound by several proteins that play a role in splicing, 5′-end-capping, and 3′-end polyadenylation. Ubiquitously expressed alternative splicing factors, such as heterogeneous nuclear ribonucleoproteins (hnRNPs) and serine-arginine rich-domain containing proteins (SR proteins), function to silence or activate splicing, respectively, and impact polyadenylation and mRNA export.[25−30] Sequence-dependent binding of these proteins, as well as other tissue- and developmental-stage specific alternative splicing factors, to the pre-mRNA affects its structure and, consequently, its interactions with additional RNA-binding proteins. The ensuing sequence of hierarchical binding events ultimately determines the splicing potential of any given pre-mRNA splice site.[31,32] Another mechanism of alternative splicing involves riboswitches, RNA structural motifs embedded in intergenic regions, and 3′-UTRs that bind small metabolites, which in turn induce RNA conformational changes.[33] Unlike in bacteria, where transcription and translation are coupled and hence regulation of gene expression by ubiquitous 5′-UTR-encoded riboswitches generally involves direct transcription termination or inhibition of translation initiation,[34,35] in eukaryotes riboswitches are typically embedded next to splice sites that they obscure through formation of secondary structure. Once the riboswitch (or, more precisely, its "aptamer" motif) binds the cognate metabolite, the ensuing conformational change makes the splice site accessible, leading to changes in splicing pattern. The end result is an alternatively spliced mRNA that may, for example, contain internal stop codons that cause translation of aberrant peptides, premature translation termination, or destabilization of the transcript.[33]

While some splicing events are constitutive, high-throughput sequencing studies have revealed that nearly all multiexon gene transcripts can be alternatively spliced, thus promoting transcriptomic and proteomic diversity in eukaryotic cells.[36,37] One of the most profound examples of alternative splicing occurs in the DSCAM (down syndrome cell adhesion molecule) gene in *D. melanogaster* that codes for 38 016 protein isoforms.[38] We note that this extreme example is most likely an exception, at least in mammals, as it has recently been shown that most mammalian genes code for one dominant transcript.[39] However, given the vast number of possible exon combinations and the challenge to maintain single-nucleotide splicing accuracy to avoid loss of the codon reading frame, it is not surprising that aberrant alternative splicing can result in the malfunction of proteins and ultimately disease.[40,41] In fact, it has been suggested that 60% of all human disease causing genetic mutations act through altering the splicing code.[42]

The spliceosome itself is a dynamic macromolecular RNP machine, containing five small nuclear RNAs (snRNAs) termed U1, U2, U4, U5, and U6 that function in concert with cognate proteins to form snRNPs.[43] The snRNAs function as structural scaffolds and mediators of splice site selection.[44] Most snRNAs are transcribed by RNA Pol II, with the exception of U6, which is transcribed by RNA Pol III.[45] In total, over 200 individual RNA and protein components are assembled and disassembled during spliceosomal mediated excision of an intron, ultimately linking together two exons via two transesterification

dx.doi.org/10.1021/cr400496q | *Chem. Rev.* 2014, 114, 3224−3265

reactions.[23] In human cell lines, approximately 80% of splicing occurs cotranscriptionally, while it has been proposed that post-transcriptional splicing occurs within interchromatin foci termed nuclear speckles.[46] Nuclear speckles consist of active, highly dynamic spliceosomal protein components, yet their direct role in post-transcriptional splicing remains debated.[47] Once an intron is excised from the pre-mRNA, a multiprotein exon-junction complex (EJC) is deposited ~20 nucleotides (nt) upstream of the adjoined exon−exon boundary, and in turn affects mRNA transport, translation and stability.[48,49]

In contrast to RNP-mediated splicing, self-catalyzed RNA splicing occurs in group I and group II introns, largely based on structural rearrangements of the RNA.[50−52] In most cases, it has been shown that high salt (and Mg^{2+} in particular) promotes RNA catalysis of these introns in vitro, proving that they are RNA-based enzymes or "ribozymes", yet some proteins are necessary in vivo. In addition to self-splicing introns, numerous other naturally occurring ribozymes have been characterized, including the hairpin, hammerhead, hepatitis delta virus (HDV), Varkud satellite (VS), and *glmS* ribozymes, in some cases using single molecule fluorescence tools in vitro.[53−66] Interestingly, structural motif searches, in vitro selections, and biochemical validations of ribozyme catalytic activity have led to the discovery that the hammerhead and HDV ribozymes in particular exist as ncRNA elements within the genomes of diverse organisms, including humans.[67−71] The finding that RNA can catalyze enzymatic reactions supported the RNA World hypothesis, wherein RNA spawned life as we know it by both self-replicating and catalyzing the metabolic reactions necessary to sustain life independent of proteins.[72−75]

2.1.2. Capping and Polyadenylation of Pre-mRNA. In addition to intron removal, pre-mRNA is modified within the nucleus with a 5′-end 7-methylguanosine cap (5′-cap) and a 3′-end poly(A) tail. The 5′-cap protects the mRNA from nucleolytic cleavage, serves as signal for the ribosome to start translation, and has been shown to have roles in mRNA splicing, nuclear export and stability.[76] A 3′-end canonical hexanucleotide polyadenylation signal, AAUAAA, is found 10−30 bases upstream of the polyadenylation site. The length and location of poly(A) tails can vary, both of which can affect mRNA stability, translational efficiency and transport from the nucleus to the cytoplasm.[77] The resulting mature mRNA typically contains a 5′-cap, a 5′-UTR, protein coding exons, a 3′-UTR, and a poly(A) tail. UTRs, just like introns, are cis-acting regulatory ncRNA elements, whose primary sequence and secondary structure directly affect protein and RNA binding and ultimately play critical roles in the regulation of gene expression.[22,78] Interestingly, the length of UTRs and the fraction of alternatively spliced genes scale with the developmental complexity in animals, indicative of the greater sophistication of mRNA regulation in higher organisms.[22]

2.1.3. Nuclear Export of mRNA. Processed, mature mRNAs remain coated with RNA-binding proteins, including the EJC, TREX complex, Aly, Nxfl, and SR proteins, that serve to package and compact the mRNA during transport across the nuclear envelope (from the nucleus into the cytoplasm) through the nuclear pore complex (NPC)[79−83] or through the recently discovered nuclear envelope budding.[48] Such transport processes, especially via the nuclear pore, have been extensively investigated using microscopy techniques, to unravel structural and mechanistic details.[48,81,84−88] Classically, the NPC is considered the prevalent mode of RNP shuttling between the nucleus and cytoplasm. The nuclear pore is an almost cylindrical macromolecular complex comprised of nucleoporin protein building blocks.[82] Recently, it was found that RNPs can also be transported from the nucleus into the cytoplasm by nuclear envelope budding using a mechanism similar to the release of herpes virus capsids.[87] Single molecule microscopy presents an exciting avenue to study these yet-to-be characterized RNP transport processes.

2.1.4. Translation of mRNA. Once in the cytoplasm, mRNAs contain numerous signals that are recognized by the cytoplasmic processing machinery that ultimately determines the individual fate of each mRNA. Some mRNAs will be destined to be translated by the ribosome, while others will be targeted for translational repression and decay by miRNAs or siRNAs (see section 2.2). As transcription and mRNA maturation are not fully accurate, some transcripts will contain premature stop codons and are destroyed by the cell via nonsense-mediated mRNA decay (NMD). Each of these processes occurs in subcompartments of the cytoplasm and has been the focus of numerous studies that are nicely summarized by, for example, Martin and Ephrussi.[89]

To be efficiently translated, mRNAs must contain a 5′-cap, appropriately positioned EJC, and a poly(A) tail greater than 50 nt with a poly(A) binding protein (PABP)[90,91] bound. The translating ribosome in eukaryotes is comprised of a small (40S) and a large (60S) subunit, together referred to as the 80S ribosome. The 40S subunit is comprised of one ribosomal RNA (18S rRNA) and 33 proteins, while the 60S subunit is comprised of three RNAs (5S rRNA, 5.8S rRNA and 28S rRNA) and 46 proteins. Most rRNAs are transcribed in the nucleolus by RNA Pol I, with the exception of 5S RNA, which is transcribed by RNA Pol III. rRNAs are chemically modified by small nucleolar RNA(snoRNA)-directed methylation and pseudouridylation.[92] The individual rRNA and ribosomal protein components assemble in a hierarchical manner and form preribosomal components in the nucleus that are exported into the cytoplasm where assembly is completed.[93]

snoRNAs represent one of the best characterized classes of ncRNAs.[94−96] Localized to the nucleolus, snoRNAs are often transcribed from intronic regions of the genes they modify. The two major classes of snoRNAs are distinguished by the type of modification they mediate on rRNAs, snRNAs, and tRNAs: C/D box snoRNAs define the target sites for 2′-*O*-ribose methylation, whereas H/ACA box snoRNAs define the target sites for pseudouridylation. The RNA structure varies between these classes and likely mediates the binding between a snoRNA and its cognate modifying protein to produce a mature snoRNP.[97] Recent data have linked snoRNAs to cancer and as precursors to miRNAs, suggesting that these RNAs will need to be examined in new contexts.[98,99]

Once eukaryotic initiation factors (eIFs) bind distinct segments of the 5′UTR, such as eIF4E the mRNA cap, translation is primed. The full 80S ribosome is then assembled and the ribosome begins to translocate along the mRNA to synthesize proteins via the sequence specific recognition of three nucleotide codons by aminoacyl-tRNAs. tRNAs are transcribed by RNA Pol III (similar to 5S rRNA) and are heavily site-specifically modified by snoRNAs.[100] tRNAs are evolutionarily ancient and characterized by a compact L-shaped tertiary structure, in aggregate carrying over 100 types of modifications, discovered by the first ever RNA crystallization experiment.[101] In many organisms, multiple copies of tRNA genes give rise to distinct levels of any given tRNA species, which may affect translation rates.[102−104] Maturing tRNAs are

dx.doi.org/10.1021/cr400496q | *Chem. Rev.* 2014, 114, 3224−3265

processed by endonucleolytic 5′-end cleavage by RNase P, an evolutionarily conserved RNP found in all three kingdoms of life and one of the first catalytic RNAs to be discovered.[105,106]

Nascent polypeptides sequester another RNP highly conserved in all three kingdoms of life, termed signal recognition particle (SRP), which in eukaryotes contains one conserved RNA and at least six proteins, that direct the nascent peptide to the endoplasmic reticulum (ER) or plasma membrane.[104,107,108] The RNA component serves both as a scaffold and mediates global rearrangements of the SRP in response to binding its polypeptide cargo. The SRP directs the translocation of the growing polypeptide into the lumen of the ER, where the protein is then folded into its native form.[109]

2.1.5. Nonsense-Mediated Decay and mRNA Turnover. Nonsense-mediated decay (NMD) is a mechanism by which the cell eliminates mRNAs that contain premature stop codons, many of which result from alternative or aberrant splicing. Numerous RNA-binding proteins, including UPF1, UPF2, and UPF3 (the latter two are components of the EJC), mediate NMD and are associated with the mRNA, at least transiently, within cytoplasmic processing bodies (P-bodies),[110] cellular foci that are enriched in RNA processing and degrading enzymes.[111] One proofreading round of translation is sufficient to target the mRNA for NMD. We direct the reader to some reviews for further mechanistic details of NMD.[112−114]

Protein expression is highly correlated with the amount of its mRNA available. To be able to modulate the expression pattern of a cell over time, it is advantageous for aging mRNAs to be degraded.[115] Degradation occurs via two pathways, the first involving shortening of the poly(A) tail by a deadenylase followed by decapping of the 5′-cap by Dcp1p and Dcp2p, which exposes the RNA to digestion by 5′-to-3′-exonucleases. The second mechanism requires mRNA deadenylation, followed by digestion by the cytoplasmic exosome.

Certain disease-related proteins have been shown to affect mRNA localization and gene expression. For example, fragile X syndrome-associated fragile X mental retardation protein (FMRP) has been shown to bind mRNAs to direct their localization within the cell and ultimately affect protein expression of target mRNAs.[116,117] In addition, it was shown that fragile-X-mental-retardation-related protein 1 (FXR1) and Argonaute 2 (AGO2) bind AU-rich elements (AREs) in a microRNA dependent manner within the 3′-UTR of mRNAs to activate translation during cellular quiescence, thereby providing mechanistic evidence of the importance of cis-activating regulatory elements in 3′-UTRs.[118] In addition to FMRP, several other RNA binding proteins (RBPs), such as Staufen and zip-code binding proteins (ZBP), bind specific sequences within UTRs to localize a large fraction of transcripts to distinct subcellular domains.[89] In the following sections, we will discuss more broadly the mechanisms by which small and long ncRNAs control gene regulation.

2.2. Small Noncoding RNA

2.2.1. Types and Functions of Small ncRNAs. RNA silencing is an evolutionarily conserved mechanism of gene silencing involving three main classes of small ncRNAs, including microRNAs (miRNAs), small interfering RNAs (siRNAs) and PIWI-interacting RNAs (piRNAs).[119] The classical biogenesis and cytoplasmic mechanisms of miRNA- and siRNA-mediated gene silencing are similar, as both types of ncRNAs are processed from a relatively longer RNA duplex into an ∼22 nt single strand that engages an Argonaute-containing protein complex to bind and silence target mRNAs. However, miRNAs, siRNAs, and piRNAs differ in origin, structure, and their detailed mechanism of silencing. miRNAs are endogenously expressed (genome-encoded), highly sequence-conserved, ncRNAs that display imperfect complementarity to mRNA targets (typically the 3′-UTR) and mediate translational repression and mRNA decay. In contrast, siRNAs are found either endogenously or administered exogenously and bind to mRNAs by perfect sequence complementarity to mediate site-specific mRNA cleavage.[120] Since target destruction is more immediate and absolute, siRNA mediated repression tends to be stronger than that achieved by miRNAs. Finally, piRNAs are ∼26−30 nt in length, engage PIWI proteins, and function to silence transposons in the animal germline.[121] In addition to their canonical functions, the last several years have revealed important roles of these and similar small ncRNAs in epigenetic gene regulation[122] and the DNA damage response.[123,124]

In 1993, Victor Ambros and colleagues described the first miRNA, lin-4, as a protein expression regulator during normal larval development of the nematode worm *Caenorhabditis elegans*, although the mechanism remained somewhat elusive.[125] In 1998, Andrew Fire and Craig Mello laid the foundation for RNA interference (RNAi), a tool that exploits the introduction of exogenous siRNAs into the cellular RNA silencing pathway to mediate mRNA cleavage, for which they shared the 2006 Nobel Prize in Physiology or Medicine.[126] Since these initial reports, small ncRNAs have been identified in plants, animals, and even bacteria (although these sRNAs are often processed from protein-coding transcripts)[127] and have been found to be a predominant mechanism for regulating gene expression in eukaryotes.[128,129] On the one hand, it is now estimated that at least 60% of protein coding genes are regulated by at least one miRNA.[130] On the other hand, siRNAs are routinely exploited in functional genomics, and their therapeutic implications are slowly being realized, although off-target effects and cell-specific delivery remain challenging.[131] There are also numerous emerging classes of small and midsized ncRNAs that will not be discussed here for brevity but are summarized in a recent review.[132] Given the relatively recent discovery of small ncRNAs and their expanding repertoire of types and functions, we will discuss, where appropriate, outstanding questions and the potential of single molecule microscopy to address them. We will specifically focus on the biogenesis, localization and function of siRNA and miRNAs because of their pervasive functions and the emergence of reports that use single molecule microscopy for functional and mechanistic probing.[133−136]

2.2.2. Biogenesis of Small ncRNAs. miRNAs are the most ubiquitous small ncRNA in humans, with over 1500 different mammalian miRNA sequences discovered to date that represent more than 1% of the entire genome and thus the largest gene family.[137−139] These RNAs are usually transcribed by RNA Pol II as long primary miRNA (pri-miRNA) transcripts.[140,141] pri-miRNAs adopt hairpin structures with numerous bulges that are recognized and cleaved by the nuclear endonucleolytic microprocessor complex, mainly comprised of the RNase III enzyme Drosha and its cofactor DGCR8 (Pasha in invertebrates).[142] The resulting pre-miRNA hairpin, ∼65 to 70 nts in length and containing a 2-nt 3′-overhang, is then bound by Exporin-5 and RanGTP for export from the nucleus to the cytoplasm through the NPC.

Once in the cytoplasm, pre-miRNAs as well as long double-stranded RNAs are recognized and cleaved by the RNase III

dx.doi.org/10.1021/cr400496q | Chem. Rev. 2014, 114, 3224−3265

enzyme Dicer and its cofactor TRBP into short, 20−24 nt duplexes, with characteristic 2 nt 3′-overhangs bearing 3′-OH groups and 5′-phosphates.[139] The mature miRNA duplex is loaded into the multiprotein RNA-induced silencing complex (RISC) loading complex (RLC) that includes an Argonaute (AGO) protein.[143] Strand selection, thought to be dependent on the thermodynamic stability of the duplex and/or presence of RISC-associated protein components,[144] occurs within the RLC, wherein one strand of the duplex (the passenger strand) is cleaved and/or dissociates from the complex. The mature RISC complex contains the miRNA guide strand bound by Argonaute and can now seek out its complementary RNA sequence. Of note, the cytoplasmic portion of the siRNA biogenesis pathway in mammals is very similar.[119]

In addition to this canonical miRNA biogenesis pathway, whose multistep nature allows for tight regulation,[145] miRNAs are also generated using the mirtron pathway[146,147] wherein short hairpins derived from excised introns serve as Dicer substrates to generate miRNAs. Since mirtons are initially processed by the spliceosome, they bypass regulation of the nuclear Drosha processing step and merge with the canonical cytoplasmic miRNA biogenesis pathway only upon nuclear export.

2.2.3. Spatial and Functional Requirements of Small ncRNAs in the Cytoplasm. In the cytoplasm, miRNA-loaded RISC (miRISC) binds mRNA targets to repress translation and then promote mRNA decay, possibly within P-bodies,[135,148−150] through specific sequence requirements. Nucleotides 2−7 located on the 5′-end of the miRNA guide strand comprise the seed sequence that is the primary determinant for stable binding to the 3′-UTR of miRNA targets.[130] Additional structural elements in the 5′-UTR of targeted mRNAs have been recently shown to elicit synergistic effects with miRNA binding sites in the 3′-UTR to enhance RNA silencing.[151] Although several bioinformatic portals are available to predict putative miRNA targets (TargetScan, PicTar, and miRanda, to name a few), few have been experimentally validated and their accuracy is still poor, largely owing to their reliance on relatively short seed sequences whose frequency of occurrence is high despite a requirement for phylogenic conservation.[152,153] In light of recent reports that have underscored the importance of target site accessibility[154] and seed-independent miRNA binding,[155] these target prediction algorithms warrant an overhaul. Furthermore, apart from specific seed matches miRNA-mediated decay requires the recruitment of additional protein components, in particular the Argonaute-associated proteins GW182, CCR4-NOT and RNA helicase eIF4A2.[151,156] One such protein is also thought to be responsible for the spatial organization of RISC assembly and miRNA mediated target repression. Li et al. described the altered meristem program1 (AMP1) protein dependent localization of miRNA-loaded AGO1 to the ER, proposing the ER as the main subcellular site of repression in *Arabidopsis*.[157] Stalder et al. further reported evidence that the rough ER is the nucleation site for RNA silencing, where both miRISC assembly and target repression occur,[158] and hypothesized that ER localization is mediated by TRBP and PACT. Regardless of spatial and sequence constraints, it is still unclear whether reduced protein output is achieved by a miRNA efficiently repressing only a subset of molecules of a given type of mRNA or less efficiently repressing a large number of the same mRNA molecules. Moreover, the binding stoichiometries of miRNAs to mRNAs are yet to be fully determined. Such questions are only accessible via single molecule microscopy.

A novel class of noncoding circular RNAs (circRNAs) was recently identified and characterized in mammals.[159,160] These RNAs are processed by the spliceosome in an unusual head-to-tail fashion, resulting in circular transcripts that contain multiple miRNA binding sites and act as miRNA sponges or decoys to deplete the cell of specific miRNAs, essentially alleviating repression of the mRNAs they target.[161] Single molecule fluorescence in situ hybridization (FISH) studies have shown that circRNA−miRNA complexes localize to P-bodies,[160] although the reasons are unknown. Further functional characterizations of this abundant class of ncRNAs will be necessary to determine how universal this mechanism is for sequestering miRNAs inside cells.

2.2.4. Nuclear Localization and Function of Small ncRNAs. Recent reports, summarized here, have provided support for novel roles of miRNAs and siRNAs within the nucleus,[128] including their canonical function of post-transcriptional gene regulation. How do ncRNAs that are processed and function in the cytoplasm localize to the nucleus? In human cancer cell lines, a 3′-end hexanucleotide nuclear localization signal, AGUGUU, has been shown to regulate the import of miR-29b from the cytoplasm into the nucleus where it may function to bind a unique set of targets.[162] However, it has also been shown that miRNAs that lack such canonical import sequences are also imported into the nucleus, but indirectly.[163,164] Nucleocytoplasmic shuttling proteins like Importin8 or TNRC6A (a GW182 isoform) associate with miRISC for transport into the nucleus, possibly triggered by specific cellular cues.[165]

Numerous research groups, working predominantly with *C. elegans*, have shown that small ncRNAs and the RNAi machinery have critical roles in epigenetic DNA modification and heterochromatin formation.[166,167] For example, exposing the nematode worm to double-stranded RNA results in heritable expression of siRNAs and the heritable epigenetic modification of DNA in the form of histone 3 lysine 9 methylation (H3K9).[122,168] Certain miRNAs also influence DNA methylation and histone modification of protein-coding and ncRNA genes, thereby affecting gene expression.[169] In another report, it was shown that Argonaute CSR-1 associates with small RNAs (termed 22G-RNAs) and other cofactors to target and efficiently segregate chromosomes during cell division.[170] Many 22G-RNAs are antisense to germline-specific protein coding genes, suggesting this mechanism as a potentially common mode of regulation. Another abundant small RNA in *C. elegans* is 21U-RNA,[171] which was found to associate with PIWI-like proteins, and thus to have germline-related functions.[172,173] In fission yeast, small RNAs termed pri-RNAs were shown to be Dicer-independent mediators of RNAi involved in heterochromatin formation.[174]

Small ncRNAs have also been found to associate with pre-mRNAs in the nucleus. For example, it was shown in *C. elegans* that Argonaute-associated siRNAs are able to inhibit RNA polymerase II and silence pre-mRNAs cotranscriptionally in a process termed RNA induced transcriptional silencing (RITS).[175] Another report suggested that human AGO1 and AGO2, which are generally associated with their RNAi functions, can also be involved in alternative splicing of pre-mRNA, a process that is possibly mediated by a small ncRNA component.[176] Small ncRNAs have also been shown to autoregulate their own biogenesis, as shown with Argonaute-

dx.doi.org/10.1021/cr400496q | *Chem. Rev.* 2014, 114, 3224−3265

associated mature let-7 miRNA binding and cleaving the 3′-end of let-7 pri-miRNAs to promote let-7 maturation.[129]

Finally, a novel class of DNA damage response associated RNAs (DDRNAs) has recently been identified and characterized in mammals, zebrafish and plants.[123,124,177] Similar to miRNAs, these RNAs are processed by Dicer and Drosha to generate short, 20−35 nt products. Yet, unlike miRNAs, DDRNAs are not further processed and instead localize to specific DNA damage sites in the nucleus where they may function to recruit proteins involved in DNA damage repair. With the sophisticated high-throughput sequencing and screening tools available today, we will likely discover many more yet unknown small ncRNA-mediated pathways, all of which can in principle be probed by the single molecule techniques highlighted here.

2.3. Long Noncoding RNA

2.3.1. Discovery of Long ncRNAs. Long noncoding RNAs (lncRNAs) or long intergenic noncoding RNAs (lincRNAs) are an abundant class of ncRNAs that have recently emerged from deep-sequencing data as ubiquitous cellular transcripts of high structural and functional diversity.[178−180] Unlike the "housekeeping" small ncRNAs that display clear evolutionary conservation in terms of sequence and structure, lncRNAs are more difficult to classify due to a lack of evolutionary conservation based on primary sequence and thus they have remained somewhat of an enigma, despite often exhibiting functional conservation.[32]

lncRNAs are greater than 200 nt in length with little or no protein-coding capacity. This diverse group of RNAs is expressed tissue-specifically and is classically defined by their function in epigenetics to condense chromatin and regulate DNA methylation and histone modifications, thereby positively or negatively affecting the expression of nearby genes.[181] Genetic studies from the early 1990s revealed the first lncRNA, *Xist*, as an ∼17 000 nt long RNA that coats and inactivates one X chromosome during dosage compensation in sex determination of mammals. Other lncRNAs, such as *H19* and *Air*, are also involved in genetic imprinting by silencing adjacent alleles through DNA methylation and histone modifications.[182−184] Many novel lncRNAs have been identified by high-throughput sequencing of cell type-specific transcriptomes, and subsequent characterization has only begun to illuminate the functional nuclear and cytoplasmic niches of lncRNAs. The biogenesis, cognate protein partners, and functions of lncRNAs remain the most elusive of all ncRNAs so that we discuss only a subset of the best characterized lncRNAs. For further detail, we refer the reader to several recent reviews on specific lncRNAs, including promoter-associated RNAs (PARs).[179,185−187]

2.3.2. Biogenesis of Long ncRNAs. lncRNAs are found throughout the genome, including intergenic regions (lincRNAs), in antisense, overlapping, intronic, and bidirectional regions relative to protein-coding genes, as well as in UTRs, promoters and enhancers.[8,188,189] The biogenesis of lncRNAs is quite similar to that of mRNAs, in that they are typically transcribed by RNA Pol II, spliced and further processed to contain a 5′-cap and polyA tail. In fact, some mRNAs have been shown to function as lncRNAs.[190] In addition, recent studies suggest that lncRNAs can be chemically modified, a feature classically associated with rRNAs and tRNAs.[179] It is possible that chemical modifications are present to stabilize lncRNA secondary and tertiary structures, or that they have evolved to preclude activation of the innate immune response. For example, it was recently shown that modified, but not unmodified, tRNAs avert activation of the innate immune response protein dsRNA-activated protein kinase R (PKR).[191] Yet another layer of lncRNA complexity pertains to the presence of adjacent snoRNAs (sno-lncRNAs) loci.[192] Thus, this novel class of ncRNAs harbors many surprises, leading to many functionally interesting questions that can be addressed using single molecule approaches.

2.3.3. Epigenetic Gene Regulation and Other Functions of Long ncRNAs. lncRNAs were first characterized for their nuclear functions related to epigenetic gene regulation by DNA methylation and chromatin remodeling. These functions require lncRNAs to associate with proteins such as polycomb complexes or histone modifying proteins.[188,193,194] The lncRNAs guide modifying proteins to specific DNA sites to repress gene expression though histone methylation of H3K9 and trimethylation of H3K27. Within the last five to ten years, however, numerous reports have expanded the functional roles of lncRNAs to the cytoplasm where they have been shown to associate with importin-β proteins to prevent nuclear import of a transcription factor (i.e., *NRON* lncRNA), bind an antisense mRNA to increase protein synthesis in response to stress (i.e., *UCHL2* lncRNA), and bind the 3′UTRs of mRNAs to induce decay by dsRNA-recognition protein Staufen1.[195−197] Recent studies have also revealed that pseudogenes can act as ncRNAs to regulate gene expression of their protein-coding counterparts.[198] Further characterization of the elusive class of lncRNAs will be necessary to determine the full extent of their cellular functions.

2.4. Telomerase RNA

Telomerase RNA is a specialized type of lncRNA that, similar to other lncRNAs, acts on DNA in the nucleus. DNA telomere sequences are located at the ends of chromosomes and function to delay cellular senescence.[199,200] These sequences are maintained by telomerase, a large ∼1000 kDa (in vertebrates) RNP, whose function was discovered by Blackburn, Greider, and Szostak, for which they received the Nobel Prize in Physiology or Medicine in 2009. Telomerase is comprised of an RNA component containing a template sequence, a reverse transcriptase protein component that extends the telomere as guided by the template, and numerous accessory proteins. Aberrant telomerase activity has profound cellular consequences, where telomerase up-regulation in most immortalized cancer cell lines is thought to prevent cellular senescence whereas its inactivity expedites cell death in some diseases.[201,202] Telomerase recruitment to chromosome ends has been investigated using single molecule fluorescence approaches, as described in section 4.10.

3. PRINCIPLES OF INTRACELLULAR SINGLE MOLECULE FLUORESCENCE MICROSCOPY OF RNA

As surveyed above, our appreciation for the diversity of cellular RNAs has exponentially increased over the past decade. With the rapid advancement of deep-sequencing and bioinformatics technologies, we are likely to unearth still other classes of RNAs, a further increased functional diversity, as well as novel RNA−protein interactions. The current ensemble-averaged approaches clearly will continue to provide a wealth of information on RNA biology. However, biology is fundamentally stochastic in nature, leading to diverse, spatiotemporally inhomogeneous distributions of molecules within cells as well as across individual cells, even within a clonal cell line or

dx.doi.org/10.1021/cr400496q | Chem. Rev. 2014, 114, 3224−3265

(tumor) tissue. The resulting heterogeneities, short-lived and/or rare pathway and reaction intermediates, dispersed cellular localization and time evolution, multitude of parallel mechanisms of action and nonlinear responses from complex, multihub networks together form the very foundation of biomolecular function. The omnipresence of such molecular dispersions warrants the development of ultrasensitive, noninvasive techniques that expose them, leading to the application of emergent single molecule microscopy techniques to biological samples. Some of the earliest implementations of single molecule microscopy have been used to characterize biological processes in unprecedented detail, as exemplified by the observation of single β-galactosidase molecules trapped in microdroplets in the presence of a fluorogenic substrate,[203] tracking of single (oftentimes tethered) beads or particles in vitro or in cellulo,[204−208] recording of the absorption or fluorescence of single pentacene molecules in *p*-terphenyl crystalline matrices at liquid-helium temperature,[209,210] and measurement of single enzyme turnovers.[211]

Single molecule microscopy (SMM) can broadly be divided into two categories, optical observation and mechanical manipulation tools. In this review, we will focus on optical methods that employ single molecule fluorescence microscopy (hereon referred to as SMM) to probe the intracellular function of RNA. Imaging tools such as atomic force microscopy (AFM) and methods that apply mechanical manipulation to single molecules such as optical and magnetic tweezers are beyond the scope of this article, but a broad overview of such techniques can be found in several reviews.[212,213]

It turns out that SMM is primed to break the classical optical diffraction limit. According to Abbe's law or Rayleigh's resolution limit,[212] diffraction limits our ability to distinguish two features located closer (on the lateral plane) than half the wavelength of the illuminating or emitted light, thereby imposing a theoretical limit on the resolution of fluorescence microscopy of 200−300 nm (using visible, ∼500 nm illumination light). Consequently, the image of a single fluorescent probe, typically a few nanometers in diameter, is spread after passing the microscope optics over a few 100 nm on the detector. The intensity distribution of such a diffraction-limited spot can be mathematically described by a point spread function (PSF) and approximated as a simple two-dimensional (2D) Gaussian function. The center of the Gaussian curve, which coincides with the intensity maximum of the diffraction limited spot, can be localized with accuracy similar to the size of the fluorescent emitter, effectively breaking the diffraction barrier. Recent advancements in instrumentation have thus facilitated our ability to visualize single molecules under ambient conditions in situ at nanometer spatial resolution,[212,214,215] previously accessible only to biologically invasive techniques such as electron microscopy.

However, the application of intracellular SMM presents a unique pair of challenges: (i) the need to reach an appropriately low sample concentration to delineate individual molecules within the dense and complex milieu of a cell and (ii) the requirement to detect photons (signal) from individual molecules within the uneven background (noise), contributed mostly by both autofluorescence and signal from out-of-focus molecules, with minimal phototoxic effects on the cell. The former is specifically difficult to control when probing endogenous biomolecules, especially RNA, whose intracellular abundance can vary from a few to several (tens of) thousand(s of) molecules per cell. The latter, especially autofluorescence that is primarily contributed by fluorescent intracellular metabolites, cofactors and pigments, is omnipresent. Put together, these obstacles render the successful implementation of intracellular SMM nontrivial. Nevertheless, a careful choice of labeling strategies and imaging conditions can make this seemingly daunting task relatively seamless. For instance, titratable reporters,[216] controlled delivery of labeled probes[135,217,218] and ultrahigh resolution microscopy methods that systematically probe only a subset of all labeled probes at any given time[212,215,219] have judiciously tackled the concentration challenge, whereas improved optical configurations (illumination sources, strategies and detectors) and fluorescent probes have successfully dealt with the latter. In this section, we will review and present a "panorama" of the fluorescent probes, labeling strategies and imaging schemes that have been employed to achieve in cellulo single RNA/RNP molecule detection, along with their respective advantages and disadvantages.

3.1. Fluorescent Probes

During the early stages of intracellular single particle tracking (SPT) and single molecule microscopy large (0.25−2 μm), either fluorescent or nonfluorescent beads were popular as reporters.[204,220] Their large size enabled convenient high-precision imaging without the risk of undesired signal photobleaching, even when using microscopes with unsophisticated optics. However, conjugating biomolecules to large beads comes with the caveat that the attachment of a bulky load may skew the molecule's function, localization, and/or diffusion, or introduce other artifacts.[220] Moreover, limited options for multiplexing means that nonfluorescent beads cannot be used to probe multiple types of biomolecules simultaneously. Thus, small fluorescent probes, available in various colors, soon superseded beads as the primary choice of visual reporters in SMM.

Upon their discovery in the 1960s[221] and cloning in the 1990s,[222] fluorescent proteins (FPs) quickly became a mainstay of intracellular fluorescence microscopy.[223] The ease with which FP genes can be expressed as fusions with cellular protein targets and the availability of a broad FP "color-palette" that spans the entire visible and near-IR part of the spectrum[224] make them attractive probes. One of the main caveats of this labeling method is that protein fusions are often expressed exogenously, thus resulting in overexpression compared to endogenous levels, which jeopardizes physiological relevance. Additionally, overexpression typically increases intracellular particle density to an extent that it becomes refractory to single molecule visualization. Using weak promoters, inducible expression systems, controllable viral transduction or creating/selecting for stable cell lines with low expression are a few adaptations that can be employed to mitigate the effects of overexpression.[225,226] In addition, recent genome editing technologies using zinc-finger nucleases (ZFNs), transcription activator-like effector nucleases (TALENs) and clustered regulatory interspaced short palindromic repeat (CRISPR)/Cas-based methods have emerged as powerful tools that can function to regulate endogenous expression of FP fusions, and thus, future implementation of these technologies may help circumvent the above hurdles.[227] Despite suffering from frequent intensity fluctuations (blinking) and limited photostability,[228] FPs are still preponderant in intracellular single molecule microscopy of RNA due to the ease of creating and delivering them as genetically encoded fluorescence markers.

dx.doi.org/10.1021/cr400496q | *Chem. Rev.* 2014, 114, 3224−3265

Even otherwise deleterious blinking properties have found compelling applications in super-resolution imaging,[219,229,230] enhancing our ability to image samples of high probe density. The emergence of photoactivatable, photoconvertible and fluorescent dimer proteins[224,231] has further improved super-resolution imaging schemes[219] and tremendously aided in photosynchronization experiments.[232] Moreover, a majority of current RNA labeling schemes invoke the binding of multiple FPs per RNA,[233] wherein a few well-folded FPs compensate for the blinking or photobleaching of a subset of others within the complex.

Organic fluorophores (of the rhodamine, cyanine, oxazine, bodipy, perylene, and other structural scaffolds) are typically preferred over FPs in intracellular SMM for their small size and superior photophysical properties, i.e., they do not blink as often, they typically emit more fluorescence photons prior to photobleaching, and their undesired photophysical properties can be suppressed using several additives (as discussed in section 3.1.1). In further contrast to FPs, organic dyes are predominantly conjugated to biomolecules ex vivo, via several well standardized conjugation chemistries.[234−237] This labeling scheme often mandates the careful purification of probe labeled molecules from unlabeled molecules and unbound dye impurities and, for intracellular imaging, the specific delivery of tagged molecules to cells. Such hurdles are potentially overcome by the use of various genetically encodable tags that form a covalent adduct with organic dye substrates, such as SNAP tags (NEB), Halo tags (Promega), and tetracysteine motif bearing peptides (Invitrogen). These labeling strategies effectively combine the elegance of intracellular labeling via genetic engineering with tagging photophysically superior organic dyes. The development of bioorthogonal labeling strategies[238,239] and fluorogenic photoaffinity probes[240,241] has further broadened the scope of in cellulo labeling methods.

Fluorescent beads and quantum dots (QDs) have several favorable photophysical properties, as they are typically brighter and more photostable and the latter specifically have narrower emission spectra than organic fluorophores.[242] However, akin to nonfluorescent beads, these probes are typically large (similar in size to a protein or small RNA) and have a high propensity to affect the intracellular physicochemical characteristics and function of the conjugated biomolecule. Their large size additionally inhibits efficient intracellular delivery and imposes steric constraints during target binding of QD/fluorescent bead labeled probes. Additional limitations of QDs include the potential for cytotoxicity of the composite transition metal ions and tendency for frequent blinking,[243] where the latter is a bane for both single molecule counting (as it confounds intensity values that are used to measure copy number) and particle tracking (as it introduces difficulty in assigning contiguous tracks when particles temporarily vanish from observation).

3.1.1. Photophysical Properties Required for Detecting Single Fluorescent Probes. A fluorophore suitable for intracellular SMM should have high quantum yield (i.e., ratio of the rate of fluorescence to the sum of all relaxation rates; reflects the net efficiency of fluorescence), high brightness (i.e., measure of photon output calculated as the product of a fluorophore's extinction coefficient and quantum yield), favorable photophysical properties and sufficient inertness so that the label does not interfere with the function of the molecule to be tagged. Among these, brightness and inertness are inherent characteristics of the probe's chemical nature, and the brightness in particular is significantly influenced by the immediate chemical environment of the probe. It is thus critical to evaluate several probes and choose an appropriately bright fluorophore, such that the fluorescent signal is significantly more intense than the cellular autofluorescence. This cellular background is caused by naturally fluorescent molecules present inside cells, such as NADH, FADH, and heme. Two ways to circumvent such background is to use (i) cell culture media devoid of any naturally fluorescent molecules, especially vitamins[244] and (ii) fluorophores that absorb light and fluoresce in the far-red visible or NIR part of the electromagnetic spectrum where cellular components show minimal emission.[228,245,246] Another dye and environment dependent, important photophysical property of fluorophores is their fluorescence lifetimes, i.e., the time taken for an excited singlet electron to transition back to the ground state and concomitantly release a photon (Figure 2). As fluorophore excitation (at femtoseconds, or fs) occurs much faster than photon emission (at nanoseconds, or ns; Figure 2), excited singlet states have a propensity for electronic saturation, limiting the maximally possible yield of photons.

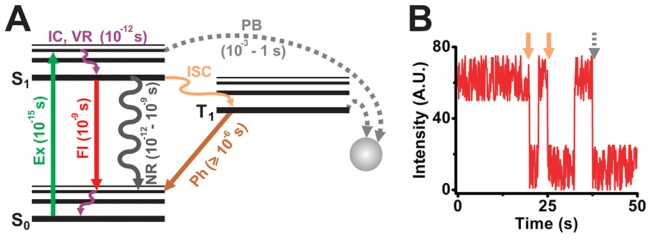

Figure 2. Photophysical properties of fluorophores. (A) Simplified Jablonski diagram representing excitation (Ex), fluorescence (Fl) emission, internal conversion (IC), vibrational relaxation (VR), nonradiative decay (NR), intersystem crossing (ISC), phosphorescence (Ph) and photobleaching (PB), and the respective time scales at which these processes occur. S_0, singlet ground state; S_1, singlet excited state; T_1, triplet state. (B) A simulated intensity trajectory of a single molecule with two blinking events (orange arrow) and a single photobleaching step (dotted gray arrow).

In contrast to its intrinsic brightness, undesirable photophysical processes affecting a given fluorophore, such as large intensity fluctuations and photobleaching, to an extent can be controlled extrinsically. Intensity fluctuations are typically characterized by reversible changes of the fluorophore between bright and dark states (i.e., blinking), whereas photobleaching signifies an irreversible switch to a dark state (Figure 2). Both processes markedly affect the quality and length of single molecule recordings. Blinking is predominantly induced by intersystem crossing (ISC, Figure 2), wherein fluorophore excitation populates electronic triplet states instead of singlet states. Relaxation back to the ground state from triplet states, which is a prerequisite for further cycles of electronic excitation and subsequent fluorescence, is quantum mechanically forbidden and takes ∼1000-fold longer than relaxation from singlet states so that probes are temporarily rendered dark. Blinking and photobleaching may also occur due to the chemical reaction of excited state molecules with radical species, induced by the excitation light or provided by the chemical environment of the dye. In certain cases, the excitation light may itself suffice to transform a fluorescent dye into its dark state in a phenomenon termed photochromism. However, several chemical agents such as cyclo-

dx.doi.org/10.1021/cr400496q | Chem. Rev. 2014, 114, 3224−3265

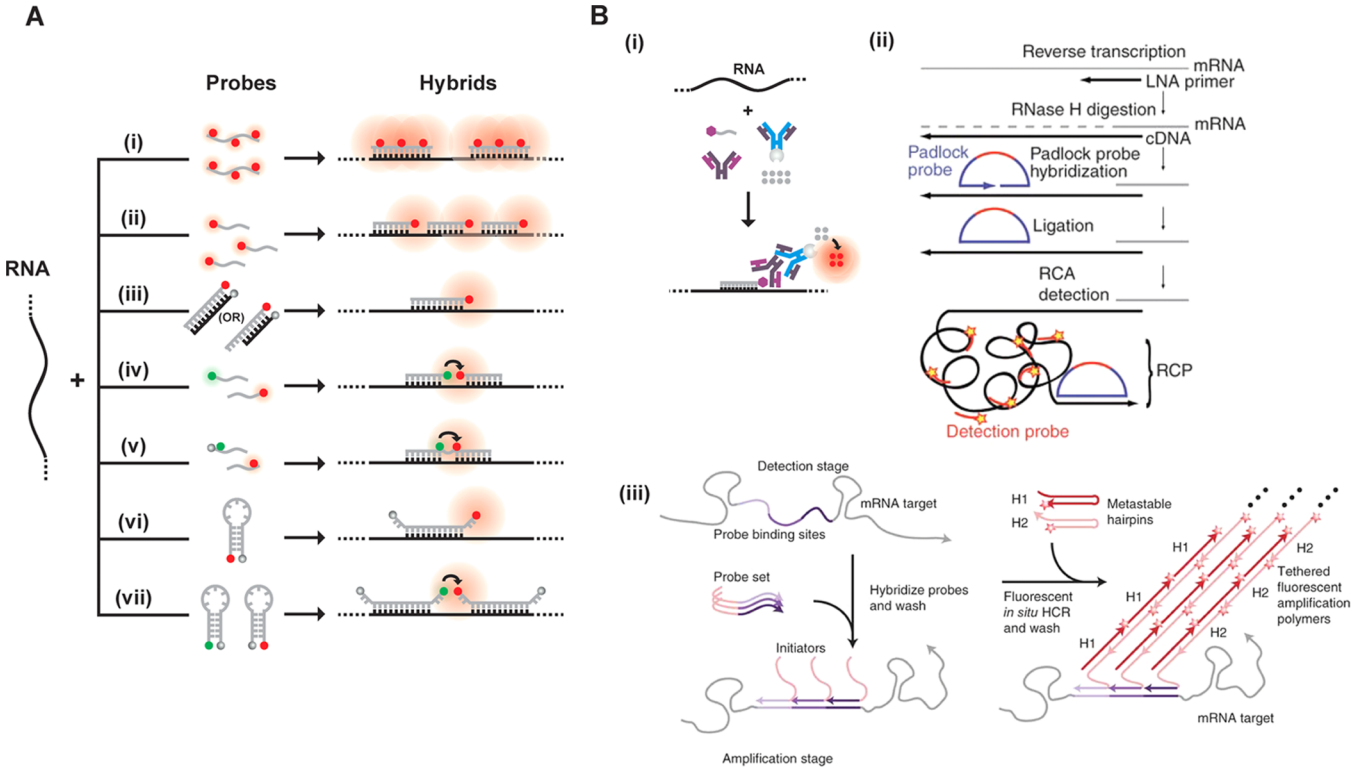

Figure 3. Fluorescently labeling RNA by hybridization of labeled probes. (A) Hybridization probes that do not employ signal amplification strategies. Represented here are schematics of the Singer approach using few multiply labeled probes (i), the Tyagi method of many singly labeled probes (ii), competitive hybridization (iii), and inherently quenched molecular beacons (iv). Green and red circles are spectrally distinct dye molecules and shaded gray circles are quenchers. Schematics iv–v and vii represent hybridization methods that have been widely used in ensemble imaging of intracellular RNA, with immense potential in single molecule imaging. Side-by-side probes[493] (iv) are designed to bind target RNAs at adjacent positions, such that the binding configuration brings fluorophores on the two probes into close proximity to enable FRET. In a variant of this scheme, called quenched-autoligation[494,495] (v), the probe containing the FRET donor also contains a quencher to suppress the fluorescence from unbound oligonucleotides. Once the functionalized probes bind side-by-side, they self-ligate, removing the quencher from the vicinity of the donor probe, thereby resulting in unquenched FRET. Another variant of the side-by-side scheme consists of dual molecular beacon FRET probes[436,496] (vii); here signal specificity is enhanced by two beacons, one containing the FRET donor and another containing the FRET acceptor, which bind at adjacent locations to generate a FRET signal. Each probe contains a quencher to reduce fluorescent background from unbound probes. (B) Signal amplification in hybridization probes. Schematics representing the ELF approach (i), padlock probes (ii) (Reprinted with permission from ref 273. Copyright 2010 Nature Publishing Group.), and the HCR approach (iii). Reprinted with permission from ref 290. Copyright 2010 Nature Publishing Group. RCP, rolling circle product.

octatetraene (COT), trolox, ascorbic acid, mercaptoethylamine (MEA), 4-nitobenzyl alcohol, 1,4-diazabicyclo[2.2.2]octane (DABCO) and *n*-propyl gallate can be used to quench triplet states and radical species and, thus, reduce blinking and increase fluorophore longevity.[228,247−249] It is noteworthy that the quenching action of some chemical agents is dye specific, for instance, MEA has proven to effectively quench triplet states of Rhodamine 6G[250] but increase blinking in cyanine dyes like Cy5.[247] Although it is still unclear, this detrimental action of MEA is attributed to its function as a reducing agent, especially considering that other reducing agents such as dithiothreitol (DTT), *β*-mercaptoethanol (BME) and tris(2-carboxyethyl)-phosphine (TCEP) also induce such deleterious effects. This effect, termed redox blinking, can be induced by oxidants such as methyl viologen as well. Regardless of whether they enhance photophysical characteristics, the addition or removal of any of these chemical agents should be contingent upon their tolerability by and the viability of cells, especially in live cell imaging, whereas such stringency is not required for imaging fixed cells, where the choice of reagents can be purely dye-based. Another chemical that has been widely attributed as the cause of photobleaching, presumably via photooxidation of the fluorophore, is molecular oxygen and related species. Especially during intracellular imaging, excited fluorophores can react with molecular oxygen within cells, resulting in the accumulation of phototoxic free radicals that can compromise subcellular compartments or even the entire cell's livelihood.[251] Enzymatic oxygen scavenging systems (OSS), such as those containing glucoseoxidase and catalase (GODCAT),[252] protocatechiuc acid and protocatechuate-3,4-dioxygenase (PCA/PCD)[247] or oxyfluor[253] utilize molecular oxygen as a substrate in enzymatic reactions, thereby effectively depleting it. These OSS prevent fast photobleaching and oxygen induced free radical production, resulting in increased signal longevity. However, it is critical to reduce the exposure of cells to OSS as they may lead to hypoxic shock,[254] as well as to include good buffering agents in the imaging solution to overcome harmful effects of pH changes induced by certain OSS.[255] As molecular oxygen is also an efficient quencher of triplet states, addition of OSS may increase fluorophore lifetimes at the cost of increased blinking rates.[256] Thus, it is mandatory to include triplet state quenchers in imaging solutions that also contain OSS. Other deleterious photophysical effects, such as light induced free radical production and phototoxicity, are reduced by striking a balance

dx.doi.org/10.1021/cr400496q | *Chem. Rev.* 2014, 114, 3224−3265

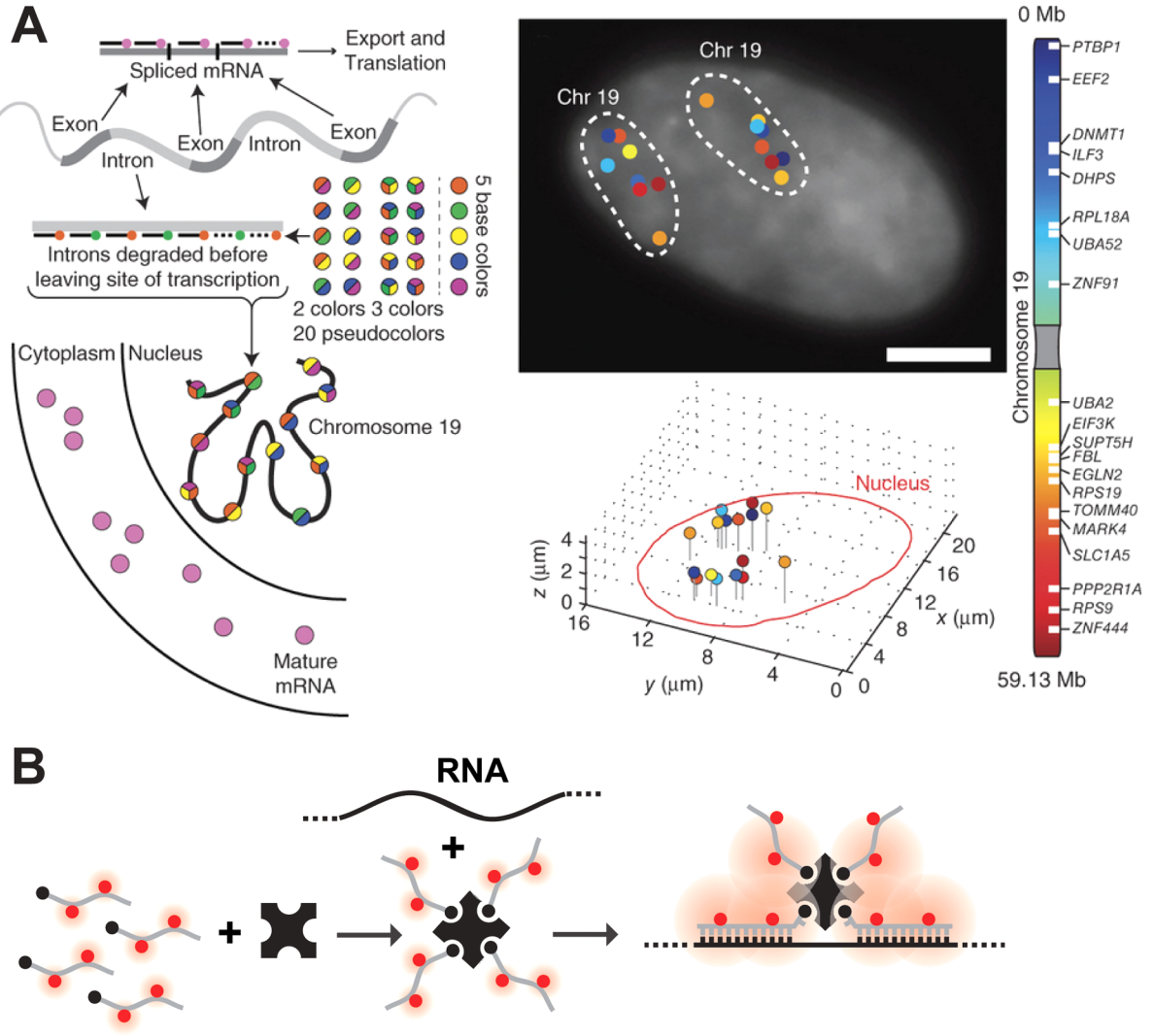

Figure 4. Recent techniques for fluorescently labeling RNA by hybridization of labeled probes. (A) A pseudocolored scheme for spectral barcoding in iceFISH to simultaneously detect 20 transcript (left panel). The right panel contains a representative cell with the transcriptional activity of 20 genes spatially annotated. Reprinted with permission from ref 292. Copyright 2013 Nature Publishing Group. (B) Schematic of the MTRIPs labeling method.

between the excitation laser power (and wavelength) and the time over which the sample is illuminated while maintaining single molecule sensitivity.

3.2. Labeling Strategies of RNA for Intracellular Single Molecule Fluorescence Microscopy

RNA labeling strategies may be crudely divided into two main categories, indirect and direct labeling schemes. The former employs sequence-complementary oligonucleotides (Figures 3 and 4) or fluorophore labeled RNA binding probes, such as RNA binding proteins, RBPs (Figure 5), which associate with appropriate RNA motifs to (indirectly) tag RNA with fluorophores. Conversely, direct labeling schemes exploit chemically reactive functional groups or structural motifs within the RNA, naturally present or introduced by chemical synthesis or RNA modifying proteins, for fluorophore conjugation (Figure 6). Currently, indirect labeling schemes are more predominant in intracellular SMM of RNA as they have the capability to probe endogenous targets, in addition to exogenous constructs, thereby finding widespread application in in situ gene expression profiling with single molecule sensitivity.[21] In this review, we will focus on well-established

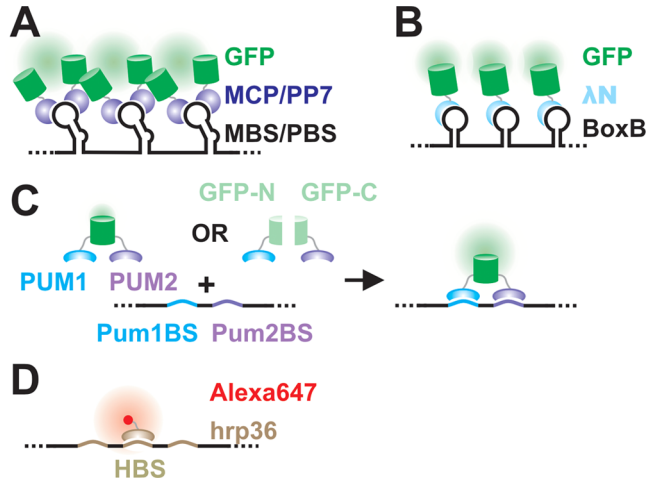

Figure 5. RNA labeling by various protein–RNA tethering approaches. A detailed description is provided in section 3.

dx.doi.org/10.1021/cr400496q | Chem. Rev. 2014, 114, 3224–3265

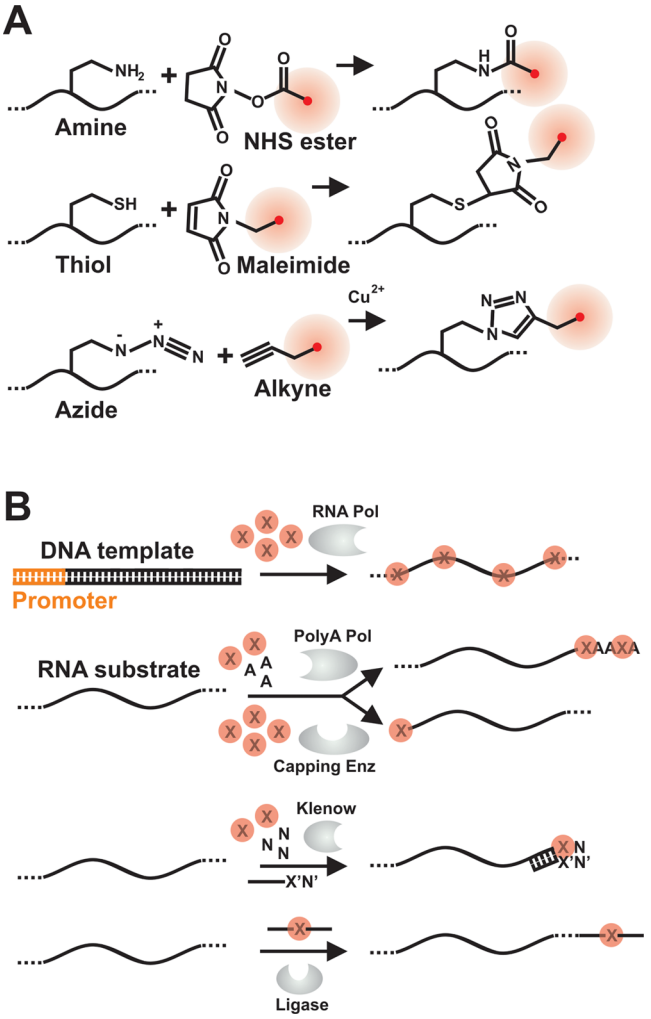

Figure 6. Chemical (A) and enzymatic (B) methods for direct fluorophore labeling RNA. (A) Direct labeling of RNA by chemical methods. Red circles are dye molecules. (B) Direct labeling of RNA by enzymatic methods. X represents appropriately modified NTPs that are either directly conjugated to fluorophores or contain functional groups for subsequent chemical conjugation of dyes. RNA Pol, RNA polymerase; PolyA Pol, PolyA polymerase; Capping Enz, 5′ end-capping enzyme; Klenow, Klenow fragment of DNA polymerase I from *E. coli*; Ligase, typically one of the two T4 RNA ligases.[24]

RNA labeling schemes used in intracellular SMM but also describe a few methods that have strong potential. A majority of these labeling strategies has been optimized to probe mRNAs; however, applications to the world of ncRNAs are slowly emerging.

3.2.1. Labeling by Fluorescence in Situ Hybridization (FISH): An Early Glimpse at the Power of Intracellular SMM. Labeling target RNAs by hybridizing sequence complementary oligonucleotides in situ upon fixing and permeabilizing a cell was one of the earliest strategies to reach single molecule sensitivity. The method quickly gained widespread use because of its ability to probe the subcellular distribution and abundance of endogenous RNA and led to the inception of single cell gene expression analysis, the importance of which is underscored by the ubiquitous occurrence of cell-to-cell variations in gene expression.[21,257,258] For instance, tumors that are often considered as a single lump of cells are comprised of many distinct cell types, each bearing distinct gene expression programs.[259] Furthermore, the microenvironment of such tumors influences gene expression;[259] for example, a cell in the center of a tumor or tissue expresses a different set of transcripts than one in the periphery. As an additional layer of complexity, gene expression is spatially organized even within individual cells.[260−262] Such heterogeneities are often hidden within the averaged measurement or statistical error of an ensemble method (such as Northern blotting, quantitative reverse transcription PCR (qRT-PCR), microarray, or deep-sequencing), traditionally used to quantify gene expression at high-throughput on a genomic scale. Techniques to access these important heterogeneities, such as single-cell RNA sequencing, microfluidics aided single-cell qRT-PCR, micro-dissection, fluorescence activated cell sorting, and subcellular fractionation, are slowly emerging as attractive technologies for single cell transcriptome analysis[263,264] but are still not very efficient and/or introduce quantification or sequence biases through amplification steps in the protocol. Moreover, these ensemble methods still do not provide critical information on the spatiotemporal distribution of transcripts within tissues or individual cells. Therefore, it is becoming increasingly important to complement bulk measurements with techniques that characterize gene expression within individual cells in situ to decipher the stochastically driven, essential dispersities of gene expression within complex genetic networks. Progress in solid state synthesis of fluorophore labeled oligonucleotides and imaging/image analysis technology coupled with incessant advances of sequencing and bioinformatics analysis are now culminated in our ability to probe, in principle, any transcript, coding or noncoding, within the entire transcriptome at single molecule resolution in cellulo.

Traditionally used for DNA profiling and later modified for RNA detection,[265] in situ hybridization (ISH) protocols generally entail a sequence of fixation, permeabilization, hybridization of long (>100 nt) oligonucleotide probes to their corresponding complementary sequences, thorough washing to remove unbound probes, and image acquisition. Oligonucleotides are either directly labeled with fluorophores (fluorescence in situ hybridization, or FISH) in a stochastic fashion via enzymatic reactions (for example, transcription, 3′-end extension, nick translation and ligation; Figure 6B) or coupled to haptens, such as biotin or digoxigenin. In the latter case, the sample is then treated with avidin or antibody to digoxigenin, which are either directly labeled with fluorophores or coupled to chromogenic enzymes like alkaline phosphatase (AP) or horseradish peroxidase (HRP) whose enzymatic products yield an amplified light signal. Alternatively, secondary antibodies specific to avidin or primary antibody to digoxigenin are fluorophore or enzyme labeled to further amplify the signal from a single hybridization event. Even though these protocols are extremely useful in providing qualitative information on gene expression and localization patterns, they lack quantitative detail due to three main reasons: (i) Random distribution of fluorophores within oligonucleotides often results in a heterogeneously labeled population of probes and sometimes even localizes fluorophores close enough to mutually quench each other, both of which shroud intensity measurements that are critical for calculating the molecule copy number; (ii) long probes are poorly cell-permeable and thus result in incomplete labeling of RNA in situ; and (iii) this original protocol suffered from low sensitivity due to high background caused by unbound and nonspecifically bound probes not removed by the washing. To overcome these caveats, multiple short

oligonucleotide probes complementary to adjacent sequences within an RNA of interest effectively have now replaced long probes when performing FISH at the single molecule level[266,267] (Figures 3 and 4). Each of these short oligonucleotide probes, small enough to surpass the permeability issue, are labeled with multiple[266] or single fluorophores[267] and designed such that the distance between fluorophores within individual hybridization probes and between different probes minimizes proximity mediated fluorescence self-quenching. Moreover, the fluorophore is attached to a specific nucleotide within the probe, resulting in more homogeneous labeling. The collective fluorescence arising from the binding of multiple such probes to a single RNA molecule is much higher than the fluorescence from a single labeled oligonucleotide, effectively delineating specific signal from unbound, nonspecifically or suboptimally bound oligonucleotides and cellular autofluorescence. In an alternative experimental scheme, endogenous transcripts containing multiple repeats of a specific sequence[268] or exogenous transcripts tagged with such a repeat sequence array[269,270] are labeled with multiple copies of a single fluorophore tagged oligonucleotide sequence, essentially mitigating oligonucleotide synthesis costs. Following the basic principle of signal amplification, other modifications to the ISH procedure include the use of molecular beacons,[269,270] modified nucleic acid backbone,[271,272] padlock probes,[273] branched DNA oligonucleotides,[274] or multivalent RNA hybridization probes.[217] With the appropriate calibration controls, instrumentation, and image analysis methods (described below) such modifications to the traditional ISH protocol result in single RNA molecule sensitivity.

Singer and co-workers spearheaded single molecule FISH (smFISH) methods by using five or more short (∼50 nt) oligonucleotide probes that bound complementary sequences within an RNA of interest[266] (Figure 3A, (i)). Each probe was labeled with 3 or 5 fluorophores at predefined positions and had a GC content of ∼50%, suitable for optimal hybridization at relatively low temperatures (37−47 °C). Probes were then independently imaged in vitro at different concentrations to derive a calibration curve, which was consequently used to confirm the identity of individual fluorescent particles as single RNA molecules. To this end, various dilutions of the fluorophore labeled oligonucleotide were imaged in vitro in a sample chamber of known volume, using the same microscope settings as during intracellular imaging. A calibration curve of fluorescence signal versus number of oligonucleotide molecules (calculated from the concentration and sample holder volume) per voxel (a 3D pixel element) was plotted and the intensity of individual oligonucleotides was extrapolated from this curve. The authors found that the number of dye labeled oligonucleotide probes within individual fluorescent particles in a deconvolved image, as computed by dividing the particle signal by the signal of a single oligonucleotide, coincided with that expected to bind to a single mRNA.[266,275] This method has been employed by several groups for spatial annotation of transcripts and counting;[276−279] however, it suffers from one major drawback: high variability in the number of oligonucleotide probes bound per target.[266,267,275] More specifically, >50% of all fluorescent spots contain only one or two of the possible five or more oligonucleotide probes, which complicates the reliable distinction of specific over nonspecific binding. As each oligonucleotide probe has 3−5 dye labeling sites, incomplete labeling and inefficient separation of fully from partially labeled probes may result in the false annotation of probe density per transcript and thus have an impact on the quantification accuracy.

Tyagi, van Oudenaarden and co-workers modified Singer's protocol by targeting a single transcript with 48−96 oligonucleotide probes, each spanning ∼17−22 nt and labeled at the 3′ end with just one fluorophore to allow for the efficient purification of labeled from unlabeled oligonucleotides, thereby improving labeling homogeneity of the target (Figure 3A, (ii)).[267] Such short probes also require less stringent conditions for hybridization and washing: compare 28−37 °C and 10% formamide[267,280] to 37−47 °C and 50% formamide[266,275] in the Singer protocol or 65 °C and 50% formamide[281] in traditional FISH. Less harsh conditions allow for combining FISH with immunofluorescence or immunohistochemistry to probe both RNAs and (associated) proteins, frequently referred to as immunoFISH.[282] Probes are designed to bind adjacent sequences on a single transcript such that the minimum spacing between them is 3 nt, thus minimizing self-quenching. Compared to the Singer approach, this strategy results in an increased fluorescence enhancement from individual transcripts, to an extent that even transcripts bound by endogenous RBPs or partially degraded are more efficiently detected. By contrast, signal arising from the nonspecific binding of just one or two probes is typically insignificant enough to avoid false positives. The single molecule sensitivity of this method was validated by multiple complementary approaches.[267,280,283] The method's sensitivity and inherent simplicity have led to its rapid commercialization (Biosearch Technologies) and to the availability of intuitive Web sites for probe design (http://www.singlemoleculefish.com) for any RNA target. However, the approach cannot be employed to detect short transcripts and small ncRNAs. In an effort to overcome this caveat, Shepherd et al. developed a competitive hybridization-based approach (Figure 3A, iii).[284,285] Herein, double-stranded probes contain a fluorophore on the 5′-end of the strand complementary to target and a quencher on the 3′-end of the other probe strand such that the former probe strand's fluorescence is quenched as long as the two oligonucleotides remain in the duplex.[286] The target gradually replaces the quencher strand to bind the fluorophore labeled probe strand, leading to loss of quenching. Shepherd et al. exploited this property to reduce background fluorescence from free probe. To probe smaller RNAs, they additionally reduced the number of probes (5−10 compared to 48−96) and relaxed several probe design criteria, including requirements for ∼50% GC content and large separation between probes. However, this method also suffers from variability in the number of probes bound per target, largely due to reduced stringency in probe design. Inefficient labeling due to poor kinetics of probe strand separation is another possible drawback. One solution is to make the fluorophore labeled, target-binding strand longer than the quencher strand, such that the overhang of their duplex is complementary to the target RNA. This allows for a more rapid removal of the quencher by strand displacement.[285] Xie's group has reportedly overcome these drawbacks by probing single mRNA molecules with a single fluorophore labeled oligonucleotide in *E. coli*.[287]

The use of probes bearing a modified oligonucleotide backbone that allows them to hybridize more stably to RNA has enabled the detection of short transcripts with high specificity. Hybridization is sensitive enough to distinguish single nucleotide differences and detect single RNA molecules with just a single probe. These properties were exploited by Lu

and Tsourkas[272] to detect miRNAs in situ at single molecule sensitivity using locked nucleic acid (LNA or 2′-O, 4′-C-methylene-linked ribonucleotide) probes aided by enzyme labeled fluorescence (ELF) based signal amplification (Figure 3B, i). The LNA oligonucleotide probe is labeled with digoxigenin at its 3′-end to be recognized by an anti-DIG-AP chimeric antibody. ELF is achieved by the cleavage of a pro-luminescent substrate by AP (or HRP). Precipitation of the product and multiple turnover by the enzyme result in a fluorescent spot at the site of enzyme activity that is 20- to 40-fold brighter than a single fluorophore. The authors confirmed single molecule sensitivity based on the similarity in copy number distribution of ectopically expressed control transcripts that were detected by either standard smFISH or LNA-ELF-FISH.[272] Probes with other backbone modifications, such as peptide nucleic acids (PNA), have been used to detect telomeres and assess their length in situ.[271]

The possibility of fluorescent ELF amplification products diffusing away during washing or detection has spurred the development of other signal amplification methods. Initially standardized for DNA, Larsson et al.[273,288] developed "padlock" probes to detect single nucleotide polymorphisms (SNPs) in RNA, i.e., distinguishing transcripts that differ only by a single nucleobase, via enzyme independent signal amplification. They first reverse transcribed the RNA to cDNA using LNA primers, RNase H treated to degrade any portion of the RNA complementary to the cDNA, hybridized linear padlock probes to the target such that the 5′- and 3′-ends are juxtaposed, enzymatically ligated the ends and used them as templates (and the cDNA as the primer) for rolling circle amplification by Phi29 DNA polymerase (Figure 3B, ii).[273] A single-stranded DNA containing tandem repeats of the padlock probe was thus created at the mRNA localization site, to which fluorophore labeled detection oligonucleotides were hybridized to yield a bright fluorescent spot. The specificity of LNA hybridization contributes to the initial specificity in targeting transcripts and tethering the cDNA to the intracellular transcript location, whereas the target dependent padlock probe ligation aided SNP detection. Another signal amplification approach uses branched DNA hybridization.[274,289] Here, a single gene specific probe contains flanking sequences that hybridize to a preamplifier probe, which in turn binds multiple amplifier oligonucleotides. Each amplifier oligonucleotide binds multiple detection oligonucleotides, thereby resulting in bright fluorescent spots, especially when multiple gene specific probes target a single transcript. This technology has been commercialized as QuantiGene ViewRNA (Affymetrix), with the advantage of using universal preamplifier, amplifier, and detection oligonucleotides for any gene specific set of probes. A related system, named hybridization chain reaction (HCR[290]), uses flanking sequences on gene specific probes (initiator oligonucleotide) to initiate self-assembly of metastable fluorescent RNA hairpins into large amplification polymers (Figure 3B, iii). All of these protocols improve signal quality and quantity, yet they have a major drawback of amplifying false positive signals as well, necessitating stringent probe design criteria.

Although multiplexing has been achieved with many of these methods by using distinct fluorophore colors, conventional optics and broad emission spectra typically limit the number of simultaneously detectable transcripts to three, beyond which nonspecific excitation and spectral bleed-through confound signal identification. To overcome this limitation, Singer and colleagues developed an approach they termed "spectral barcoding"[291] wherein gene specific probes are divided into groups labeled with spectrally distinct fluorophores. Hybridization of these groups of probes with their cognate transcripts and careful registration of multiple fluorescent channels results in fluorescent spots that are multicolored. With each gene designed to bind probes with a specific color combination, one can, in theory, have $2^n - 1$ color combinations of n spectrally resolvable fluorophores, effectively multiplexing and increasing throughput. Recently, Levesque and Raj[292] doubled the number of simultaneously detected transcripts (from 10 to 20) in an adaptation of Singer's method they called intron chromosomal expression FISH (iceFISH). The authors took advantage of the fact that most introns are unstable upon their removal from a pre-mRNA by splicing near their site of transcription and labeled introns to thus probe chromosomal structure (Figure 4A).

A majority of smFISH approaches are not extendible to living cells because it is difficult to deliver such a large number of probes into cells by methods other than irreversible membrane permeablization. Moreover, FISH protocols rely on hybridization under (mildly) denaturing conditions and multiple wash steps to remove unbound probes, both of which are difficult to accomplish in living cells. Tyagi and co-workers[269] addressed these drawbacks by microinjecting molecular beacon probes (Figure 3A, vi) into live cells. Molecular beacons are designed to have small complementary sequences on either end such that they adopt a (weak) hairpin structure (with a small stem and a large loop), bringing a fluorophore at the 5′-end close to a quencher at the 3′-end for effective quenching of fluorescence from unbound probes. Upon target hybridization, the hairpin stem is disrupted and the fluorophore becomes unquenched. 2′-*O*-Methyl (2OMe) oligonucleotides were used instead of DNA probes to alleviate RNase H mediated cleavage of RNA within DNA-RNA hybrids and to prevent probe degradation by cellular nucleases. For fluorescence enhancement from individual transcripts, the authors created an exogenous transcript that binds 96 copies of the probe, thereby requiring only a single probe sequence for target hybridization. To demonstrate that each fluorescent spot contained a single RNA, the group prepared in vitro transcribed RNA containing 16, 32, 64 or 96 probe binding sites, prehybridized the probes in solution and microinjected them into cells. As expected, the intensity of particles was proportional to the number of binding sites, the intensity distribution of particles was well represented by a single Gaussian, and the average particle counts per cell coincided with qRT-PCR results. The establishment of live cell single RNA detection allowed the group to understand nuclear trafficking of RNPs. A similar approach was used by Kubitscheck and colleagues to probe endogenous Balbiani ring (BR) 1 and 2 mRNPs. The group used a fluorophore labeled oligonucleotide that substoichiometrically targeted a stretch of repeat sequences (~80 repeats) within the mRNA.[268] Ishihama and Funatsu similarly used microinjection to track the diffusive behavior of polyA-tailed ftz mRNA, prehybridized with QD labeled oligonucleotide $U_{(22)}$, within the nucleus of mammalian cells.[293]

As microinjection may lead to the passive transport of probes into the nucleus and consequently hamper cytoplasmic RNA labeling, Santangelo and co-workers[217] used a combination of reversible permeabilization by streptolysin O (SLO) for intracellular delivery and a unique set of hybridization probes called multiply labeled tetravalent RNA imaging probes (MTRIPs; Figure 4B). Individual detection probes were created

by binding streptavidin to 2′-*O*-methyl RNA−DNA chimera that contained a 5′-biotin and 3−5 well spaced internal fluorophores. As streptavidin contains four biotin binding sites, a tetravalent probe forms with a 4-fold fluorescence enhancement over a single probe. SLO allowed for the delivery of such large probes into the cells. Single molecule sensitivity was supported by assessing intensity distributions of single probes immobilized to glass and those in cells and further confirmed by comparisons of the signal from monovalent with that of tetravalent probes and the intracellular distribution of scrambled with that of specific probes. Major advantages of this method include the need for fewer tetravalent probes (2−3) per RNA and the ability to visualize the dynamics of endogenous (as opposed to engineered) RNA. Recently, the same group replaced streptavidin with multiarmed PEG[294] covalently attached to fluorescent oligonucleotides to reduce toxicity from spurious binding of streptavidin to endogenous biotin and to increase the number of oligonucleotides, and thus fluorophores, per MTRIPs.

RNA labeling via hybridization, although popular, still suffers from several drawbacks. The cross-linking of RBPs to RNA during fixation and tightly formed secondary structures severely affect probe accessibility and binding,[295] which may compromise imaging sensitivity. Additionally, accurate RNA counting within large, intracellular aggregates, such as transcription sites or RNA−protein aggregates is seldom straightforward and often error-prone. Another concern pertains to RNA probing in live cells, wherein hybridization of oligonucleotides, especially a large number of them, may compete with endogenous RBP binding or regulatory RNA elements vital to RNA function or trigger antisense or RNA silencing responses that degrade the RNA. Moreover, the translation machinery and other RNA helicases may denature probe-RNA hybrids, resulting in reduced sensitivity. Probes should therefore be designed within the UTRs of RNA, specifically selecting binding sites that do not affect RNA function. Finally, the abundance of unbound probes (that cannot be washed away) can contribute to high background and false positive signal in live cells.

3.2.2. Labeling with RNA Binding Proteins. Since proteins can be easily appended with FPs, labeling RNAs using FP tagged proteins that bind them, rather than using oligonucleotide probes, is a logical extension. This method has allowed for the real-time detection of RNA localization and trafficking, and has provided valuable information on the temporal signature of gene expression in living cells, complementary to transcript counting in fixed cells.[296] As a result, it promises the possibility of investigating the entire life cycle of an RNA, from transcription, transport and translation to degradation, in a single experiment, a feat that is difficult to achieve with smFISH. The labeling strategy entails the intracellular expression of the RNA of interest as a fusion with multiple copies of an RNA motif that binds a specific protein. FP-tagged-RBP (RBP-FP) chimeras are simultaneously expressed and the binding of many copies of these fusion proteins to the RNA labels the target above background (Figure 5). Both the target RNA and the RBP, or just the RBP, are genetically engineered into plasmids that are either transiently transfected or stably integrated into the cellular genome for intracellular synthesis. The binding of multiple RBP-FPs through a repetitive RBP binding sequence (RBS) renders a single RNA molecule much brighter than a single FP molecule so that it becomes well distinguishable from unbound RBP-FP molecules and cellular autofluorescence.[233] Additionally, certain schemes favor fluorescence enhancement by confinement of individual nucleic acid bound FPs.[297] Here, the experiment is designed such that unbound RBP-FPs are highly expressed and diffuse much faster than the time resolution of image acquisition, constituting a fluorescent blur spread over the entire cell. Once RBP-FPs associate with slow moving or immobile RNAs via their cognate RBS, they are confined to the extent that acquisition time is not a limiting factor. Fluorescence from such slowly diffusing complexes supersedes that of the unbound probes and can be detected as distinct diffraction limited spots, effectively enhancing the signal-to-background ratio for single molecule detection. However, in either case unbound RBP-FPs still contribute significant background fluorescence, especially when overexpressed. To mitigate this issue, a nuclear localization signal (NLS) needs to be tagged to the RBP-FP gene as a means to concentrate unbound RBP-FPs in the nucleus and improve the sensitivity of (m)RNA detection in the cytoplasm.[233] Alternatively, fluorescence recovery by reconstitution of split GFP fragments can be employed.[298] Here, two distinct RBPs are fused to the nonfluorescent N-terminal and C-terminal halves of GFP. Binding of both RBPs to their respective, adjacently located RBS's brings the two fragments in close proximity to promote association, resulting in a fluorescent protein. In this fashion, unbound and singularly bound RBP probes are effectively rendered nonfluorescent. To robustly label the RNA, it is essential that the RBP binds the RBS with great specificity and affinity (preferably with a K_D of <10 nM), and that fluorescence recovery from the assembled fragments is reasonably efficient.

One archetypical high-affinity protein−RNA tethering system, pioneered by Singer and co-workers, consists of the MS2 coat protein (MCP) and matching MCP binding sequence (MBS, Figure 5A).[233] Derived from the MS2 bacteriophage (or its closely related R17 bacteriophage), the MCP is an ∼13.7 kDa regulatory RBP that readily dimerizes in solution, whereas the MBS is an ∼21 nt RNA fragment that spontaneously adopts a stem-loop structure.[299] Other viral protein−RNA tethering systems that have been derivatized for tagging RNA with FPs include a system derived from the PP7 bacteriophage, an evolutionary cousin of the MS2 bacteriophage, which infects *P. aeruginosa*.[300,301] As in the MS2 system, two copies of the PP7 coat protein (PCP) bind one copy of the stem-loop structure of the PP7 RNA binding site (PBS) with high affinity (K_D = ∼1 nM).[300] Despite the functional similarity, the PCP bears only ∼15% sequence identity to the MCP and the PBS differs from the MBS in both size and nucleotide composition. This feature results in orthogonality between the PP7 and MS2 systems, i.e., the PCP does not recognize the MBS and vice versa.[300] Another orthogonal system comprises the λ_N peptide, which spans ∼22 amino acid (aa), and its corresponding ∼15-nt long RNA binding motif, box B,[299,302,303] derived from lambda bacteriophage (Figure 5B). In the virus, the λ_N protein (12.2 kDa and 107 aa), which contains the λ_N peptide at its N-terminus, binds box B stem-loop motifs in a 1:1 stoichiometry and with equal specificity and affinity (K_D = ∼1.5 nM) as the full-length version.[299] These three orthogonal protein−RNA tethering systems provide the opportunity to simultaneously image up to three different mRNAs[303] or probe three discrete segments of a single mRNA. Furthermore, they have evolved in nature to minimize nonspecific interactions with other proteins or RNAs so that

dx.doi.org/10.1021/cr400496q | *Chem. Rev.* 2014, 114, 3224−3265

they can be expected to serve as "inert" tags for probing the intracellular localization and dynamics of target RNAs.

In its earliest manifestation, 24 copies (24×) of the viral RBS were appended to an RNA, resulting in the binding of up to 48 molecules of FP labeled RBPs,[233] although versions that utilize lower[304] or significantly higher[305,306] number of RBS repeats have also been reported. mRNA labeling via these large appendages is typically achieved by incorporating the RBS into the 5′- or 3′-UTR such that the tag does not affect the transcript's translation or UTR-mediated regulation.[233] Nevertheless, control experiments need to be performed to test whether a tagged RNA retains its biological function. Additional control experiments should be performed to verify that individual intracellular fluorescent particles represent single RNA molecules.[233,307] To this end, Singer and co-workers used a combination of FP titration and cross-validation by smFISH.[233,307] The FP titration aided calibration curve was constructed similar to that discussed in section 3.2.1, with purified FPs replacing fluorophore labeled oligonucleotides. This measurement was complemented with smFISH, performed on the same set of RBP-FP expressing cells, to exclude the possibility that clusters of suboptimally labeled mRNAs were misidentified as single mRNAs. Colocalization of smFISH probes with FP labeled particles and calibrations curves that identified the number of oligonucleotide probes bound per RNA (as also described in section 3.2.1) further supported the FP titration data.

Both the MS2 and PP7 systems have been well characterized, yet similar characterizations of the λ_N:boxB pair have so far been lacking. Notably, such characterizations have shed light on surprising anomalies and led to the development of improved MCP and PCP probes.[308] Anomalies included incomplete and heterogeneous occupancy of MBS by MCP,[233,307,308] i.e., the observations that only a subset of the 24 or so MBS is bound by FP tagged MCPs and that MBS or PBS tagged mRNAs were not uniformly labeled across different cells or sometimes within the same cell. Especially the latter undermines the ability of this labeling method to quantify gene expression at single molecule sensitivity. For instance, a single RNA-containing particle that is half as bright as another owing to nonuniform labeling may be scored as harboring half the number of RNA molecules even though the two are stoichiometrically identical. These limitations were attributed to the expression-level dependent dimerization of MCP or PCP.[308] At low RBP abundance, dimerization as a prerequisite to RBS binding is compromised and results in incomplete RBS occupancy. As the RBP expression increases, the extent of dimerization and hence occupancy increases, but saturates based on the number of RBS repeats and concomitantly increases background fluorescence from unbound RBP-FPs. In an alternative strategy, Singer and co-workers created tandem dimers of MCP (tdMCP) or PCP (tdPCP) conjugated to an FP, wherein two copies of the RBP are engineered in tandem with a flexible linker in the middle.[308] This scheme promotes concentration independent intramolecular dimerization, thus effectively resolving issues of expression level mediated nonuniform labeling. While maximum occupancy is achieved with the PCP-PBS system (∼48 copies of the PCP or 24 copies of tdPCP bound to 24× PBS), the MCP-MBS pair always shows substoichiometric labeling (only ∼26 MCPs or 13 tdMCPs associated with 24× MBS), for reasons still unknown.[308]

Regardless of their widespread use and efficacy, the protein−RNA tether labeling strategies discussed so far are only useful to probe genetically engineered constructs. Recently, two groups independently developed distinct methods capable of labeling both engineered and endogenous RNAs with single molecule sensitivity.[213,268,309,310] Both methods exploit the binding of fluorophore labeled RBPs to specific RNA sequences, rather than structured motifs. In the first technique, Ozawa and co-workers[213,309,310] utilized the RNA binding properties of PUMILIO, a protein that mediates eukaryotic posttranscriptional gene regulation (Figure 5C).[311] This protein binds RNA via the Pumilio homology domain (PUM-HD), which contains an array of eight modular elements that specifically recognize the RNA sequence UGUANAUA[312,313] (where N is any nucleotide), also termed PumBS. As each module recognizes a single RNA base,[312] the binding specificity of PUM-HD can be altered by simply changing the base recognizing amino acid residues within each element such that it matches a specific sequence within an RNA of interest. Notably, just a single base mutation within the first half of the consensus sequence results in an ∼100- to 3000-fold loss in affinity for the wild-type PUM-HD that can be rescued by appropriate PUM-HD mutants.[312,313] This modular RNA binding feature was exploited to create FP labeled tandem PUM-HD probes, wherein each engineered PUM-HD recognizes a distinct, yet closely located sequence within an endogenous target[213,309,310] (Figure 5C). This tandem binding approach utilizes two different 8-nt PumBS's located adjacent to each other and can theoretically distinguish one among 4^{16} ($\sim 4.3 \times 10^9$) transcripts, unique enough to identify a specific target RNA within a single cell. In one version, endogenous mitochondrial ND6[309] or β-actin mRNA[314] were visualized by the split-GFP approach. Here, the two mutants of PUM-HD (mPUM1 and mPUM2) were fused to the nonfluorescent N-terminal and C-terminal segments of GFP, respectively; binding of both PUM-HDs to their respective PumBS reconstituted GFP. A variant of this strategy was employed to image β-actin mRNA,[213] in which a single RBP-FP fusion was constructed by bridging GFP between two PUM-HDs. In contrast to the split-GFP approach, this version necessitates the construction and intracellular delivery of only one RBP-FP probe (as opposed to two) and overcomes limitations of slow GFP reconstitution. The loss of the background reduction through the split GFP, however, had to be compensated by targeting unbound RBP-FP to the nucleus, and imaging sensitivity was further improved by fluorescence enhancement via confinement. Both versions of this technique utilize tags that are significantly smaller than viral protein-RNA tethering systems, a preferable trait, and can use single-step photobleaching of FPs to confirm detection of single RNAs. The system, however, suffers from diminished fluorescence enhancement and short observation windows, as the RNA is labeled with just one fluorescent RBP that binds its cognate RBS only for a limited amount of time. Disappearance of signal in a single step, often assumed to be photobleaching, can also occur by dissociation of the RBP from the RBS or from the abrupt diffusion of the RNA out of the focal plane. Additional limitations are related to the "metastability" of the reconstituted GFP, wherein the reconstructed probe persists beyond the dissociation or degradation of the RNA that nucleated assembly of the split GFP, often leading to false-positive signal.

The second endogenous RNA probing technique exploits the binding of hrp36, an hnRNPA1-like protein found in *C. tetani*, to hrp36 binding sites in BR2 mRNA (Figure 5D, shown is a general labeling scheme).[268,315] Although the hrp36 binding

dx.doi.org/10.1021/cr400496q | *Chem. Rev.* 2014, 114, 3224−3265

site is found in other mRNAs, its copy number in BR2 mRNA is significantly higher. Thus, at any given moment a larger number of hrp36 molecules bind BR2 mRNA than any other mRNA, allowing for selective fluorescence enhancement.[268,315] In these studies, organic dye labeled hrp36 was used instead of FP for three reasons: (i) It was difficult to genetically manipulate primary cells extracted from *C. tetans* salivary glands; (ii) overexpression of FP labeled hrp36 was expected to result in high background of hrp36 free or bound to other mRNAs; and (iii) intracellular delivery and density of labeled hrp36 could be controlled by microinjection. Orthogonal in its approach, multiple repeats of the hrp36 binding site can be tethered to any exogenous RNA, although the system has limited application in probing other endogenous mRNAs. Additional protein−RNA tethering system labeling approaches include the use of PABP,[316] two split eIF4A domains,[317] and MCP-zipcode binding protein (ZBP),[318] none of which have yet been utilized for intracellular SMM.

Although a majority of these FP-based labeling schemes has the foremost advantage of genetic tractability, they suffer from a few drawbacks. First, the relatively high molecular weight of protein−RNA tethering systems limits their application to large RNAs. mRNAs in particular are bound by endogenous RBPs and the translation machinery, and therefore exist as bulky messenger ribonucleoprotein complexes (mRNPs); thus, the molecular weight of large mRNAs does not appreciably change upon introduction of a few tethered RBPs, but these can adversely affect the mobility of smaller mRNAs. Second, the inclusion of the NLS to the RBP-FPs may affect the labeled RNA's function and localization by increasing the propensity of NLS-RBP-FP bound cytoplasmic RNAs to localize within the nucleus. Third, the presence of unbound RBP-FPs in the cytoplasm, mediated by their overexpression and/or their limited binding affinity and resulting significant dissociation from the target RNA, results in significant background noise the removal of which often requires image processing algorithms such as deconvolution.[233] Fourth, single molecule counting is not straightforward and entails the painstaking construction of fluorescence calibration curves,[233,307] as well as requires the implementation of other complementary methods like FISH.[233,307] Fifth, nonuniformity of labeling further confounds counting (discussed above), but strategies to overcome this issue are slowly emerging.[308] Sixth, RBPs, especially PumHDs, are not strictly specific to their corresponding RBS and can generate spurious signal by nonspecifically binding to other RNAs. Nonetheless, the reliability of these well-standardized labeling schemes is evidenced by the availability of general methods to tag and image any mRNA with the MCP-MBS system in both lower eukaryotes, such as yeast,[304] and complex mammals like mice.[226] The transgenic mouse model[226] in particular allows for probing the intracellular distribution of any mRNA over different cell types, tissues, and even whole animals.

Another approach to overcome some of the drawbacks of FPs is to reduce the protein in size to its chromophore and bind it to a specifically in vitro selected aptamer incorporated into the target RNA. Early versions of this approach used malachite green as the fluorophore with an aptamer that modulates the dye conformation and increases its fluorescence.[319,320] A more recent incarnation of the approach uses a GFP-derived group of fluorophores bound by an RNA aptamer termed "spinach" that again enhances their fluorescence.[321,322] Because of their relatively low binding affinity and rapid exchange with free dye, the GFP-derived chromophores appear to photobleach only slowly,[321] but whether such comparably weak binding of small-molecule fluorophores will allow for single molecule detection of spinach-tagged RNA remains to be seen.

3.2.3. Direct Labeling of RNA. The direct, covalent coupling of fluorescent probes, typically organic dyes, to an RNA of interest can be achieved by several chemical and enzymatic methods[234−237,323−330] (Figure 6). Generally, small RNAs (<100 nt) are chemically synthesized to contain fluorophore labels or reactive functional groups, which in turn are conjugated to fluorophores (Figure 6A), at predefined positions. Larger RNAs are either labeled at random positions using modified NTPs during transcription or specifically labeled, mostly at the 5′- or 3′-end or internally through ligation, by chemical or enzymatic modification (Figure 6B). Even here, modified NTPs directly coupled to fluorophores or containing reactive functional groups can be used; however, the larger size of the former may inhibit labeling.[331] In any case, two critical steps in this labeling strategy are the removal of free dye from the sample and separation of labeled from unlabeled RNA. As the molecular weight of the free dye is much smaller than that of the RNA, the first purification step is easily and efficiently achieved by, for example, ultrafiltration, gel filtration, or gel electrophoresis. Size cannot be used, however, for the second purification step, as the difference in molecular weight between labeled and unlabeled RNA is often negligible. Small RNAs are efficiently purified by reversed-phase HPLC since labeled RNAs are more hydrophobic than their unlabeled counterparts;[328] however, this difference becomes less for large RNAs. The ligation of unique sequences to large RNAs can aid purification of the product via beads coupled to complementary hybridization probes, whereas other enzymatic reactions require thorough and time-consuming standardization to achieve high labeling efficiencies.[237] Moreover, the incorporation of modified NTPs during transcription results in a heterogeneous population of labeled RNAs, with both varying location and number of modifications. Nevertheless, nonspecific RNA labeling via transcription[332] or alkylating agents[333] has been used to incorporate multiple fluorophores within individual RNA molecules as a fluorescence enhancement strategy.

Although intracellular delivery of directly labeled RNA has challenges, it also offers three main advantages over other labeling strategies. First, RNA counting by stochastic photobleaching of fluorophores, wherein the stepwise reduction in intensity of labeled particles is a proxy of molecular count, is more accurate and straightforward.[135,334,335] Other methods require calibration curves and read out the intensity with little ability to consider the broad distribution of intensity fluorophores typically exhibit.[336] Second, this method does not require any elaborate probe design or attachment of significant RNA extensions, only that fluorophores are appropriately positioned to not affect RNA function. Finally, particularly small ncRNAs such as siRNAs and miRNAs, which cannot be probed via conventional hybridization or protein−RNA tethering strategies, can be directly labeled and visualized in both live and fixed cells at single molecule resolution.[135]

3.3. Intracellular Delivery of Fluorophore Labeled RNA

The choice of labeling strategy directly influences that of the intracellular delivery method. For instance, a majority of protein-RNA tether labeling strategies largely employ chemical transfection[213,233,308−310] or viral transduction.[226,307,308,337]

dx.doi.org/10.1021/cr400496q | *Chem. Rev.* 2014, 114, 3224−3265

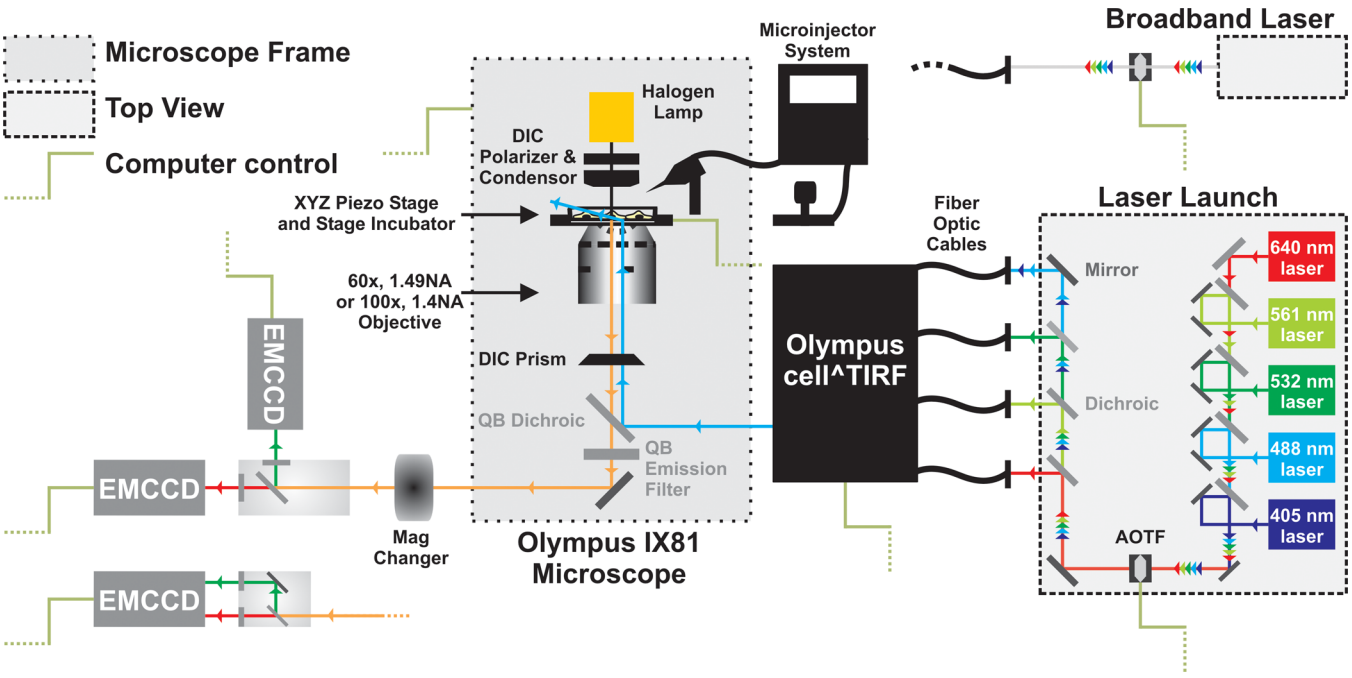

Figure 7. Schematic of our home-built single molecule microscope. Our Olympus IX81 microscope is equipped with two high NA, 60×, and 10×, oil-immersion objectives. The microscope also has low NA, 10×, and 20×, objectives. It features an internal 1.6× magnification and is additionally equipped with a 1−4× magnification changer (Olympus). Thus, a maximum magnification of 740× (100 × 1.6 × 4) can be achieved. Samples are positioned on a nanometer-precision piezo-controlled stage. The microscope also contains an infrared laser based zero-drift control module (Olympus) to correct for focal drift. Solid state lasers with wavelengths of 405, 488, 532 and 640 nm are directed through an acousto-optical tunable filter (AOTF) and split into separate fiber-optic cables within a laser launch system. The AOTF allows for computer-guided selection of the appropriate laser wavelength for illumination and modulation of laser intensity. AOTF coupling also enables submillisecond switching between multiple laser wavelengths, forming the basis for alternating or interlaced excitation schemes. Alternatively, a broadband supercontinuum laser capable of emitting multiple wavelengths of excitation light in a pulsed fashion (ns to ps) can replace the multilaser system. The fiber-coupled laser beams are directed into a cell-TIRF laser-combining module (Olympus). All laser beams are focused on the back-focal plane of the objective and aligned to travel parallel to the optical axis such that the incident angle of illumination at the dish-medium interface can be controlled electronically by changing the distance of the beam from the optical axis at ~0.01° angular resolution using the cell-TIRF module. Fluorescence from the sample is detected typically via an EMCCD. For multicolor imaging, the emitted light is split onto two different detectors using a single beamsplitter or onto two regions of the same detector. The former strategy can be used even with a point detector such as an APD or PMT, whereas the latter requires a large detector area and can be implemented only with a CCD. Appropriate mirrors, filters and dichroic beamsplitters are used to guide and spectrally filter the light source and emitted light. QB, Quadband. Cells grown on dishes (Bioptechs) are maintained at 37 °C on the microscope stage while imaging using a stage incubator. The micromanipulator of a microinjection system (Eppendorf Femtojet) is attached to the microscope for intracellular probe delivery.

Plasmids encoding both the RBP and RBS are transiently expressed or stably integrated into the cellular genome using either of these delivery methods. Numerous transfection reagents are available in various chemical formulations, cationic lipids, polyethyleneimine, DEAE dextran, calcium phosphate and cationic or neutral dendrimers to name a few, and serve to neutralize the innately negatively charged DNA (or RNA), which allows for the efficient uptake of the resulting self-assembled particles through negatively charged cell membranes, presumably via endocytosis. As transfection reagent-plasmid complexes are heterogeneous in size and distribution, each cell receives a different amount of the plasmid (or RNA). Thus, transient transfection leads to heterogeneous (over)expression of both the RBP and RBS, a major obstacle for uniform RNA labeling.[308] Creation of stably transfected cell lines may mitigate nonuniform expression. Transduction with a lenti- or adenovirus that harbors only a single copy of the DNA offers better control over intracellular delivery but is often a laborious process. Furthermore, direct synchronization of experiments using any of these methods is difficult because self-assembly, endocytosis, exit from endocytosed vesicles, migration into the nucleus, and subsequent gene expression each take significant amounts of time that have a wide distribution across cells. In addition to these steps, viral transduction also requires virus production, which further adds to the time prior to RNA visualization. However, the presence of inducible expression systems [see refs 225, 269, 270, 303, 304, 317, and 338−340] for plasmids can aid in defining a more precise experimental start time, albeit often accompanied by a basal level of "leaky" expression.

RNAs labeled via other strategies are predominantly delivered by physical force [see refs 133−135, 268−270, 293, 315, 333, and 341−345] or via cell membrane permeabilization [see refs 217, 225, 226, 267, 270, 272, 273, 278, 282, 292, 294, 303, 307, 337, 340, and 346−348]. The former includes electroporation and microinjection, whereas the latter utilizes pore forming peptides or detergents and organic solvents that partially dissolve the cell membrane. More specifically, pore forming peptides function by reversible permeabilization,[217,294,346,347] making them popular for intracellular SMM of hybridization-labeled RNA in live cells. SLO is a classic example of a pore forming peptide, which is produced by gram-positive bacteria as a cytolytic toxin.[349] The addition of SLO, typically under serum free conditions, results in its binding to

dx.doi.org/10.1021/cr400496q | Chem. Rev. 2014, 114, 3224−3265

cholesterol on the cell membrane and subsequent oligomerization to form pores of ∼25−30 nm diameter that permits the influx of hybridization probes or directly labeled RNA.[350] Once the SLO containing medium is removed and replaced with fresh growth medium, SLO dissociates and the membrane reseals. However, based on a cell type's cholesterol composition, the incubation temperature, time, cell number, and SLO concentration needs to be optimized and, as is the case for transfection, nonuniform delivery of probe and/or RNA across the cell population is commonplace, and SLO cannot per se be used for intranuclear delivery. Permeabilization of the cell membrane by detergents (Triton-X100, NP40, deoxycholate, etc.) or organic solvents (acetone, ethanol, and methanol) is irreversible and is only used to mediate the delivery of hybridization probes into fixed cells.

In contrast to membrane permeabilization methods, delivery methods employing physical force are amenable for the intracellular delivery of both plasmids and RNA without any additives and are often the method of choice in hard-to-transfect cells. Among them, microinjection offers maximal control over delivered amount and flexibility in experimental design, especially for RNA that is directly labeled.[135,343,345] The process is conceptually simple and uses a micromanipulator, which can traverse distances as low as ∼10 nm, and an injector pump. First, injection samples are filled into glass capillaries whose openings are typically ∼0.5−1 μm wide, small enough not to puncture cells. Microinjection is then achieved via three precisely timed steps that occur within 1 s: (i) assisted by the micromanipulator the capillary pierces the cell, (ii) the pump applies a preset pressure (∼10−150 hPa) to the capillary that allows for sample ejection, and (iii) the capillary is removed from the cell. In this fashion, cells are sequentially and uniformly microinjected with a few femtoliters of RNA solution, and controlled delivery is achieved by modulating the sample concentration and injection pressure. Furthermore, the ability to inject RNA selectively into either the cytosol or nucleus provides for the opportunity to evaluate RNA function in distinct cellular compartments and to study nucleocytoplasmic transport processes.[351] Disadvantages of this technique include the requirement for expensive instrumentation and its applicability only to relatively large cell types (i.e., not bacteria), and that only a limited number of cells can be manipulated in a given time period. However, the latter has the advantage that different RNA types or concentrations, as necessary for titrating and measuring reaction kinetics, can be injected into small, spatially separated groups of cells, maximizing experimental throughput within a single culture dish. Compared to SLO and transfection mediated intracellular delivery that take ∼30 min and >6 h, respectively, fluorophore labeled RNA can be visualized immediately after microinjection, allowing for precise temporal control. Additionally, transfection often leads to the entrapment of probes within endocytic vesicles and their degradation via the endosomal/lysosomal pathway.[158] Emerging alternatives employ CPPs,[294,352] such as HIV-Tat, that are transported across the cell membrane via cell surface receptors. Here, RNA is directly tagged with the CPP and the addition of this fusion molecule to cell culture medium results in close to quantitative intracellular delivery.

3.4. Instrumentation

As with any ultrasensitive technique, intracellular SMM requires sophisticated instrumentation. However, the availability of a plethora of fluorescence enhancement strategies has made it possible to visualize single bright RNA molecules even with simple microscopes. In addition to the labeling strategy, the choice of excitation source, optics, illumination scheme and detector contribute toward single molecule sensitivity. In the following we provide a broad overview of available instrumentation options and, in Figure 7, describe a typical single molecule fluorescence microscope.

3.4.1. Light Source. Lamps were initially popular light sources in both ensemble and single molecule microscopy. Due to their polychromatic light, a single lamp could be used to excite distinctly colored fluorophores by spectrally refining the excitation light with relatively inexpensive narrow-bandwidth filters. However, inefficient filtering is typical and leads to the leakage of other excitation light colors that either spuriously excites the sample or adds to the noise of the detector and severely compromises sensitivity. Additionally, most of these arc-based lamps suffer from limited lifetime and nonuniform illumination intensity over their spectral range of operation. Since lasers emit monochromatic, coherent and collimated light, they now have effectively replaced lamps as the primary light source in intracellular SMM. To minimize phototoxicity, especially during live cell imaging, and to reduce photobleaching, lasers operating at 1 μW to 100 mW power, with a power density (i.e., the light flux or number of photons per unit area) of 1 W/cm^2 to 100 kW/cm^2 is typical in intracellular SMM applications.[353,354] The choice of illumination wavelength depends on the spectral properties of the fluorescent probe, but typically spans the visible part of the electromagnetic spectrum (∼400−700 nm) because transmission properties of available optics are best in the visible range and the best-documented fluorophores emit within this regime. Imaging at wavelengths greater than ∼500 nm is preferred to overcome cellular autofluorescence and to increase sample penetration depth via reduced scattering so that far-red and near-infrared (NIR) probes and lasers are slowly gaining popularity. Ultraviolet (UV) light is not suitable for imaging living cells as it induces DNA damage and apoptosis.[355]

3.4.2. Optics. At the heart of a microscope lies the objective lens. It transmits light from the illumination source and collects (fluorescent) light from the sample to create a focused image on the detector. Two important parameters, the numerical aperture (NA), an indirect measure of photon collection ability, and the magnification together define objectives. High NA (1.25−1.65) and optimal magnification (60−150×) are preferred to collect as many photons as possible, especially under the low light conditions of single molecule experiments. Notably, a further increase in magnification without a corresponding increase in the brightness of the light source reduces the number of photons collected per unit square area of the detector, thoroughly compromising the visibility of single molecules. A good objective additionally minimizes chromatic aberrations (distortions in an image caused by differential focusing of different wavelengths of light). Thus, achromat or apochromat versions of objectives are mandatory for multicolor imaging. Downstream of the objective lens are other optical elements that mediate spectral selection/filtering, important aspects of intracellular SMM and multicolor imaging. These include dichroic beamsplitters and emission filters, whose choice is based on the spectral characteristics of the light source and the fluorescent probe. The former is oriented at an angle of 45° with respect to the illumination or emission light to spectrally separate them, typically reflecting the light source and transmitting fluorescence from the sample (in which case it is

dx.doi.org/10.1021/cr400496q | Chem. Rev. 2014, 114, 3224−3265

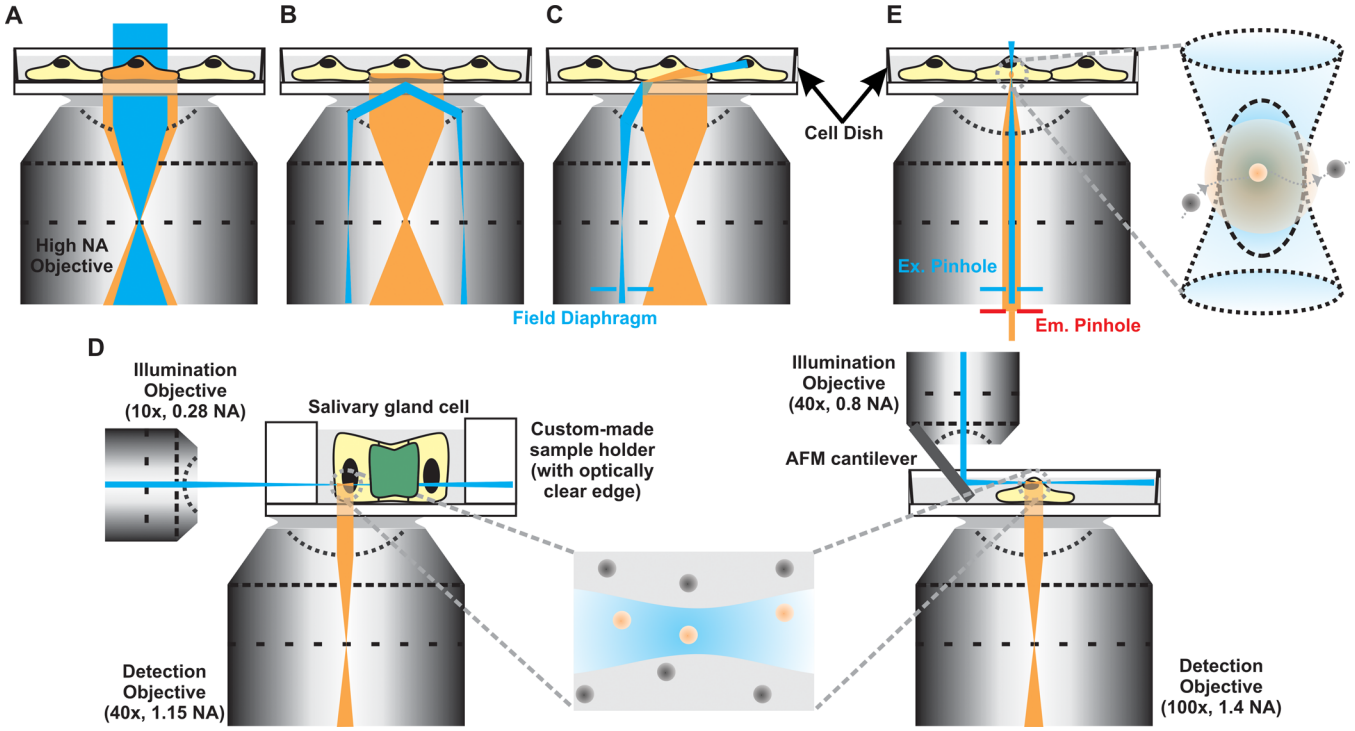

Figure 8. Various types of illumination geometries. (A) Wide-field, (B) TIRF, (C) HILO/VAEM with a field diaphragm to reduce illumination light diameter, and (D) SPI with LSFM (left) and RLSM (right) with a magnified view of the illumination plane. Although the geometry is similar for the two approaches, the dimensions of the illumination plane are very different. (E) Standard narrow-field illumination, with an enlargement of the illumination spot. Pinholes for the excitation (Ex.) light and emitted (Em.) light are used to reduce excitation volume and decrease background from out-of-focus fluorescence, respectively.

called as a long-pass dichroic). This property is also used in multicolor imaging to separate colors above and below the dichroic's wavelength cutoff. Emission filters placed further downstream are oriented orthogonal to the incoming light to selectively transmit only the fluorescent light and effectively block other stray radiation, including a significant amount of excitation light that leaks past the dichroic.

Although the basic optical elements (objective, other focusing lenses, beamsplitters, filters, etc.) suffice for intracellular SMM of RNA over the lateral (x,y) plane of the sample, 3-dimensional (3D) motion inherent to all biomolecules including RNA is not captured. To extract such axial (z) information, certain optical accessories, such as astigmatic lenses can be used. First introduced by Kao and Verkman,[356] and later modified by Zhuang and co-workers,[357] the method uses a cylindrical lens in the optical path to adjudicate axial localization based on the intensity profile of the sample under investigation; particles in focus have evenly distributed radial intensity profiles whereas particles just above or below the focal plane have elliptical/ellipsoidal intensity profiles elongated along different major axes. Recently, Moerner and co-workers used the combination of achromatic lenses and a spatial light modulator in a so-called 4f imaging system to extract 3D diffusional information of mRNPs in yeast[358,359] at 25 nm lateral and 50 nm axial accuracy. In this case, the PSF of each single molecule is bilobed, whose relative position varies with the particle's axial position, essentially carving out the backbone of a DNA double helix through the axial movement of the particle; hence the eponym double helical PSF (DH-PSF). Other accessories such as a defocusing lens[360] and wedge prisms[361] have also been used to resolve 3D diffusion of particles and hold promise in 3D SPT of RNA.

3.4.3. Illumination Geometry. In intracellular SMM, far-field illumination geometries are typically used, wherein the distance between the objective lens and sample is at least an order of magnitude greater than the wavelength of illumination light (Figure 8). There are primarily two types of far-field illumination: wide-field (WF) and narrow-field (NF) illumination. The main difference between the two types of illumination geometry arises in the sample area (the field of view, or FoV) they excite: >100 μm^2 of the sample is illuminated in WF illumination, whereas it is <1 μm^2 in NF illumination. Examples of WF illumination include epi-, total internal reflection (TIR), highly inclined and laminated optical sheet (HILO, also termed near-TIR), and various other forms of selective plane illumination (SPI), whereas examples of NF illumination include confocal and single point edge excitation subdiffraction (SPEED) schemes (Figure 8).

Simplest to implement, WF epi-illumination (Figure 8A) is widely used in intracellular SMM of RNA, largely due to several fluorescence enhancement strategies that render single RNA molecules significantly brighter than the cellular background. However, excitation light passes through the entire depth of the sample and out-of-focus fluorescent molecules contribute toward significant background noise, limiting the method to samples with molecules sparsely distributed over all three spatial dimensions. In contrast, only a thin lamina of ~150 nm at the sample surface is illuminated using TIR fluorescence microscopy (TIRF, Figure 8B), effectively reducing background fluorescence from outside regions.[362] This scheme is based on Snell's law, wherein light that is transmitted through a medium of higher refractive index (n_i; e.g., coverglass) into one of lower refractive index (n_r; e.g., water), is totally reflected within the first medium at incident angles (θ_i) greater than the critical

dx.doi.org/10.1021/cr400496q | Chem. Rev. 2014, 114, 3224−3265

angle given by $\theta_c = \sin^{-1}(n_r/n_i)$. Because of the wave properties of light, TIR creates a thin lamina of "evanescent" wave within the aqueous phase, only exciting molecules that are within ~150 nm of the coverglass-sample interface. TIR is rarely used in intracellular SMM of RNA because it only excites the basal plasma membrane and ~100 nm of the adjacent cytoplasm, whereas most RNAs are present also throughout the cell and in cellular compartments (such as the nucleus) that the evanescent wave cannot penetrate. To achieve greater penetration into the sample without significantly compromising the signal-to-noise ratio, HILO microscopy (HILO, Figure 8C), also termed variable angle epi-fluorescence microscopy (VAEM) or near-TIR fluorescence microscopy (near-TIRF), was developed.[363,364] Here, $\theta_i < \theta_c$ so that the light is refracted into the sample at high inclination from the optical axis, thus illuminating an angled layer within the sample and reducing illumination of molecules not in focus. A field diaphragm that maintains the laminar width of the beam controls the width of this illuminated layer within the sample. The excitation beam path for epi-illumination, through-objective (or objective-type) TIRF and HILO are so similar that a single microscope can be used to implement all three schemes (Figure 7).

Several alternative SPI methods have been developed to further increase the penetration depth of illumination and restrict sample excitation to the focal plane, such that single molecules can be visualized within tissues or even whole organs, a realm that is not accessible to WF-epi, TIRF or HILO. One such advancement is called light sheet based fluorescence microscopy (LSFM, Figure 8D).[268,315,365−367] In its most recent embodiment,[315] the method uses two perpendicular objectives, one with low NA (~0.3) and the other with higher NA (>1) for illumination and detection, respectively. Such a configuration allowed focusing the illumination light as an ~3 μm thick elliptical sheet, which can be moved across the z-axis of the specimen for optical sectioning. Depth of imaging is only limited by the working distance of the detection objective. A possible alternative to LSFM is reflected light sheet microscopy (RLSM, Figure 8D).[354] In this method a small disposable mirror, such as an aluminum coated tipless AFM cantilever, is attached at an angle of ~45° to a high (0.8) NA illumination objective, positioned to face the detection objective with a slight lateral offset. The mirror reflects the light sheet from the illumination objective by 90° and projects it horizontally across the sample, thus attaining optical sectioning capabilities. The upright geometry allowed for imaging samples mounted on standard sample holders and results in a light sheet thickness of ~1 μm (fwhm). However, the positioning of the mirror and the shape of the light sheet introduce a gap between the surface and light sheet that cannot be illuminated. The RLSM illumination geometry holds promise for optical sectioning of thick specimens, but so far has been primarily used to image cultured cells.[354]

A majority of NF illumination schemes aims to increase spatial resolution by physically reducing the focal volume to a small, typically ellipsoidal or spherical, spot rather than a large plane (Figure 8E). In this fashion, only a few molecules are excited within this small volume element, typically ~500 nm wide and ~1 μm deep. Conventional confocal microscopes are augmented by more sophisticated optical configurations, such as spot-scanning 4Pi microscopy (4PiM)[368] and other reversible saturable optical fluorescence transitions (RESOLFT) techniques,[369] which achieve significantly higher spatial resolution by further reducing the illumination volume by at least an order of magnitude. Unlike WF illumination, throughput is minimal with NF illumination; that is, the sample is illuminated only one volume element at a time and has to be scanned, but NF illumination has advantages of superior spatial (axial) resolution. Modifications to the standard confocal setup, such as the spinning-disc or Nipkow-disc confocal microscopy,[370] significantly improve scanning rates and throughput by simultaneously illuminating distinct regions of the sample. Recently, Ma and Yang[371] increased the FoV of NF illumination by incorporating oblique angle illumination (projected onto the sample at an angle of 45° with respect to the optical axis) and an ~400 μm wide pinhole in the excitation path within a standard WF microscope, in what they termed SPEED microscopy. This modification results in an inclined ellipsoid excitation volume, tilted at an angle of 45° with respect to the optical axis, that selectively illuminates ~320 nm of the sample in all three dimensions, leading to ~6-fold larger lateral FoV and ~3-fold smaller axial FoV than standard confocal microscopy. By restricting the acquisition area on an EMCCD camera, the time resolution of acquisition was improved to ~1 ms,[371] which is ~20- to 100-fold better than standard WF imaging using the entire CCD chip.

3.4.4. Detectors. Illumination geometry dictates the choice of detector. Intensified charged coupled devices (ICCDs) or electron multiplying CCDs (EMCCDs), which feature a relatively large detection area (~8 × 8 mm^2), are the detectors of choice in WF illumination. For NF illumination, where photons are collected from only a small region of the entire sample, point detectors like avalanche photodiodes (APDs) or photomultiplier tubes (PMTs) are used. Almost unlimited in time resolution, APDs and PMTs are sensitive enough to detect and accurately count single photons in the submillisecond regime, showcasing the superior sensitivity and better time resolution of NF imaging (with the caveats of low throughput and the need for scanning a larger sample). Although current CCDs also have photon counting capabilities, they still suffer from limited time resolution (millisecond time regime) and spectral range of detection. The complementary metal oxide semiconductor (CMOS) is an emerging technology that promises faster acquisition rates for WF imaging, but suffers from lower quantum efficiency (the ratio of detected photons over total photons that reach the detector) than CCDs.

3.4.5. Specialized Illumination Schemes. Once a specific illumination geometry is chosen, several illumination schemes can be employed to enhance sensitivity and spatiotemporal resolution. For instance, alternating excitation (ALEX) schemes[372] have been routinely used in multicolor imaging to spectrally and temporally separate photon acquisition from multiple fluorophores by sequential imaging. Other multicolor acquisition schemes rely on spatially separating fluorescence signals from distinct fluorophores onto different regions of the same detector or onto multiple detectors, adding to the cost of instrumentation, whereas ALEX is useful in multicolor imaging on a single detector. ALEX is especially useful in reducing background associated with simultaneous multicolor illumination and in fluorescence resonance energy transfer (FRET) applications to confirm the presence of both the donor and acceptor fluorophores through the course of image acquisition. Another illumination scheme, termed stroboscopic illumination,[220,373] can be employed to detect rapidly moving single particles that typically look blurry under slow CCD frame rates. Here, high-powered laser pulses, much shorter than the camera integration time, are used to briefly excite the sample. During

dx.doi.org/10.1021/cr400496q | Chem. Rev. 2014, 114, 3224−3265

this excitation period, single particles do not move over large distances and appear as distinct PSFs. In this fashion, the temporal resolution of acquisition is controlled by the duration of the pulse, however, at the cost of very high laser intensity that may be phototoxic to cells. The method also relies on relatively slow moving particles distributed at a very low density, such that it is easy to track the position of a single particle over time despite the pulse train's dark periods and the presence of other proximal particles, which can obscure particle identity. Finally, when photoactivatable or photoconvertible probes are used, tandem excitation schemes of photoactivation followed by sample excitation can be used to execute stochastic optical reconstruction microscopy (STORM) or photoactivation localization microscopy (PALM) and attain ∼10 nm-scale spatial resolution, even within densely populated samples.[212,219]

3.5. Single Molecule Observables

A single intracellular SMM experiment allows the user to monitor a multitude of observables, each of which provides information about the molecule under study and its immediate surroundings.[212] Experiments are typically performed on one of two distinct sample types, live cells or fixed cells, where each provides mutually complementary information. Among the two, live-cell intracellular SMM or SPT experiments shed light on the dynamic aspects of cellular function, such as the mobility of individual molecules and the extent of interaction between multiple distinct sets of molecules. Although fluorescence recovery after photobleaching (FRAP)[374] and fluorescence correlation spectroscopy (FCS)[133,134,344,375] have been traditionally used to extract such dynamic information, they only measure ensemble-averaged properties and probe a small subcellular section at any given time, frequently missing variations in molecular motion that occur over the entirety of the cell. SPT microscopy by WF illumination overcomes this caveat by accounting for almost all fluorophore labeled molecules within a cell in a sequence of images (or video). Individual particles are localized in each frame of the video at nanometer-scale accuracy and this position is linked between frames to construct particle trajectories. Several well-established methods are available to execute both of these steps[205,376−379] whose choice is dependent on the signal-to-noise ratio for the former and the ratio of particle density to interframe displacement for the latter. Mobility of RNA is then expressed in the form of velocity and a 1D, 2D, or 3D diffusion coefficient (the average spatial unit a molecule traverses per unit time given any constraints on its movement). Particle velocity and displacement are physical properties that provide valuable insight into the processivity and overall directionality of motion, which are important, for example, in the characterization of motor protein-mediated RNA transport.[380] Diffusion coefficients encode information about the molecular mass of the mRNPs or the nature of its surrounding milieu, in terms of subcellular viscosity and the presence of potential interaction partners.[381,382] Furthermore, the diffusive pattern (Brownian, biased, corralled, or stationary) can be used to predict the role of motor proteins or the nature and amount of obstacles in the path of a diffusing molecule.[233] For instance, prolonged observation and analytical methods like velocity autocorrelation[359] have shown that the diffusive pattern of a single RNP often varies even within an individual trajectory,[233,359] highlighting the different intracellular interactions a molecule experiences through its lifetime. More specific interactions are revealed by simultaneous tracking and colocalization dwell times of molecules that are labeled with spectrally distinct fluorophores[307,347] in two-color imaging schemes. Concordant motion adds another layer of confidence to traditional colocalization studies that often obfuscates noninteracting particles bearing similar x,y coordinates but distinct z positions with physical association (complex formation). The protein−RNA,[233,307] hybridization by molecular beacons[269] or MTRIPs,[217,346,347] and direct labeling systems[135] have all been used in SPT of RNA in living cells; however, the protein−RNA tethering systems are particularly popular among cell biologists because of their arguably easier and gentler conditions for delivering probes, which may better preserve cell integrity.

Subcellular localization and counting of individual mRNA molecules yields single cell gene expression data and thus has revolutionized our understanding of cellular homeostasis and the effects of deviations from it.[21,135,383−385] Stoichiometry measurements by stepwise photobleaching, which assess the number of molecules within individual, not further resolved fluorescent particles, increase the accuracy of counting and are useful in discerning the ubiquitous assembly/disassembly of molecular complexes[135,334] and in functionally annotating subcellular localizations.[282,347] However, the abrupt change in intensity by the diffusion of particles out of the focal plane in conventional 2D imaging confounds single molecule counting and stoichiometry measurements in live cells. FCS is useful in such cases, wherein the diffusion of molecules through a well-calibrated focal volume results in intensity bursts whose frequency is used to measure intracellular concentration. This method, however, has the inherent disadvantage of having to assume a homogeneous distribution of the molecule throughout the cell or, conversely, requires the slow, sequential probing of different regions within the cell to correct for heterogeneity. Molecule counting and stoichiometry analysis are more reliable in fixed cells, where particles are easily tractable and spatially confined. A majority of single molecule counting experiments of RNAs, especially mRNAs, has been achieved by smFISH. 3D image stacks of probe-treated cells are acquired and individual particles are detected by image processing steps that include image enhancement and intensity thresholding.[267,283] Gaussian fitting,[205] deblurring by deconvolution,[217,266,275] and image convolution by high-pass filtering,[267,280] such as a Laplacian of Gaussian (LoG) filter, are a few image enhancement strategies that have been applied to particle detection via smFISH. Molecular stoichiometry in fixed cells can be measured either by particle counting in smFISH images or by stochastic photobleaching of fluorophores.[135,334] The latter is more effective when single RNA molecules are labeled with relatively few fluorophores, typically achieved by direct labeling schemes. Photobleaching of RNPs decorated with a large number of fluorophores, as in the case for most protein−RNA tethering and hybridization labeling schemes, yields nondiscernible and frequently overlapping photobleaching steps that yield incorrect molecular count.[335] In such cases, calibration curves are constructed by imaging (free) fluorescent probes[266,275] at various concentrations, from which the intensity of a single probe is extrapolated. The number of probe repeats per RNA is considered in calculating the approximate intensity of a single RNA molecule, which is then used to compute the molecular copy number within individual particles. Alternatively, the mean intensity value of smFISH-detected particles is used as a measure of molecular count.[267,283] Although stoichiometries extracted from these curves are often either error-prone or

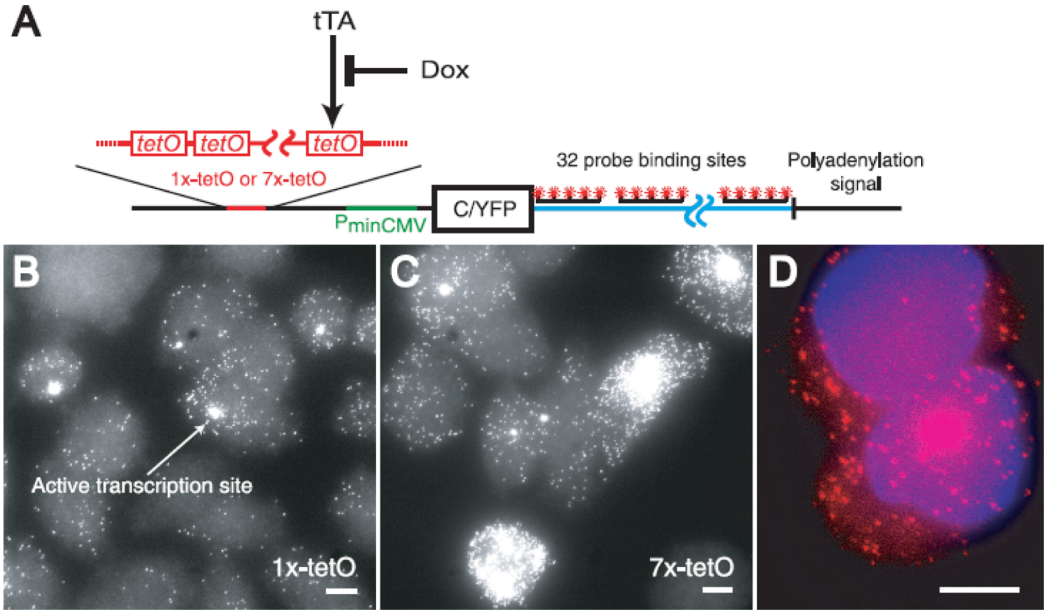

Figure 9. Transcriptional bursting measured by smFISH in mammalian cells. (A) Schematic of the doxycycline controlled yellow fluorescent protein gene containing 32x smFISH probe binding sites in the transcript's 3′-UTR used in this study. (B and C) Representative images of cells with active or inactive transcription sites. (D) A representative image of two sister cells with variable mRNA localization. The upper cell displays primarily cytoplasmic localization of mRNA (shown in red), while the bottom cell displays both nuclear (stained blue with DAPI) and cytoplasmic mRNA distributions. The scale bar represents 5 μm. Reprinted with permission from ref 400. Copyright 2006 Public Library of Science.

approximate, they are useful in observing trends. Overall, both live and fixed cell imaging are powerful in discerning the spatiotemporal organization of intracellular RNAs.

In the next section, specific recent examples of characterizing the biological function of RNAs and the mechanisms of their biogenesis, transport, regulation and turnover through single molecule observation are presented.

4. RECENT APPLICATIONS OF SINGLE MOLECULE APPROACHES TO RNA IN CELLULO

Earlier in this review, RNA was introduced in its various forms as a highly versatile molecule, coding for proteins, serving as structural scaffold, performing enzymatic functions, and regulating gene expression. To perform such widespread functions, RNA production, maturation, interactions, and spatial distributions require tight regulation, which in turn is the foundation of cellular homeostasis and survival. Intuitively, the bulk properties observed of such processes and others are potentially the sum of all single molecule events. For example, ensemble experiments have convincingly shown that a significant fraction of β-actin mRNA localizes to the leading edge of a cell,[260,386] while a majority of transcripts still seems to be spread throughout the cytoplasm. Yet only with the aid of intracellular SMM it could be resolved that their diffuse cytoplasmic distribution is a cumulative result of individual transcripts either remaining stationary or undergoing (i) Brownian diffusion, (ii) corralled motions and (iii) active transport.[233,346] It was additionally found that transcripts are not in a constant diffusive state but rather switch between multiple modes of movement.[233] Despite the fact that only ∼9−20% of all transcripts exhibit biased motion, interrupting active transport significantly alters intracellular distribution and almost abolishes localization at the leading edge.[233,260,346,386] Thus, intracellular SMM has been indispensable for understanding mechanisms of cellular RNA localization and the underlying kinetic parameters controlling them. To fully appreciate these findings, this section will detail the results of select studies performed over the last 15 years and how they have contributed to our understanding of cellular biology. By necessity, this selection will be incomplete, due to the rapid and accelerating progress in intracellular single molecule fluorescence studies of RNA.

4.1. Stochasticity of Transcription

Gene expression is canonically, and minimally, perceived to result from the transcription of genetic information into mRNAs (i.e., mRNA synthesis), followed by transcript decoding and protein synthesis (translation).[387,388] The intracellular copy number of a given mRNA is quite low (∼1−500 copies is typical),[389] yet each mRNA molecule can be translated tens to hundreds of times. Thus, small fluctuations in mRNA production or degradation will potentially result in large changes in protein concentration[257,390,391] and potentially alter the cellular phenotype.[392−395] As transcriptional fluctuations are ubiquitous,[21,395] it is critical to understand the causes and impacts of such bursts with special attention to perturbation of gene regulation programs. A variety of single molecule techniques have been applied over the years to probe the extent of transcription variability and its impact on gene expression. Below is a comprehensive discussion of their findings.

In first approximation, a stochastic model of gene expression can be assumed to follow a Poisson process,[396] wherein the synthesis and degradation of transcripts occur at random, but the probability of transcript production is time-invariant; that is, the rate of transcript production is constant. Consequently, the mean expression level of the transcript for a single cell and all cells in a clonal population should coincide with the distribution's variance, or the Fano factor (variance/mean) should equal unity. Conversely, describing gene expression patterns using Poisson distributions assumes that they are completely random. Deviations of the Fano factor from unity

dx.doi.org/10.1021/cr400496q | Chem. Rev. 2014, 114, 3224−3265

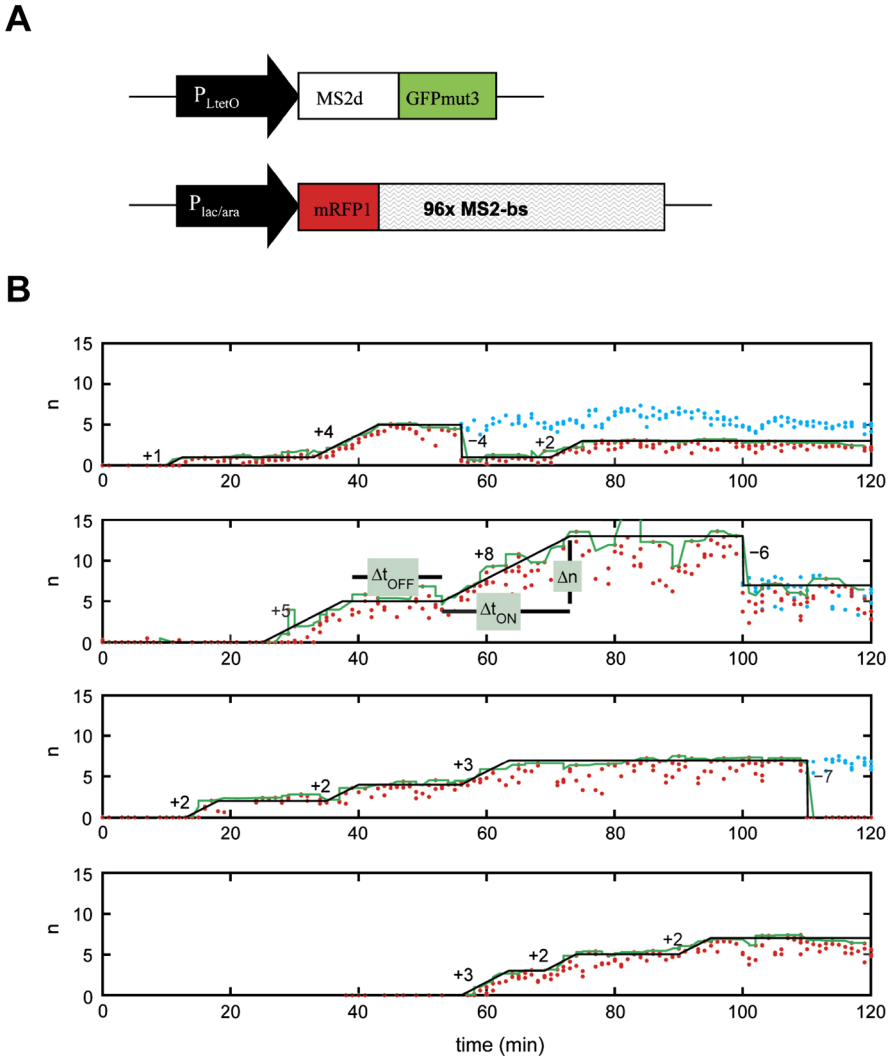

Figure 10. Transcriptional bursting as measured by mRNAs bound by MCP-GFP in individual *E. coli* cells. (A) Schematic of MCP-GFP and mRFP constructs with 96xMS2 binding sites used in this study. (B) Plots from four cells depicting typical estimated numbers of transcripts (n) as a function of time. Red dots indicate raw data, the green line represents smoothed fit, and the black line depicts a linear function that shows periods of transcriptional activity and inactivity. Cyan dots represent the number of transcripts in the daughter cell after cell division. The numbers represent the change in the number of transcripts. Reprinted with permission from ref 306. Copyright 2005 Elsevier.

entail either transcriptional bursting (super-Poissonian or Fano factor >1) or synchronized and homogeneous transcript production over the cell population (sub-Poissonian or Fano factor <1), implying highly regulated transcription.[267,397]

Transcriptional bursting is a term that is used to describe genes that are synthesized discontinuously, typically with a temporally varying rate of transcript synthesis.[398,399] Tyagi and co-workers used smFISH to count individual transcripts and determine that the mean cellular production of an inducible exogenous mRNA in mammalian cells is significantly less than the variance, indicating super-Poissonian trends[400] or bursting. They determined that the extent of intercellular gene variability is not heavily weighted on transcription initiation events, as genes bearing multiple promoter sites failed to alter the noisiness in mRNA number. Additionally, modeling the distributions of transcriptional states, cellular locations of single molecule mRNA (nuclear, cytoplasmic, or both), and number of mRNAs produced within the assayed time period for a colony of cells lent additional evidence to transcriptional bursting (Figure 9).[400] Transcription was found to be intrinsically random and dependent on single gene activation and deactivation processes, as transcription factor concentrations have little impact on the extent of randomness. Furthermore, genes within a similar DNA locus have synergistic bursting kinetics, unlike instances where they are located within dissimilar loci. One can argue that smFISH only provides a snapshot of events within a fixed cell that cannot account for the temporally changing contributions of mRNA degradation, cell division, and RNA aggregates on the calculated super-Poissonian trends. In a complementary line of experiments, Golding et al. used the MS2 labeling system to detect transcriptional behaviors in live *E. coli* cells.[306] Despite the change in techniques and species, transcriptional bursting was equally seen within single cells, whereby RNA is created by pulses of transcription that are interspersed by longer periods of inactivity (Figure 10).[306] Unlike in mammalian cells, the randomness of bacterial transcription appears dependent on extrinsic factors, such as transcription factor or inducer abundance.[306,401] Recently, Golding and co-workers used smFISH to probe the transcription of another artificial mRNA construct mRNA when driven by one of 20 different promoter sequences in *E. coli* and unveiled a correlation

dx.doi.org/10.1021/cr400496q | *Chem. Rev.* 2014, 114, 3224−3265

between promoter activity and increased "burstiness" during transcription.[340] Their work suggests that only the duration of gene activity dictates the oscillatory behavior of transcription, regardless of the stimulus that initiates transcription or the specific promoter sequence controlling it. These and other data suggest that bursting results from topological DNA changes, RNA polymerase dynamics, or some effects of broad-target DNA binding proteins.[287,402,403] Transcriptional bursting has also been demonstrated using single molecule techniques in social amoeba,[404] humans,[291,403,405] and yeast.[278]

Contrary to the work by Golding and co-workers, Muthukrishnan et al. demonstrated that select genes in *E. coli* exhibit sub-Poissonian behavior.[401] While they too used the MS2 labeling system, these authors elected to monitor gene transcription at the active site, rather than counting mRNA numbers. This group relied on the monotonic increase in signal of the MCP-FP once it is bound to the MBS at the transcription site, so that a stepwise increase in signal (per unit time) reflects the appearance of a novel transcript. This increase persists until the eventual release of the RNA from the transcription site, at which point the relatively low time resolution of data acquisition blurs the signal from fast moving transcripts. Plotting the various lag times between transcriptional events for these mRNA resulted in a Fano factor <1, or sub-Poissonian behavior, which was further corroborated by the low intercellular mRNA variability. Based on these results, the authors argued that transcription cannot be dictated solely by the randomness of binding and release of transcription factors from the DNA surface. Similar observations were made in an earlier study by Kandhavelu et al.[406]

Not all mRNA production is dependent on an external stimulus or the stage of the cell cycle, as some mRNAs are constitutively expressed. For constitutively transcribed genes in yeast cells, specifically housekeeping genes, the variance in intercellular protein expression is remarkably small,[407] despite the low transcript numbers. Zenklusen et al.[278] concluded that these low variances are related to production of translated mRNA molecules. Intracellular mRNA copy number, as detected by smFISH, is best fit with a Poisson distribution, which along with computational modeling suggests that the transcription of constitutively expressed genes is dependent on the probability of forming the transcription initiation complex.[278] The authors discuss these effects as contributed by transcription initiation events that are digitally "separated in time" instead of "bursts".[278]

Thus far, we have discussed the variability that surrounds gene transcription in a cell culture context. However, cell culture conditions of bacterial or immortalized mammalian cells might not represent those that transpire in tissue or primary eukaryotic cells. For example, in aggregative slime mold development, each endogenous gene exhibits its own unique transcriptional profile, with increased RNA production correlating with increased 'bursting' behavior.[402] It was further found that transcriptional variability is minimized for transcripts produced in low quantities and for proteins that require tight regulation. Similar effects were observed in developing *C. elegans* embryos, where intestinal specification during the initial stages of organogenesis is initiated by various environmental cues that induce the transcription of select developmental genes.[283] These genes then initiate a signal cascade that instigates heterochronic gene expression and exhibits sub-Poissonian transcription properties enabling their tight regulation in the cell.[280] To understand the effects of "bursting" on nonbursting genes, the authors introduced a mutation into an upstream developmental gene that resulted in highly variable mRNA expression profiles of the remaining downstream genes.[283] Increasing variability in the transcription of these genes results in a defective intestinal tract. Such strict developmental control is also observed during the induction of pluripotent stem cells.[408]

The possibility that stochastic transcription may be associated with chromosome structure spurred Levesque and Raj to adopt a spectral barcoding approach that simultaneously visualizes transcript production and relative chromosomal localization.[292] Using the iceFISH method, the authors simultaneously visualized 20 different transcripts spread over individual chromosomes. They found that genes on the t(13:19) chromosome of HeLa cells were up to 5-fold more active than those on chromosome 19. Although a majority of genes within a given chromosome were transcribed independently, one specific pair of transcripts had anticorrelated expression, even if several megabases apart on the chromosome. Moreover, such an effect was not found on the other allele, suggesting that the effect is mediated by cis- and not trans-acting elements.

These single molecule experiments have demonstrated that transcription is controlled by a wide variety of mechanisms that can vary in a gene- and species-dependent manner. The sensitivity associated with intracellular SMM has revealed that transcription can produce RNA in a highly controlled fashion with low variability (sub-Poisson),[306,401,406,409] in a completely random fashion (Poisson),[278,340,402] or in a highly fluctuating, burst-like fashion (super-Poisson).[278,291,306,400,404] Based on these data, a great deal of effort is currently focused on modeling the transcription process as a predictive tool for gene expression.[410−413] However, more work in this field is necessary to tease out mechanistic details that control the fate of gene production and the variability surrounding it.

4.2. Transcription Inhibition and Silencing by Long ncRNA

Cell survival, maintenance and self-destruction are all dependent on the well-timed transcription of select genes and the silencing of others. To keep the activity of RNA transcribing polymerase molecules in check, the cell has adopted numerous mechanisms for the short- or long-term silencing of select genes. Important regulators and, at times, targets of such silencing activities are lncRNAs.[414,415] smFISH studies have demonstrated that lncRNAs have the ability to inhibit transcription of proximal or overlapping genes in cis, at the site of synthesis,[416,417] and in trans, distal to site of synthesis,[188,416,418] such as the silencing mediated by *Xist* lncRNA that inactivates one of the two X chromosomes in female mammals.

In yeast, many genes give rise to antisense transcripts. Some of these transcripts are stable, while others, termed cryptic unstable transcripts (CUTs), are rapidly degraded by the nuclear exosome.[419] For example, PHO84 AS is an antisense transcript that is involved in the transcriptional silencing of the protein coding gene PHO84 from the same genomic locus and was hypothesized to accumulate at the locus to sustain repression.[420] Contradicting this hypothesis, Castelnuovo et al. found using smFISH[421] that PHO84 AS is always weakly expressed in wild-type yeast cells, and in fact, a majority of transcripts are localized in the cytoplasm. The latter observation suggested that the antisense transcript essentially behaves like a protein coding mRNA as it is transcribed, polyadenylated, and

transported to the cytoplasm. However, the expression modes of the sense and antisense transcripts were found to be distinct, with the sense RNA abundantly transcribed in bursts and the antisense synthesized constantly at very low numbers. Although PHO84 and PHO84 AS were expressed within a clonal population of cells, individual cells seldom coexpressed both, an observation often masked in ensemble experiments. Put together, the authors hypothesized that regulation occurs via a switch-like mechanism instead of one where the slow accumulation of one silences the other RNA. Moreover, low expression of the antisense transcript is sufficient for silencing and ensures that sense expression is only activated in the presence of a stronger opposing signal.

4.3. Splicing of Pre-mRNA

Nuclear speckles are membraneless protein aggregates that are enriched in pre-mRNA splicing factors and are located in the interchromatin region of the nucleoplasm.[47] Their specific function is still debated as they are not always found near sites of active transcription, but they have been shown to contain pre-mRNAs and thus presumably are sites of post-transcriptional splicing.[46] Co-transcriptional splicing is thought to be advantageous as it ensures the fidelity of exon-intron recognition in the RNA molecule before it is released into the nucleoplasm. However, during alternative splicing, post-transcriptional splicing is arguably more important as the complete synthesis of all exons and introns provides greater options for exon selection. To test the frequency of co- and post-transcriptional splicing, Vargas et al. performed smFISH and molecular beacon-mediated live cell imaging of a set of GFP reporter genes, bearing 12 distinct arrays of intronic oligonucleotide binding sites.[270] The 3′-UTR or GFP coding sequence (CDS) was simultaneously labeled to annotate spliced and unspliced transcripts − fluorescent spots only containing signal for the 3′-UTR (or GFP CDS) were considered spliced, whereas those that showed colocalization with the intronic array signal were annotated as unspliced transcripts. Using this system, the authors found that the nucleoplasmic distribution of pre-mRNAs varied based on the identity of their intronic array, wherein pre-mRNAs with accessible spicing recognition sites were found almost exclusively at the transcription site (TS), while ones with recognition sites obscured by RNA secondary structure were found diffusely distributed throughout the nucleoplasm. The latter type of pre-mRNA was observed to interact with, but not enter, speckle sites as marked by immunofluorescence.[270] Secondary structure analysis predicted that the post-transcriptional splicing phenotype was well correlated with the accessibility of particularly the intron's polypyrimidine tract. Burying this tract in introns known to splice near the TS within strong secondary structure predictably recapitulated the distal splicing phenotype and thus the uncoupling of transcription and splicing.[270]

Recently, real-time imaging of cotranscriptional splicing has been used to characterize the kinetics of intron excision in live cells.[422] In this report, single-molecule sensitivity was achieved using protein−RNA tethering systems. This study revealed the rate of transcription by RNA Pol II (3−6 kb min^{-1}) is the rate-limiting step in splicing, thus providing mechanistic insight into genetic regulation.

Most mRNAs within the human genome are known to undergo alternative splicing[36,37] to generate protein isoforms in the various tissues of an organism. Vargas et al. suggested that the relative abundances of alternative splicing factors dictate the relative quantities of transcript isoforms.[270] Waks et al. set out to use smFISH to probe the extent of isoform heterogeneity of a clonal population for noncancerous and cancerous cells.[423] Using bioinformatics approaches, they found CAPRIN1 and MKNK2 to each express two isoforms that differ in either their terminal exon sequence or their 3′-end length. By designing smFISH probes that bind sequences unique to each isoform, the authors were able to use a two-color approach to quantify the copy number of each isoform. MKNK2 pre-mRNA is located near the TS and is thought to be spliced constitutively, whereas as an alternatively spliced pre-mRNA CAPRIN1 is found distal from the TS. In noncancerous Rpe1 cells, mRNA isoform ratios varied as minimally as could be expected given the stochastic nature of transcription, whereas HeLa cells demonstrated significantly more cell-to-cell variability in the isoform ratios in a manner driven by alternative splicing factor activity. Taken together, these data suggest that the splicing pathway has acquired control mechanisms to reduce isoform fluctuations in noncancerous cells.[423]

4.4. Nuclear Diffusion of RNA

Regardless of the relative distances between the transcription and pre-mRNA processing sites, RNA must eventually traverse the nucleoplasm to reach the nuclear envelope for exportation. Active transcription sites are not always located at peripheral regions of the nucleus, but can occur in chromatin dense regions.[424,425] Transcribed RNA molecules in these regions traverse chromatin free tracks towards the nuclear envelope,[426] sparking the hypothesis that RNA may be actively transported via motor proteins along the nucleoskeleton as a more efficient means of RNA delivery to processing centers and the NPC. An electron microscopy study was the first to demonstrate that BR mRNAs in *C. tentans* salivary glands are randomly distributed throughout the nucleoplasmic space, suggesting that they move primarily via simple diffusion and not active transport.[427] Siebrasse et al. labeled and tracked the movements of single BR mRNA molecules, labeled with fluorophore-conjugated DNA or 2′-*O*-methyl-RNA oligonucleotides, or with recombinant fluorescent hrp36 (an hnRNP protein), in living *C. tentans* salivary gland cells[268] to corroborate the EM findings. Mean square displacement (MSD) analyses of the SPT data demonstrated deviations from linearity, and thus from Brownian diffusion behavior, with increased lag time, suggesting corralled motions.[268,428] This behavior is potentially mediated by the binding of BR transcripts to cellular factors or by general crowding effects that occur in the dense milieu of the nucleus. Nucleoplasmic diffusion coefficients of BR mRNA were significantly slower than those of similarly sized dextran molecules (D = 2.2 $\mu m^2/s$). These data coupled with Monte Carlo simulations suggested that BR mRNA may be slowed as the result of a series of transient interactions with nuclear components. These results effectively strengthened claims from prior ensemble microscopy experiments performed in chromatin bearing mammalian cells, where mobility of mRNPs was found to involve passive diffusion and ATP-dependent processes.[316,429]

Shav-Tal et al. employed the MCP-MBS labeling system to selectively label stably integrated and inducible exogenous genes in mammalian cells and, using SPT, studied a significant part of their lifecycle, from transcription to nuclear export.[430] Labeled RNA diffused throughout the nucleoplasm avoiding regions occupied by large nuclear structures (chromatin,

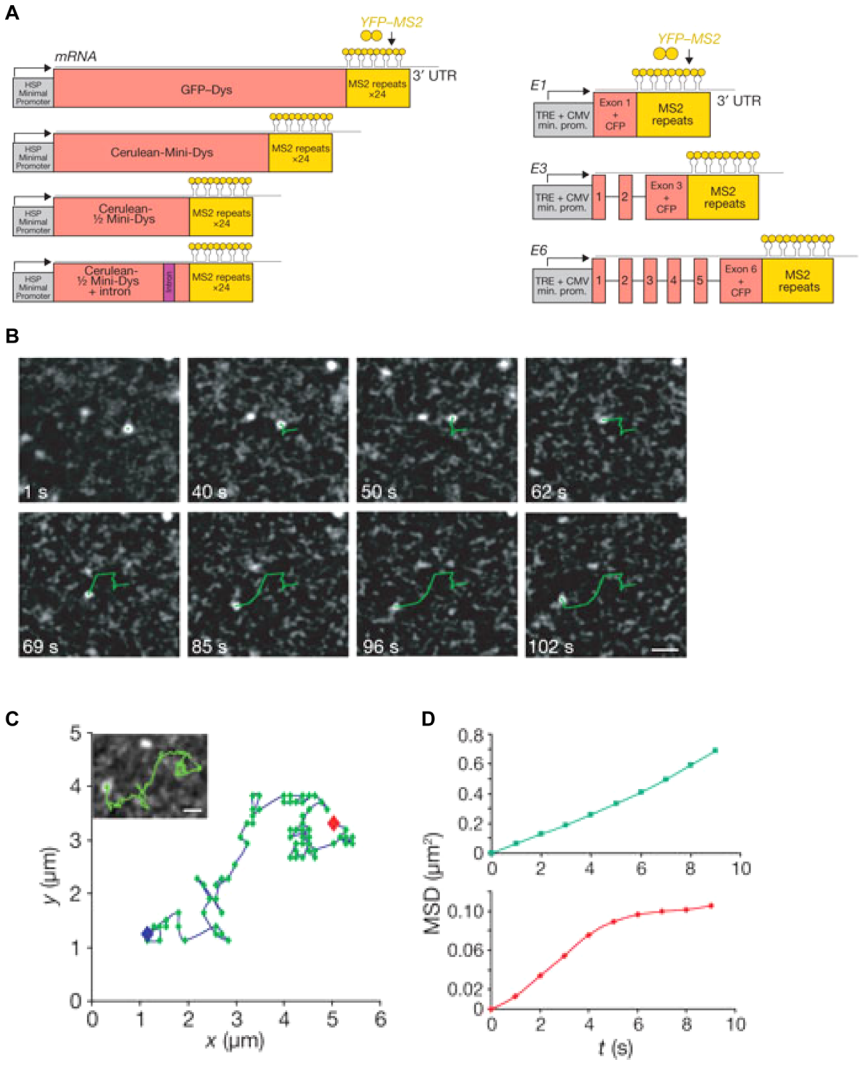

Figure 11. Single particle tracking of mRNPs in mammalian cells. (A) Schematic of the mRNA constructs with 24× MS2 binding sites used in this study. Nuclear diffusion data for each construct are summarized in Table 2. (B) Deconvolved time-series images of nuclear Cerulean-1/2 mini-Dys + intron mRNP diffusing in the nucleoplasm (green tracks). (C) Complete track of the nuclear Cerulean-1/2 mini-Dys + intron mRNP. (D) MSD analysis of single nuclear mRNPs displaying Brownian (green) or corralled (red) motions in the nucleoplasm. Corralled motions deviate from linearity at longer lag times. Scale bar represents 1 μm. Reprinted with permission from ref 225. Copyright 2010 Nature Publishing Group.

nucleolus, etc.), with 58% of the tracks Brownian in nature and 42% exhibiting corralled motion (Figure 11).[225,430] Motions were most confined or immobile when in close proximity to the TS.[269,430] Outside the transcription site, RNA molecules were not observed to stall or stop, implying that they do not make stable interactions with subnuclear compartments. Under hyper-osmolar conditions, corralled motions of mRNPs were enhanced due to the entrapment of transcripts within dense DNA regions and their sequestration into speckle domains, a process that is reversible upon returning the cells to isotonic conditions. Vargas et al. obtained similar results with temperature reduction or ATP depletion,[269] strongly suggesting a (perhaps indirect) role for DNA dynamics in modulating RNP diffusion.

The diffusion coefficients of MCP-MBS labeled mRNPs are much smaller than those reported in ensemble mRNA experiments.[428,242] To test if this effect is due to particle size or transient RNP interaction with other proteins, Mor et al. designed seven constructs of increasing size or bearing the same size but different numbers of introns (Table 2).[225] 2D and 3D SPT of these transcripts showed trends of diffusion coefficients decreasing with RNA size, eventually reaching a saturation point for the three largest mRNAs tested (Table 2). Cytoplasmic diffusion coefficients of the smaller transcripts correlated well with their nuclear diffusion coefficients; however, the larger transcripts diffused more slowly in the

Table 2. Nuclear Diffusion Characteristics of RNAs of Varying Length[a]

gene name	mRNA length (kb)	diffusion (μm^2/s)	percent corralled	percent Brownian
Full-Dys	14	0.005	60%	40%
Mini-Dys	8	0.005	75%	25%
1/2-mini-Dys	4.8	0.005	50%	50%
1/2-mini-Dys + 1 intron	4.8	0.004	45%	55%
E1	1.7	0.009	NA	NA
E3	2.1	0.010	NA	NA
E6	2.3	0.023	NA	NA

[a]Data taken from ref 225.

dx.doi.org/10.1021/cr400496q | Chem. Rev. 2014, 114, 3224−3265

nucleoplasm. 3D tracking of mRNPs in cells with Hoechst 33342-stained DNA suggested that the larger RNAs exhibit more corralled motions in the narrow interchromatin spaces than the smaller RNA, contributing to their small diffusion coefficients. Thus, the three largest mRNAs have equal nuclear diffusion coefficients but divergent, faster cytoplasmic diffusion coefficients simply due to the strong (and nondiscriminating) sieving effects of the comparably narrow interchromatin channels they traverse in the nucleus.[225]

Labeling of particles with spectrally distinct fluorophores facilitates colocalization and cotracking during the assembly of biomolecular complexes. A two-color approach was used to study the interaction of snRNPs with nuclear speckles, in an effort to understand the interaction of splicing factors with these largely elusive nuclear foci. To this end, Grunwald et al. microinjected nonspecifically labeled U1 snRNP-Cy5 conjugates into the cytoplasm of HeLa cells expressing ASF/SF2-GFP, a protein that concentrates in nuclear speckles.[343] Upon nuclear import, the snRNPs distributed into three subpopulations: immobile (77.5%), slowly diffusing (15%, with average diffusion coefficients of 0.51 ± 0.05 $\mu m^2/s$), and fast diffusing (7.3%, with 8.2 ± 3 $\mu m^2/s$). Interestingly, not all immobile snRNPs were observed to colocalize with fluorescent markers of nuclear speckles[343] where splicing occurs and most spliceosomal snRNPs are thought to reside. Notably, snRNPs that colocalized with speckles remained so over periods ranging from milliseconds to seconds, with a double-exponential time distribution, suggesting that their binding mechanisms are complex.[343] In another study, it was observed that spliceosomal components are not stored in nuclear speckles, but rather splicing proteins are found diffusing throughout the nucleus and collide randomly and transiently with pre-mRNAs.[431]

4.5. Nuclear Export of RNA

The nuclear pore complex, or NPC, is a large protein complex that creates, in first approximation, size-limited perforations on the nuclear envelope to mediate nucleocytoplasmic transport. NPC dependent transport is the primary pathway to deliver RNAs into the cytoplasm. The rate and mechanism of these transport processes are critical to understanding spatiotemporal regulation of gene expression. Due to the stochasticity and rapidity of RNA transport across the NPC, intracellular SMM is an ideal tool to probe its kinetics and mechanism.

As discussed, RNA transcribed in the nucleus traverses chromatin-free channels for the vectorial diffusion to select regions of the nuclear envelope. Regardless of the position of the transcription site or the channel, however, RNA is uniformly distributed throughout the nucleoplasm. Therefore, it seems unlikely that transcribed RNA is automatically targeted for export through the NPC. Supporting this notion, several groups have observed that the anchoring of mRNPs to NPCs does not necessitate transport and that a single mRNP can interact multiple times with a single or multiple NPCs prior to transport (Figure 12).[88,225,307] Additionally, the extent of transport, derived by transcript counting in the nuclear and cytoplasmic compartments over time, also depends on the presence of introns, thereby alluding to a splicing mediated binding of appropriate nuclear export factors.[88,225]

mRNP transport through the NPC is more rapid than nucleoplasmic diffusion (Figure 12A).[427] The distribution of translocation times for β-actin mRNP particles across the NPC is, however, very wide, stretching from milliseconds to seconds and fitting a double-exponential time distribution.[307] The

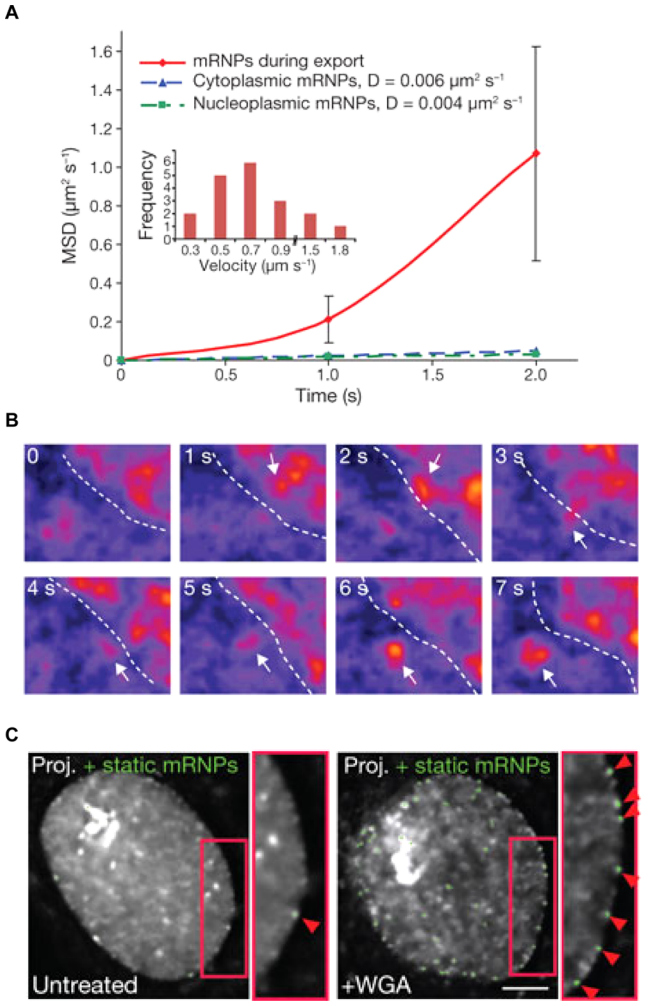

Figure 12. Nuclear export of MS2 labeled mRNA in mammalian cells. (A) MSD plot comparison of the nuclear export (red) relative to cytoplasmic (blue) and nucleoplasmic (green) diffusion. (B) Pseudocolored time-series of an mRNP (red), marked with a white arrow, during nucleocytoplasmic transport across the nuclear envelope (dotted white line). (C) Stalled (red arrows) MS2 labeled RNA (green) at the nuclear envelope before (left image) and after (right image) ATP depletion. Reprinted with permission from ref 225. Copyright 2010 Nature Publishing Group.

slowest 10% of mRNPs, predominantly resulting from direction change in the pore, exhibited monophasic transport kinetics, while the faster population exhibited biphasic kinetics, indicating two rate-limiting steps. Additionally, the slowest transported β-actin particles appeared to be positioned most centrally to the NPC, while the fastest population aligned themselves more proximal with the edges of the NPC. β-actin RNPs were also observed to stall at the nuclear and cytoplasmic sides of the NPC but not in the channel. Depleting cellular ATP levels did not affect binding of β-actin RNA with the NPC, but no fluorescent signal was discovered inside the channels, again suggesting active transport across the pore, which is possibly required to linearize the RNP to fit the pore of the NPC. Based on these data, the authors proposed a three-step mechanism for mRNP translocation across the NPC: a relatively long mRNP docking phase on the nucleoplasmic side for ~80 ms, rapid translocation through the channel within 5–20 ms, and release on the cytoplasmic side within the next ~80 ms.[307]

dx.doi.org/10.1021/cr400496q | Chem. Rev. 2014, 114, 3224–3265

One potential caveat when using the MS2 system for studying rates of nuclear export may be the loss of the (relatively weakly bound) MS2 coat protein during translocation through the NPC. Consistent with this notion, Mor et al. reported that the MS2 labeled RNA dimmed during transport, compromising the accuracy of kinetic measurements.[225] Furthermore, the addition of the MS2 stem loops and binding of MS2 coat proteins may have deleterious effects on the rates of NPC transport by adding size to the mRNP or preventing the binding of key proteins necessary for NPC interaction. However, it is known that numerous endogenous nuclear RNA binding proteins, like hrp36, will bind to transcribed mRNA in the nucleus and remain bound even during transport through the NPC. Exploiting this phenomenon, Siebrasse et al. were able to track individual BR mRNPs simply by microinjecting fluorescently labeled, recombinant hrp36, a BR mRNA binding protein, into *C. tentans* salivary gland cells.[315] Trajectories of the various moving particles displayed mRNPs that collided with the nuclear envelope and returned to the nucleoplasm (nuclear probing) or returned into the cytoplasm (cytoplasmic probing); showed active export, as well as nucleoplasmic and cytoplasmic particles binding to the NPC with no further interaction; and indicated particles that started and ended at the NPC for the duration of the observation window. Nuclear and cytoplasmic probing events, especially, were thought to be instances where collisions with the nuclear envelope or with the NPC resulted in unsuccessful docking and were the predominant phenomena in hrp36 (nuclear export protein) labeled mRNPs and Dbp5 (cytoplasmic helicase responsible for mRNA remodeling), respectively. Only 25% of all trajectories corresponded to export with time constants of 65 ± 5 ms (for 87% of that population) and 350 ± 25 ms (the remaining 13%). Taken together, the authors hypothesized that a rate-limiting step for export occurs at the nuclear basket, which may represent proper RNA orientation to penetrate the NPC.

In a recent study, SPEED microscopy[88,371] was utilized to map the 3D pathway taken by mRNPs as they traverse through the NPC of eukaryotic cells.[88] At an unprecedented spatiotemporal accuracy of 8 nm and 2 ms, the authors determined that MCP-FP labeled mRNPs decelerated at the center of the NPC during nuclear export, adopting a fast-slow-fast diffusion pattern during their brief (~12 ms) interaction with the NPC. This contrasts with an earlier report attained at a lower spatiotemporal resolution of 26 nm and 20 ms that predicted a slow-fast-slow model wherein mRNP diffusion was proposed to be attenuated at the NPC periphery.[307] Based on the faster SPEED microscopy data,[88,371] 3D reconstruction of both mRNP and small (protein) molecule export routes was possible and revealed that mRNPs primarily interact with the periphery on the nucleoplasmic side and in the center of the NPC, where they are selected for export, whereas small molecules passively diffuse via the central axial conduit. These results are consistent with a multilane traffic model wherein the transport receptor facilitated diffusion of large mRNP complexes and the passive diffusion of small molecules follow distinct paths through the NPC.[88,371,432] These observations also demonstrate how improvements in instrumentation often lead to refined biological insights.

4.6. Cytoplasmic Localization of RNA

Much like proteins, the subcellular localization of RNAs is critical to their function and regulation.[433] Localization can be diffuse, wherein RNA molecules move in a manner that allows equal sampling of the cytoplasmic space, or polarized, where the RNA is directed to and localized in or near unique subcellular features. For instance, certain neuronal mRNAs are enriched in select dendritic regions for their local and rapid production of proteins that control potentiation, a process necessary for cellular memory. These asymmetric RNA distributions were alternatively hypothesized to result from (i) continuous active transport, (ii) active transport and anchoring, (iii) diffusion and anchoring, and/or (iv) increased stability in subcellular distributions. However, it is still unclear if these processes simply occur to varying degrees or if different RNAs follow distinct localization pathways. Live cell, single molecule experiments are an ideal tool to provide answers to these questions.

The first recorded experiment utilizing the MS2 RNA labeling system was designed to probe the mechanism of mother-to-daughter (bud) Ash1p mRNA delivery and sequestration in yeast.[434] SPT of Ash1p mRNA revealed directional movements at velocities concordant with that of myosin-mediated transport (320 nm/s), strongly suggesting active transport of these mRNPs on the actin cytoskeleton. Ash1p mRNA stably resides at the bud cortex for periods of >1 min, suggesting an anchoring mechanism. It was later found that similar transport mechanisms mediate the asymmetric distribution of other yeast RNAs.[303,435] RNA transport mechanisms were found to be widespread in higher eukaryotes such as Drosophila,[436−439] *C. elegans*,[440] chicken fibroblasts,[441] and human cells.[213,345,346,442,443]

Although individual actively transported mRNPs are large and typically contain the transport and translation machinery among others, they primarily entail only single molecules of mRNA.[345,442−445] In lieu of single RNP transport, the packaging and cotransport of multiple RNPs as large granules have also been observed, in both individual cells and multicellular embryos.[303,439] In either case, RNA in route to its destination can oscillate between anterograde and retrograde transport,[436,444,446] and the extent of bidirectionality can be stimulus dependent. For instance, Rook et al. used the MS2 system to demonstrate that the dendritic localization of CaMKIIα mRNA is increased by cell depolarization.[446]

In cellulo single molecule imaging has also shed light on novel RNA transport mechanisms. Specifically, Fusco et al.[233] used the MS2 labeling strategy to demonstrate the heterogeneous and probabilistic movement of individual mRNPs in living COS cells.[233] They found that mRNPs exhibit either a multitude of diffusive behaviors (biased, corralled, and Brownian) or remain stationary and frequently switch between different diffusive patterns (Figure 13A,B), a phenomenon observed by other groups as well.[346,447] Importantly, the authors demonstrated a sequence specific bias of mRNPs toward select motion types by being able to increase the propensity for directed motion in RNPs tagged with a zipcode sequence contained in the 3′-UTR of β-actin mRNA (Figure 13C).[233] Other cytoskeleton independent RNP transport processes were also found in complex multicellular systems, wherein transport is mediated by fluid flow within the organism and localization can either be actin dependent or independent.[438,448]

4.7. Translation of mRNA

As discussed earlier, transcription can be a highly variable process that will lead to changes in cellular mRNA levels.

dx.doi.org/10.1021/cr400496q | *Chem. Rev.* 2014, 114, 3224−3265

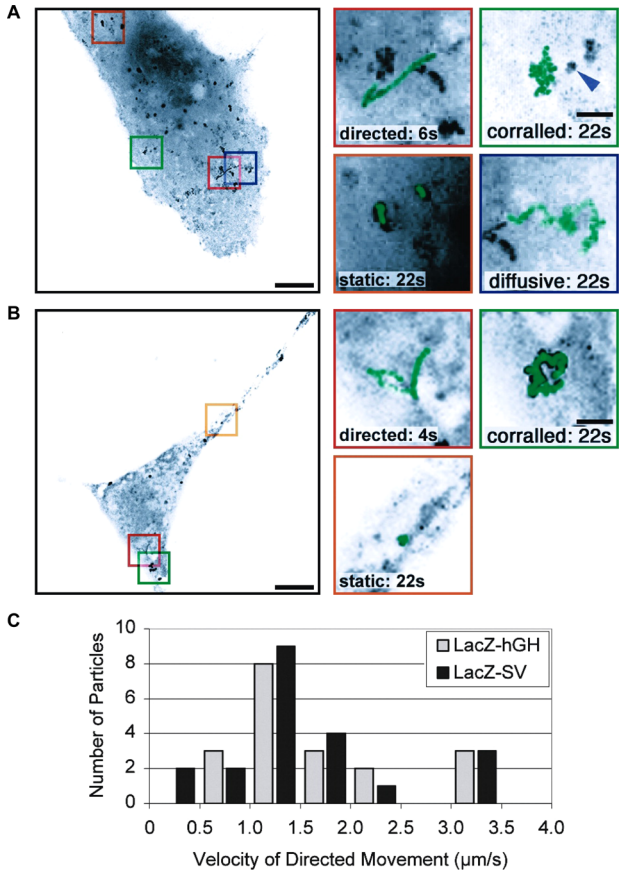

Figure 13. Cytoplasmic mRNP dynamics. (A) Movements of an MCP-FP labeled LacZ-hGH mRNA. Overlay of a 200-frame video (left image). The scale bar located in the bottom right corner represents 10 μm. Magnifications of select regions of the projection image are shown in the right images. The scale bar here represents 2 μm. Green lines represent the tracks the particles traverse. (B) Movements of an MCP-FP labeled Lacz-SV mRNA, imaged similar to panel A. (C) Distributions of LacZ-SV mRNP motions with and without a β-actin 3′-UTR. Reprinted with permission from ref 233. Copyright 2003 Elsevier.

Correlating transcript number to protein output further defines the stochastic nature of translation and its overall contribution to noise in gene expression.[399] Notably, spatiotemporally controlled, localized mRNA translation is a ubiquitous phenomenon, where proteins are synthesized at their site of activity, thus reducing the need for macromolecular transport; a prototypical example is that of actin mRNA translation at the leading edge of cells.[449] Tatavarty et al. probed the translational output of individual mRNAs in neuronal cell dendrites by taking advantage of the facts that mRNPs are typically transported within relatively slow moving granules along dendrites and that translation is primarily localized to the dendritic spine.[345] In essence, the authors had a priori knowledge of the location of translation and could visualize both the mRNA and translated protein at the temporal resolution of their microscope. To this end, they nonspecifically labeled the mRNA coding for the Venus FP with Cy5 by incorporating Cy5-UTP during in vitro transcription and microinjected the labeled mRNA into the perikaryon of cultured hippocampal cells. They used an appropriate concentration of labeled RNA such that a single granule had at most a single RNA. Correlating mRNA signal with that of translated Venus FP presented evidence for Poissonian (sporadic) or super-Poissonian (bursting) translation, where bursting was hypothesized to result from polysome formation (mRNA bearing >1 ribosome).[345] The authors demonstrated that polysome formation occurs less frequently than monosome formation and that its extent is controlled by receptor mediated elongation or initiation inhibition and excitation.[345] Intriguingly, there was no correlation between mRNA number and fluorescent protein output in *E. coli*,[287] which the authors attributed to factors extrinsic to translation, like mRNA degradation, or to the static nature of the smFISH technique.[287]

Stress conditions can also alter the extent of translation of a given gene.[450] During stress, bacterial protein RelA synthesizes alarmones (signaling molecules synthesized solely under harsh conditions), such as (p)ppGpp to suppresses translation, among other cellular processes. English et al. discovered that both RelA and the ribosomal 70S subunit have the same diffusion coefficient (~0.5 $\mu m^2/s$) at normal growth conditions, possibly due to their association.[450] Upon heat shock or starvation, RelA's diffusion coefficient increases 25-fold, suggesting its release and diffusion throughout the cytoplasm, in a reversible fashion. Taken together, the authors were able to demonstrate that RelA will 'hop off' the ribosome under stress conditions in order to induce the cellular adaptation response pathway, consequently inhibiting bacterial translation.[450]

4.8. Post-Transcriptional Control of Gene Expression

The proper development, growth, and regeneration of multicellular organisms require tight spatiotemporal control of gene expression. Any deviation from the norm, in terms of the number and spatiotemporal localizations of specific RNAs, can contribute to phenotypic changes that are either necessary or deleterious to the organism. Defining these RNA parameters provides mechanistic insight into functional and dysfunctional differentiation processes. Single molecule tools, particularly smFISH, have been used extensively to characterize RNA expression profiles in multicellular, asynchronous and heterogeneous cell populations, such as tissues and developing embryos.[273,451,452] For example, Saffer et al. used smFISH to demonstrate the impacts of genetic mutations in synMuv genes on cellular lin-3 RNA distribution and the consequent influence on vulva development in *C. elegans*.[453] A three-color smFISH study by Itzkovitz et al. discovered the location of specific stem cells in mouse intestines by probing for cell specific genes.[384] Their findings revealed that two distinct populations of stem cells are harbored in intestinal crypts, each exhibiting a unique expression profile for stem-cell specific genes that changes as a function of age and active regeneration.[384] Lionnet et al. developed a transgenic mouse that coexpresses an endogenous MCP-FP fusion protein together with a β-actin mRNA carrying MBS repeats that can be used to study mRNA expression in any tissue.[226] In addition to coding mRNAs, smFISH techniques have been utilized to probe miRNA expression patterns.[454,455] Neely et al. utilized the *Direct* miRNA assay to characterize the expression patterns of 45 miRNAs in as many as 16 different tissue types.[454] Finally, Li et al. utilized miRNA in situ hybridization (MISH) coupled with enzyme-labeled fluorescence (ELF) to show reduced quantities of miRNA-375 expression in esophageal squamous cell carcinoma cell lines relative to normal tissue.[455] Collectively, these single molecule RNA counting assays have and will continue to provide much needed spatial and temporal information of gene regulation in asynchronous and heterogeneous cellular systems.

dx.doi.org/10.1021/cr400496q | *Chem. Rev.* 2014, 114, 3224−3265

The cell has developed a multitude of mechanisms to control gene expression and prevent infection through the sequestration and degradation of both endogenous and exogenous parasitic RNAs. Mechanistic and kinetic analyses of RNA decay processes reveal important parameters to understand and predict their cytoplasmic spatial distributions and lifetimes. In cellulo single molecule counting is ideal when aiming to quantify changes in RNA levels within a single cell or a heterogeneous sample. Trcek et al. counted cytoplasmic mRNA using smFISH and uncovered a cell cycle specific mRNA decay mechanism in yeast.[456] They deduced that these mRNAs are stable from the S to the G2 phase (halftime, $t_{1/2} > 66$ min), but are more rapidly degraded during mitosis ($t_{1/2} < 2$ min). Additionally, these effects were found to be dependent on the promoter sequence and nuclear protein factors that bind them (Dbf2p and Dbf20p).[456] Together, this data present a model of degradation wherein cotranscriptional events dictate an mRNA's lifetime.

Single particle tracking is ideal for measuring kinetic parameters of rapid processes and measuring temporal changes in diffusion patterns. Pitchiaya et al. used a unique blend of SPT, photobleaching analysis and microinjection (in a technique termed intracellular single-molecule, high resolution localization and counting, or iSHiRLoC) to elucidate the spatiotemporal behaviors of microinjected, cyanine dye labeled miRNAs in HeLa cells (Figure 14).[135] The authors found that a majority of miRNAs begins to diffuse slowly enough for observation with a 100-ms camera integration time about 1 h after microinjection, suggesting that association with target mRNAs occurs on this time scale. Analysis of stepwise photobleaching trajectories in fixed cells indicated little multimer assembly (more than one miRNA per focus) up to this time (Figure 14C,D), supporting the conclusion from live cell imaging.[135] At 2 h after microinjection and beyond, miRNAs are visible as individual particles with a fluorescence signal enhanced by confinement or binding within comparatively large endogenous mRNPs. These particles exhibit four different types of diffusive motion: Brownian, corralled, directional, and slow Brownian/immobile, and distribute into (at least) two Gaussian distributions of diffusion constants that mimic the diffusion observed for mRNPs (0.26 $\mu m^2/s$) and the mRNA degrading P-bodies (0.034 $\mu m^2/s$; Figure 14B). Photobleaching analysis revealed time dependent formation of miRNA multimers (foci containing >1 labeled miRNA), whose temporal evolution fits with a double-exponential function (Figure 14D) and correlates well with the changes in miRNA diffusion coefficients.[135] An artificial miRNA with much fewer endogenous targets does not show any temporal change in assembly, unless endogenous mRNA target is co-microinjected (Figure 14D). Taken together, the authors concluded that miRNA bind and sequester their targets into mRNA degrading P-bodies within the first 2 h ($k_1 = 1.2 \pm 0.2$ h^{-1}), which are slowly ($k_2 = 0.14 \pm 0.08$ h^{-1}) released back to the cytoplasmic pool, likely after target degradation, over the remaining 32 h period. These results correlate with the timing of colocalization between smFISH probed RNA and various immunostained P-body components[282] and support a unifying two-stage RNA silencing mechanism where translational repression is kinetically followed by mRNA degradation.[135]

Stress granules (SGs) are membrane-less cytoplasmic foci that form when cells are exposed to environmental stress, and their formation is accompanied by global translation arrest of housekeeping transcripts.[457] These foci are composed of the

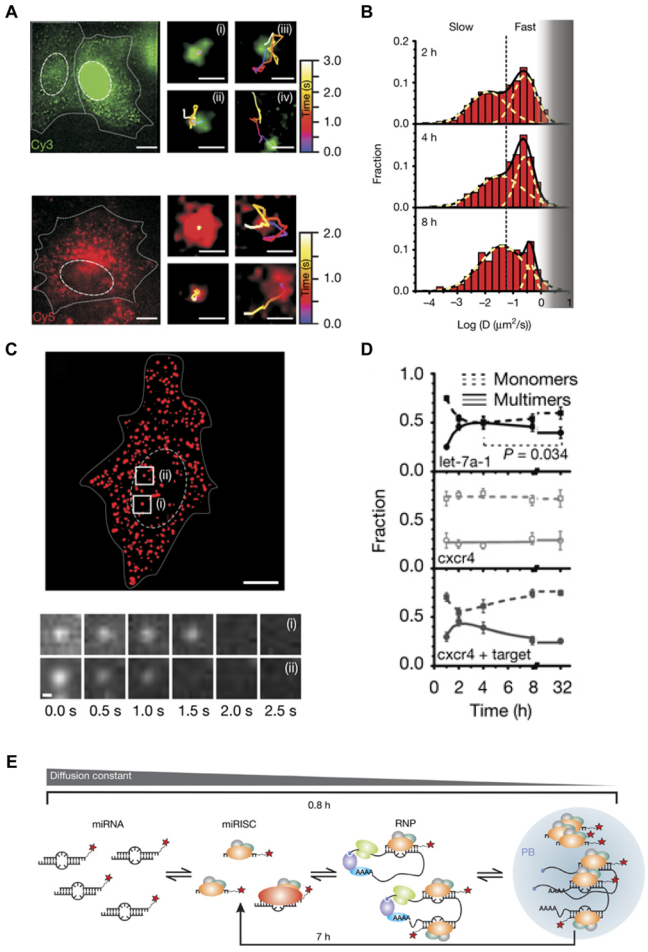

Figure 14. iSHiRLoC of miRNAs. (A) Representative pseudocolored images of live HeLa cells injected with Cy3 (green) or Cy5 (red) labeled let-7-a1 miRNAs and representative single particle tracks showcasing the multitude of diffusive patterns these miRNAs exhibit. Scale bars represent 10 μm. (B) Distribution of diffusion coefficients of miRNPs at various time points. (C) Representative pseudocolored and background subtracted image of a fixed HeLa cell microinjected with Cy5 labeled let-7-a1 miRNA. Below, two representative photobleaching trajectories of particles in the image. (D) Fraction of monomers and multimers as a function of time. (E) Unifying model of the RNA silencing pathway consistent with the experimental data. Reprinted with permission from ref 135. Copyright 2012 Nature Publishing Group.

noncanonical, translationally silent 48S preinitiation complex (containing the small ribosomal subunit-associated early initiation factors eIF4E, eIF3, eIF4A, and eIFG and PABP), several mRNA binding proteins that regulate mRNA translation and decay and proteins involved in RNA metabolism.[457] P-bodies, by contrast, are cytoplasmic foci predominantly enriched in RNA processing and degradation enzymes, which are present in healthy cells as well. Although SGs and P-bodies are often seen in proximity to each other during stress and both have common protein components, they are distinct cellular granules, with the former functioning to store and aggregate translationally inactive mRNAs and the latter representing RNA decay sites.[457] While the two types of foci have been well characterized, their interactions with native mRNAs are still poorly understood. To probe this interaction, Zurla et al. used hybridization-based MTRIPs to visualize the interaction of actin and other polyA sequence containing mRNAs with

dx.doi.org/10.1021/cr400496q | Chem. Rev. 2014, 114, 3224−3265

immunostained SGs and P-bodies in fixed cells.[347] They observed that under stressed conditions <5% of all transcripts colocalized with SGs, whereas <1% colocalized with P-bodies, and that the extent of P-body localization was similar between stressed and unstressed conditions. Stress induced specifically by translation inhibition changed the localization pattern of the transcripts and moved them closer to the nucleus. By coimaging the mRNA and tubulin, and by disrupting the cytoskeletal network, the group found that microtubule integrity was necessary for actin mRNA localization to both these foci and the exosome.[347]

4.9. Retroviral Life Cycle

Retroviruses are unique entities in that they carry their genetic information in the form of RNA, rather than DNA. Upon host infection, their genetic information is reverse-transcribed into DNA and inserted into the host's genome. Through hijacking the cellular transcription and translation machineries, new viruses are created.[458] A significant body of work has contributed to our overall understanding of the viral life cycle;[458] however, resolving key aspects of the subcellular localization of viral assembly intermediates and viral trafficking requires in cellulo single molecule tools. For example, influenza virus A contains eight unique RNA segments that comprise its genetic information. Using smFISH, it was discovered that all eight RNA segments remain associated with one another even after their release from the viral capsid. This association is retained until their entry into the nucleus where they disassemble and are subsequently reverse-transcribed and integrated into the genome.[459] Once transcribed, each of the eight influenza A RNAs is exported from the nucleus individually, but then they all assemble into a cytoplasmic RNP in a Rab11 (an endosomal binding protein) dependent process.[459] RNP formation prior to capsid assembly provides a checkpoint to ensure accurate packaging of the viral genome. Similarly, HIV-2 RNA was observed to dimerize in the cytoplasm prior to capsid assembly.[460] Boireau et al. discovered via FRAP and smFISH techniques that MCP-FP labeled HIV-1 RNA is rapidly transcribed in U2OS cells at ∼1.9 kb/min.[461] Basyuk et al. used SPT of similarly labeled viral progeny RNA molecules to discover that they are actively transported to their host's plasma membrane.[462] Actively transported viral RNA was observed to cotrack with lysosomes and transferrin-positive endosomes in a Gag and Env protein dependent process. Vesicle transport could represent an efficient means to deliver the budding virus to the plasma membrane for its secretion, as corroborated by later studies.[463,464] Jouvenet et al.[465] and Ivanchenko et al.[466] discovered that HIV-1 RNA viral assembly occurs at the plasma membrane and not within the cytoplasm, squelching the hypothesis that viral particles are cotranslationally assembled during capsid protein synthesis. Once transported to the budding site, viral RNA particles are rapidly assembled for release at $\sim 5 \times 10^{-3}$ s^{-1}.[464,466]

A host that has been infected with two parent viruses gives rise to progeny virions that either contain genetic information from a single provirus (homogeneous) or from two different proviruses (heterogeneous). Chen et al. utilized the MCP-FP system and another protein−RNA tethering system comprising of the *E. coli* RNA binding protein BglG and its cognate binding sequence to selectively label two different HIV-1 RNA molecules in vivo.[467] In this study, the authors determined that viral particles are assembled with high fidelity, wherein >90% of particles contain the appropriate number of HIV-1 genomic RNA molecules. The extent of virion heterogeneity depends on the dimer initiation sequence (DIS, a palindromic dimerization sequence in the 5′ UTR of the viral RNA) on each proviral RNA molecule.[467] If both proviral RNAs contain identical DIS sequences, the extent of viron heterogeneity will be random. In contrast, unique DIS sequences will induce bias toward the most thermodynamically stable pairing.[467,468] Additionally, HIV-1 and 2, which share very little sequence homology, can package into similar progeny viruses in a DIS dependent fashion.[460,468]

4.10. Telomerase

Telomeric DNA is a specialized, repetitive sequence on the ends of chromosomes designed to protect chromosomes from progressive shortening and fusion. Telomerase RNA is a specialized lncRNA that helps maintain the proper length of the chromosomal telomeres.[199,200] To better understand the mechanism by which the telomerase RNP is recruited to chromosome ends, Gallardo et al. designed stably integrated telomerase RNA using the in vivo labeled MCP-FP system and performed SPT at various stages of the yeast cell cycle.[469] Diffusion and cotracking indicated that telomerase RNA is associated with the telomere and telomere interacting protein Rap1 only during S phase (when telomeres are supposed to be elongated), yet the telomerase retains enzymatic activity throughout the cell cycle. Thus, active telomerase is recruited to the shortest telomeres only in the late S phase of the cell cycle.[469]

5. CONCLUSIONS

In this review, we have described numerous RNAs that are found in particularly the eukaryotic cell and have provided a detailed summary of the single molecule tools available to study RNAs intracellularly. A large fraction of single molecules studies published so far have been used to characterize protein-coding mRNAs. However, as we have highlighted in section 2, the majority of RNAs found in the eukaryotic cell do not code for protein but rather regulate gene expression via post-transcriptional gene silencing or epigenetic gene regulation. Intracellular single molecule techniques offer an unparalleled means to investigate the behavior of these emerging classes of ncRNAs.

Rapid recent advances in single molecule tool development are likely to further facilitate analysis of the multitude of cellular RNA functions. For example, more pervasive implementation of super-resolution techniques may be necessary to dissect the functions and mechanisms of ncRNAs within densely populated samples.[212] In addition, enhanced spatiotemporal resolution using, for example, SPEED microscopy,[88] more observables, and an increased field of view will likely facilitate studies of intracellular single molecule RNA dynamics. We anticipate a bright future for discoveries using intracellular single molecule fluorescence microscopy as applied to RNA.

AUTHOR INFORMATION

Corresponding Author

*Tel.: (734) 615-2060. E-mail: nwalter@umich.edu.

Author Contributions

‖These authors contributed equally to this work.

Notes

The authors declare no competing financial interest.

Biographies

Sethuramasundaram Pitchiaya received his bachelor's degree in Industrial Biotechnology from the Center for Biotechnology at Anna University in Chennai, India, in 2006. In 2011, he received a Ph.D. degree in Chemistry from the University of Michigan in Ann Arbor, Michigan, while developing iSHiRLoC under the guidance of Dr. Nils Walter. Until recently, he served as a postdoctoral fellow in the Single Molecule Analysis in Real-Time (SMART) center, is now back full-time in the Walter group, and is broadly interested in understanding the intracellular organization, trafficking, and mechanism of action of eukaryotic noncoding RNAs (ncRNAs) and ribonucleoprotein granules. Apart from assembling, maintaining, and training users on a high-resolution objective-TIRF type single molecule microscope and an atomic force microscope at the SMART center, he has been working towards unraveling the intracellular localization, assembly, and function of microRNPs and DNA damage response associated ncRNAs at single molecule resolution.

Laurie Heinicke was born in 1981 in St. Paul, Minnesota. She received her B.S. degree in Biochemistry from the University of Minnesota-Twin Cities. In 2010, she received her Ph.D. in Chemistry at The Pennsylvania State University under the direction of Dr. Philip Bevilacqua. She spent three years as a postdoctoral fellow at The University of Pennsylvania (advisors Drs. Alan Gewirtz and Russ Carstens) and was supported by an NIH Hematopoiesis training grant. She is currently a postdoctoral fellow in Dr. Nils Walter's laboratory at the University of Michigan in Ann Arbor, Michigan. Her previous experience working with in vitro RNA folding intermediates, RNA–protein interactions, and cell culture has facilitated a smooth transition into using single molecule fluorescence microscopy to examine the behavior of miRNAs and other ncRNAs in living cells.

Thomas Corey Custer received his Bachelor's degree in Chemistry from Monmouth College in Monmouth, Illinois, in 2002. He completed his Master's degree in Chemistry from the University of Colorado—Denver, Colorado, in 2006. While a Master's candidate, he spent 3 years working as a Drug Metabolism scientist for Array BioPharma in Boulder, Colorado. He continued his efforts as a Drug Metabolism scientist with Abbott Laboratories in Abbott Park, Illinois, for five years, four of which he also spent as an adjunct faculty member for the Chemistry Department at the College of Lake County in Grayslake, Illinois. He is currently a Ph.D. candidate at the University of Michigan in Ann Arbor, Michigan, in the Program in Chemical Biology. As a member of the Walter laboratory, he uses live-cell RNA detection approaches to study the kinetics and mechanisms of microRNA interactions with RNA silencing components using single molecule techniques such as iSHiRLoC.

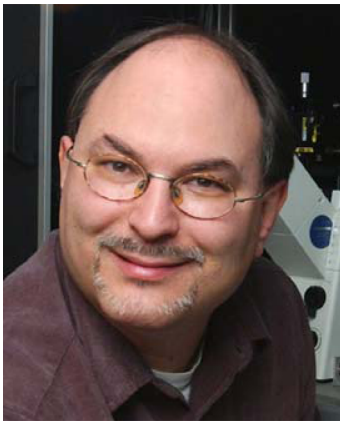

Nils G. Walter was born in 1966 in Frankfurt am Main, Germany. He received his "Vordiplom" (B.S.) and "Diploma" (Masters) from the Technical University of Darmstadt after performing research with Hans-Günther Gassen on the physiochemical characterization of a protein dehyrogenase enzyme. He earned his Dr. rer. nat. while studying molecular in vitro evolution of DNA and RNA using fluorescence techniques with Nobel laureate Manfred Eigen at the Max-Planck-Institute for Biophysical Chemistry, Göttingen. For his postdoctoral studies, he turned to RNA enzymes under the guidance of John M. Burke at the University of Vermont in Burlington, Vermont. He is currently a Professor of Chemistry at the University of Michigan in Ann Arbor, Michigan. His research interests focus on noncoding RNA through the lens of single molecule techniques. He currently directs the unique Single Molecule Analysis in Real-Time (SMART) Center at Michigan.

dx.doi.org/10.1021/cr400496q | Chem. Rev. 2014, 114, 3224–3265

ACKNOWLEDGMENTS

This work was supported by NIH Grants GM081025 and GM098023 to N.G.W.

REFERENCES

(1) Consortium, E. P.; Birney, E.; Stamatoyannopoulos, J. A.; Dutta, A.; Guigo, R.; Gingeras, T. R.; Margulies, E. H.; Weng, Z.; Snyder, M.; Dermitzakis, E. T.; Thurman, R. E.; Kuehn, M. S.; Taylor, C. M.; Neph, S.; Koch, C. M.; Asthana, S.; Malhotra, A.; Adzhubei, I.; Greenbaum, J. A.; Andrews, R. M.; Flicek, P.; Boyle, P. J.; Cao, H.; Carter, N. P.; Clelland, G. K.; Davis, S.; Day, N.; Dhami, P.; Dillon, S. C.; Dorschner, M. O.; Fiegler, H.; Giresi, P. G.; Goldy, J.; Hawrylycz, M.; Haydock, A.; Humbert, R.; James, K. D.; Johnson, B. E.; Johnson, E. M.; Frum, T. T.; Rosenzweig, E. R.; Karnani, N.; Lee, K.; Lefebvre, G. C.; Navas, P. A.; Neri, F.; Parker, S. C.; Sabo, P. J.; Sandstrom, R.; Shafer, A.; Vetrie, D.; Weaver, M.; Wilcox, S.; Yu, M.; Collins, F. S.; Dekker, J.; Lieb, J. D.; Tullius, T. D.; Crawford, G. E.; Sunyaev, S.; Noble, W. S.; Dunham, I.; Denoeud, F.; Reymond, A.; Kapranov, P.; Rozowsky, J.; Zheng, D.; Castelo, R.; Frankish, A.; Harrow, J.; Ghosh, S.; Sandelin, A.; Hofacker, I. L.; Baertsch, R.; Keefe, D.; Dike, S.; Cheng, J.; Hirsch, H. A.; Sekinger, E. A.; Lagarde, J.; Abril, J. F.; Shahab, A.; Flamm, C.; Fried, C.; Hackermuller, J.; Hertel, J.; Lindemeyer, M.; Missal, K.; Tanzer, A.; Washietl, S.; Korbel, J.; Emanuelsson, O.; Pedersen, J. S.; Holroyd, N.; Taylor, R.; Swarbreck, D.; Matthews, N.; Dickson, M. C.; Thomas, D. J.; Weirauch, M. T. *Nature* **2007**, *447*, 799.

(2) Carninci, P.; Kasukawa, T.; Katayama, S.; Gough, J.; Frith, M. C.; Maeda, N.; Oyama, R.; Ravasi, T.; Lenhard, B.; Wells, C.; Kodzius, R.; Shimokawa, K.; Bajic, V. B.; Brenner, S. E.; Batalov, S.; Forrest, A. R.; Zavolan, M.; Davis, M. J.; Wilming, L. G.; Aidinis, V.; Allen, J. E.; Ambesi-Impiombato, A.; Apweiler, R.; Aturaliya, R. N.; Bailey, T. L.; Bansal, M.; Baxter, L.; Beisel, K. W.; Bersano, T.; Bono, H.; Chalk, A. M.; Chiu, K. P.; Choudhary, V.; Christoffels, A.; Clutterbuck, D. R.; Crowe, M. L.; Dalla, E.; Dalrymple, B. P.; de Bono, B.; Della Gatta, G.; di Bernardo, D.; Down, T.; Engstrom, P.; Fagiolini, M.; Faulkner, G.; Fletcher, C. F.; Fukushima, T.; Furuno, M.; Futaki, S.; Gariboldi, M.; Georgii-Hemming, P.; Gingeras, T. R.; Gojobori, T.; Green, R. E.; Gustincich, S.; Harbers, M.; Hayashi, Y.; Hensch, T. K.; Hirokawa, N.; Hill, D.; Huminiecki, L.; Iacono, M.; Ikeo, K.; Iwama, A.; Ishikawa, T.; Jakt, M.; Kanapin, A.; Katoh, M.; Kawasawa, Y.; Kelso, J.; Kitamura, H.; Kitano, H.; Kollias, G.; Krishnan, S. P.; Kruger, A.; Kummerfeld, S. K.; Kurochkin, I. V.; Lareau, L. F.; Lazarevic, D.; Lipovich, L.; Liu, J.; Liuni, S.; McWilliam, S.; Madan Babu, M.; Madera, M.; Marchionni, L.; Matsuda, H.; Matsuzawa, S.; Miki, H.; Mignone, F.; Miyake, S.; Morris, K.; Mottagui-Tabar, S.; Mulder, N.; Nakano, N.; Nakauchi, H.; Ng, P.; Nilsson, R.; Nishiguchi, S.; Nishikawa, S. *Science* **2005**, *309*, 1559.

(3) Carninci, P.; Hayashizaki, Y. *Curr. Opin. Genet. Dev.* **2007**, *17*, 139.

(4) Harrow, J.; Frankish, A.; Gonzalez, J. M.; Tapanari, E.; Diekhans, M.; Kokocinski, F.; Aken, B. L.; Barrell, D.; Zadissa, A.; Searle, S.; Barnes, I.; Bignell, A.; Boychenko, V.; Hunt, T.; Kay, M.; Mukherjee, G.; Rajan, J.; Despacio-Reyes, G.; Saunders, G.; Steward, C.; Harte, R.; Lin, M.; Howald, C.; Tanzer, A.; Derrien, T.; Chrast, J.; Walters, N.; Balasubramanian, S.; Pei, B.; Tress, M.; Rodriguez, J. M.; Ezkurdia, I.; van Baren, J.; Brent, M.; Haussler, D.; Kellis, M.; Valencia, A.; Reymond, A.; Gerstein, M.; Guigo, R.; Hubbard, T. J. *Genome Res.* **2012**, *22*, 1760.

(5) Eddy, S. R. *Nat. Rev. Genet.* **2001**, *2*, 919.

(6) Mattick, J. S. *Nat. Rev. Genet.* **2004**, *5*, 316.

(7) Djebali, S.; Davis, C. A.; Merkel, A.; Dobin, A.; Lassmann, T.; Mortazavi, A.; Tanzer, A.; Lagarde, J.; Lin, W.; Schlesinger, F.; Xue, C.; Marinov, G. K.; Khatun, J.; Williams, B. A.; Zaleski, C.; Rozowsky, J.; Roder, M.; Kokocinski, F.; Abdelhamid, R. F.; Alioto, T.; Antoshechkin, I.; Baer, M. T.; Bar, N. S.; Batut, P.; Bell, K.; Bell, I.; Chakrabortty, S.; Chen, X.; Chrast, J.; Curado, J.; Derrien, T.; Drenkow, J.; Dumais, E.; Dumais, J.; Duttagupta, R.; Falconnet, E.; Fastuca, M.; Fejes-Toth, K.; Ferreira, P.; Foissac, S.; Fullwood, M. J.; Gao, H.; Gonzalez, D.; Gordon, A.; Gunawardena, H.; Howald, C.; Jha, S.; Johnson, R.; Kapranov, P.; King, B.; Kingswood, C.; Luo, O. J.; Park, E.; Persaud, K.; Preall, J. B.; Ribeca, P.; Risk, B.; Robyr, D.; Sammeth, M.; Schaffer, L.; See, L. H.; Shahab, A.; Skancke, J.; Suzuki, A. M.; Takahashi, H.; Tilgner, H.; Trout, D.; Walters, N.; Wang, H.; Wrobel, J.; Yu, Y.; Ruan, X.; Hayashizaki, Y.; Harrow, J.; Gerstein, M.; Hubbard, T.; Reymond, A.; Antonarakis, S. E.; Hannon, G.; Giddings, M. C.; Ruan, Y.; Wold, B.; Carninci, P.; Guigo, R.; Gingeras, T. R. *Nature* **2012**, *489*, 101.

(8) Guttman, M.; Amit, I.; Garber, M.; French, C.; Lin, M. F.; Feldser, D.; Huarte, M.; Zuk, O.; Carey, B. W.; Cassady, J. P.; Cabili, M. N.; Jaenisch, R.; Mikkelsen, T. S.; Jacks, T.; Hacohen, N.; Bernstein, B. E.; Kellis, M.; Regev, A.; Rinn, J. L.; Lander, E. S. *Nature* **2009**, *458*, 223.

(9) Belinky, F.; Bahir, I.; Stelzer, G.; Zimmerman, S.; Rosen, N.; Nativ, N.; Dalah, I.; Iny Stein, T.; Rappaport, N.; Mituyama, T.; Safran, M.; Lancet, D. *Bioinformatics* **2013**, *29*, 255.

(10) Tuck, A. C.; Tollervey, D. *Trends Genet.* **2011**, *27*, 422.

(11) Martens-Uzunova, E. S.; Olvedy, M.; Jenster, G. *Cancer Lett.* **2013**, *340*, 201.

(12) Henriques, R.; Griffiths, C.; Hesper Rego, E.; Mhlanga, M. M. *Biopolymers* **2011**, *95*, 322.

(13) Dreyfuss, G.; Kim, V. N.; Kataoka, N. *Nat. Rev. Mol. Cell. Biol.* **2002**, *3*, 195.

(14) Castello, A.; Fischer, B.; Eichelbaum, K.; Horos, R.; Beckmann, B. M.; Strein, C.; Davey, N. E.; Humphreys, D. T.; Preiss, T.; Steinmetz, L. M.; Krijgsveld, J.; Hentze, M. W. *Cell* **2012**, *149*, 1393.

(15) Huang, Y.; Steitz, J. A. *Mol. Cell* **2005**, *17*, 613.

(16) Hafner, M.; Landthaler, M.; Burger, L.; Khorshid, M.; Hausser, J.; Berninger, P.; Rothballer, A.; Ascano, M., Jr.; Jungkamp, A. C.; Munschauer, M.; Ulrich, A.; Wardle, G. S.; Dewell, S.; Zavolan, M.; Tuschl, T. *Cell* **2010**, *141*, 129.

(17) Yeo, G. W.; Coufal, N. G.; Liang, T. Y.; Peng, G. E.; Fu, X. D.; Gage, F. H. *Nat. Struct. Mol. Biol.* **2009**, *16*, 130.

(18) Zhang, C.; Darnell, R. B. *Nat. Biotechnol.* **2011**, *29*, 607.

(19) Sugimoto, Y.; Konig, J.; Hussain, S.; Zupan, B.; Curk, T.; Frye, M.; Ule, J. *Genome Biol.* **2012**, *13*, 67.

(20) Muller-McNicoll, M.; Neugebauer, K. M. *Nat. Rev. Genet.* **2013**, *14*, 275.

(21) Raj, A.; van Oudenaarden, A. *Annu. Rev. Biophys.* **2009**, *38*, 255.

(22) Mattick, J. S.; Makunin, I. V. *Hum. Mol. Genet.* **2006**, *15* (Spec No 1), R17.

(23) Wahl, M. C.; Will, C. L.; Luhrmann, R. *Cell* **2009**, *136*, 701.

(24) Abelson, J.; Blanco, M.; Ditzler, M. A.; Fuller, F.; Aravamudhan, P.; Wood, M.; Villa, T.; Ryan, D. E.; Pleiss, J. A.; Maeder, C.; Guthrie, C.; Walter, N. G. *Nat. Struct. Mol. Biol.* **2010**, *17*, 504.

(25) Nilsen, T. W.; Graveley, B. R. *Nature* **2010**, *463*, 457.

(26) Chaudhury, A.; Chander, P.; Howe, P. H. *RNA* **2010**, *16*, 1449.

(27) Dreyfuss, G.; Matunis, M. J.; Pinol-Roma, S.; Burd, C. G. *Annu. Rev. Biochem.* **1993**, *62*, 289.

(28) Long, J. C.; Caceres, J. F. *Biochem. J.* **2009**, *417*, 15.

(29) Lou, H.; Neugebauer, K. M.; Gagel, R. F.; Berget, S. M. *Mol. Cell. Biol.* **1998**, *18*, 4977.

(30) Danckwardt, S.; Kaufmann, I.; Gentzel, M.; Foerstner, K. U.; Gantzert, A. S.; Gehring, N. H.; Neu-Yilik, G.; Bork, P.; Keller, W.; Wilm, M.; Hentze, M. W.; Kulozik, A. E. *EMBO J.* **2007**, *26*, 2658.

(31) McManus, C. J.; Graveley, B. R. *Curr. Opin. Genet. Dev.* **2011**, *21*, 373.

(32) Mauger, D. M.; Siegfried, N. A.; Weeks, K. M. *FEBS Lett.* **2013**, *587*, 1180.

(33) Serganov, A.; Nudler, E. *Cell* **2013**, *152*, 17.

(34) Breaker, R. R. *Mol. Cell* **2011**, *43*, 867.

(35) Suddala, K. C.; Rinaldi, A. J.; Feng, J.; Mustoe, A. M.; Eichhorn, C. D.; Liberman, J. A.; Wedekind, J. E.; Al-Hashimi, H. M.; Brooks, C. L., III; Walter, N. G. *Nucleic Acids Res.* **2013**, *41*, 10462.

(36) Pan, Q.; Shai, O.; Lee, L. J.; Frey, B. J.; Blencowe, B. J. *Nat. Genet.* **2008**, *40*, 1413.

(37) Wang, E. T.; Sandberg, R.; Luo, S.; Khrebtukova, I.; Zhang, L.; Mayr, C.; Kingsmore, S. F.; Schroth, G. P.; Burge, C. B. *Nature* **2008**, *456*, 470.
(38) Schmucker, D.; Clemens, J. C.; Shu, H.; Worby, C. A.; Xiao, J.; Muda, M.; Dixon, J. E.; Zipursky, S. L. *Cell* **2000**, *101*, 671.
(39) Gonzalez-Porta, M.; Frankish, A.; Rung, J.; Harrow, J.; Brazma, A. *Genome Biol.* **2013**, *14*, R70.
(40) Tazi, J.; Bakkour, N.; Stamm, S. *Biochim. Biophys. Acta* **2009**, *1792*, 14.
(41) Cooper, T. A.; Wan, L.; Dreyfuss, G. *Cell* **2009**, *136*, 777.
(42) Lopez-Bigas, N.; Audit, B.; Ouzounis, C.; Parra, G.; Guigo, R. *FEBS Lett.* **2005**, *579*, 1900.
(43) Fischer, U.; Englbrecht, C.; Chari, A. *Wiley Interdiscip. Rev. RNA* **2011**, *2*, 718.
(44) Roca, X.; Krainer, A. R.; Eperon, I. C. *Genes Dev.* **2013**, *27*, 129.
(45) Matera, A. G.; Terns, R. M.; Terns, M. P. *Nat. Rev. Mol. Cell Biol.* **2007**, *8*, 209.
(46) Girard, C.; Will, C. L.; Peng, J.; Makarov, E. M.; Kastner, B.; Lemm, I.; Urlaub, H.; Hartmuth, K.; Luhrmann, R. *Nat. Commun.* **2012**, *3*, 994.
(47) Spector, D. L.; Lamond, A. I. *Cold Spring Harbor Perspect. Biol.* **2011**, *3*, 1.
(48) Singh, G.; Kucukural, A.; Cenik, C.; Leszyk, J. D.; Shaffer, S. A.; Weng, Z.; Moore, M. J. *Cell* **2012**, *151*, 750.
(49) Moore, M. J.; Proudfoot, N. J. *Cell* **2009**, *136*, 688.
(50) Cech, T. R. *Annu. Rev. Biochem.* **1990**, *59*, 543.
(51) Saldanha, R.; Mohr, G.; Belfort, M.; Lambowitz, A. M. *FASEB J.* **1993**, *7*, 15.
(52) Bonen, L.; Vogel, J. *Trends Genet.* **2001**, *17*, 322.
(53) Rueda, D.; Bokinsky, G.; Rhodes, M. M.; Rust, M. J.; Zhuang, X.; Walter, N. G. *Proc. Natl. Acad. Sci. U.S.A.* **2004**, *101*, 10066.
(54) McDowell, S. E.; Jun, J. M.; Walter, N. G. *RNA* **2010**, *16*, 2414.
(55) Doherty, E. A.; Doudna, J. A. *Annu. Biophys. Biomol. Struct.* **2001**, *30*, 457.
(56) Winkler, W. C.; Nahvi, A.; Roth, A.; Collins, J. A.; Breaker, R. R. *Nature* **2004**, *428*, 281.
(57) Lilley, D. M. *Curr. Opin. Struct. Biol.* **2005**, *15*, 313.
(58) Pereira, M. J.; Nikolova, E. N.; Hiley, S. L.; Jaikaran, D.; Collins, R. A.; Walter, N. G. *J. Mol. Biol.* **2008**, *382*, 496.
(59) Rhodes, M. M.; Reblova, K.; Sponer, J.; Walter, N. G. *Proc. Natl. Acad. Sci. U.S.A.* **2006**, *103*, 13380.
(60) Ditzler, M. A.; Aleman, E. A.; Rueda, D.; Walter, N. G. *Biopolymers* **2007**, *87*, 302.
(61) McDowell, S. E.; Spackova, N.; Sponer, J.; Walter, N. G. *Biopolymers* **2007**, *85*, 169.
(62) Walter, N. G.; Perumal, S. *Springer Ser. Biophys.* **2009**, *13*, 103.
(63) Zhuang, X.; Kim, H.; Pereira, M. J.; Babcock, H. P.; Walter, N. G.; Chu, S. *Science* **2002**, *296*, 1473.
(64) Bokinsky, G.; Rueda, D.; Misra, V. K.; Rhodes, M. M.; Gordus, A.; Babcock, H. P.; Walter, N. G.; Zhuang, X. *Proc. Natl. Acad. Sci. U.S.A.* **2003**, *100*, 9302.
(65) Ditzler, M. A.; Rueda, D.; Mo, J.; Hakansson, K.; Walter, N. G. *Nucleic Acids Res.* **2008**, *36*, 7088.
(66) de Silva, C.; Walter, N. G. *RNA* **2009**, *15*, 76.
(67) Seehafer, C.; Kalweit, A.; Steger, G.; Graf, S.; Hammann, C. *RNA* **2011**, *17*, 21.
(68) de la Pena, M.; Garcia-Robles, I. *EMBO Rep.* **2010**, *11*, 711.
(69) Chadalavada, D. M.; Gratton, E. A.; Bevilacqua, P. C. *Biochemistry* **2010**, *49*, 5321.
(70) Webb, C. H.; Luptak, A. *RNA Biol.* **2011**, *8*, 719.
(71) Salehi-Ashtiani, K.; Luptak, A.; Litovchick, A.; Szostak, J. W. *Science* **2006**, *313*, 1788.
(72) Crick, F. H. *J. Mol. Biol.* **1968**, *38*, 367.
(73) Orgel, L. E. *J. Mol. Biol.* **1968**, *38*, 381.
(74) Woese, C. R. *The Genetic Code: The Molecular Basis for Genetic Expression*; Harper & Row: New York, 1967.
(75) Gesteland, R. F.; Cech, T. R.; Atkins, J. F. *The RNA World*, 3rd ed.; CSHL Press: Cold Spring Harbor, 2006; Vol. *43*.
(76) Cowling, V. H. *Biochem. J.* **2010**, *425*, 295.
(77) Proudfoot, N. J. *Genes Dev.* **2011**, *25*, 1770.
(78) Mignone, F.; Gissi, C.; Liuni, S.; Pesole, G. *Genome Biol.* **2002**, *3*, 1.
(79) Kohler, A.; Hurt, E. *Nat. Rev. Mol. Cell Biol.* **2007**, *8*, 761.
(80) Hoelz, A.; Debler, E. W.; Blobel, G. *Annu. Rev. Biochem.* **2011**, *80*, 613.
(81) Grunwald, D.; Singer, R. H.; Rout, M. *Nature* **2011**, *475*, 333.
(82) Wente, S. R.; Rout, M. P. *Cold Spring Harbor Perspect. Biol.* **2010**, *2*, a000562.
(83) Katahira, J. *Biochim. Biophys. Acta* **2012**, *1819*, 507.
(84) Mehlin, H.; Daneholt, B.; Skoglund, U. *Cell* **1992**, *69*, 605.
(85) Davis, L. I.; Blobel, G. *Cell* **1986**, *45*, 699.
(86) Kim, J.; Izadyar, A.; Nioradze, N.; Amemiya, S. *J. Am. Chem. Soc.* **2013**, *135*, 2321.
(87) Speese, S. D.; Ashley, J.; Jokhi, V.; Nunnari, J.; Barria, R.; Li, Y.; Ataman, B.; Koon, A.; Chang, Y. T.; Li, Q.; Moore, M. J.; Budnik, V. *Cell* **2012**, *149*, 832.
(88) Ma, J.; Liu, Z.; Michelotti, N.; Pitchiaya, S.; Veerapaneni, R.; Androsavich, J. R.; Walter, N. G.; Yang, W. *Nat. Commun.* **2013**, *4*, 2414.
(89) Martin, K. C.; Ephrussi, A. *Cell* **2009**, *136*, 719.
(90) Kahvejian, A.; Svitkin, Y. V.; Sukarieh, R.; M'Boutchou, M. N.; Sonenberg, N. *Genes Dev.* **2005**, *19*, 104.
(91) Diem, M. D.; Chan, C. C.; Younis, I.; Dreyfuss, G. *Nat. Struct. Mol. Biol.* **2007**, *14*, 1173.
(92) Bratkovic, T.; Rogelj, B. *Cell. Mol. Life Sci.* **2011**, *68*, 3843.
(93) Kressler, D.; Hurt, E.; Bassler, J. *Biochim. Biophys. Acta* **2010**, *1803*, 673.
(94) Kiss-Laszlo, Z.; Henry, Y.; Bachellerie, J. P.; Caizergues-Ferrer, M.; Kiss, T. *Cell* **1996**, *85*, 1077.
(95) Tollervey, D.; Kiss, T. *Curr. Opin. Cell Biol.* **1997**, *9*, 337.
(96) Weinstein, L. B.; Steitz, J. A. *Curr. Opin. Cell Biol.* **1999**, *11*, 378.
(97) Watkins, N. J.; Bohnsack, M. T. *Wiley Interdiscip. Rev. RNA* **2012**, *3*, 397.
(98) Williams, G. T.; Farzaneh, F. *Nat. Rev. Cancer* **2012**, *12*, 84.
(99) Ono, M.; Scott, M. S.; Yamada, K.; Avolio, F.; Barton, G. J.; Lamond, A. I. *Nucleic Acids Res.* **2011**, *39*, 3879.
(100) El Yacoubi, B.; Bailly, M.; de Crecy-Lagard, V. *Annu. Rev. Genet.* **2012**, *46*, 69.
(101) Kim, S. H.; Suddath, F. L.; Quigley, G. J.; McPherson, A.; Sussman, J. L.; Wang, A. H.; Seeman, N. C.; Rich, A. *Science* **1974**, *185*, 435.
(102) Goodenbour, J. M.; Pan, T. *Nucleic Acids Res.* **2006**, *34*, 6137.
(103) Shah, P.; Ding, Y.; Niemczyk, M.; Kudla, G.; Plotkin, J. B. *Cell* **2013**, *153*, 1589.
(104) Dittmar, K. A.; Goodenbour, J. M.; Pan, T. *PLoS Genet.* **2006**, *2*, e221.
(105) Walker, S. C.; Engelke, D. R. *Crit. Rev. Biochem. Mol. Biol.* **2006**, *41*, 77.
(106) Guerrier-Takada, C.; Gardiner, K.; Marsh, T.; Pace, N.; Altman, S. *Cell* **1983**, *35*, 849.
(107) Akopian, D.; Shen, K.; Zhang, X.; Shan, S. O. *Annu. Rev. Biochem.* **2013**, *82*, 693.
(108) Pool, M. R. *Mol. Membr. Biol.* **2005**, *22*, 3.
(109) Hebert, D. N.; Molinari, M. *Physiol. Rev.* **2007**, *87*, 1377.
(110) Durand, S.; Cougot, N.; Mahuteau-Betzer, F.; Nguyen, C. H.; Grierson, D. S.; Bertrand, E.; Tazi, J.; Lejeune, F. *J. Cell Biol.* **2007**, *178*, 1145.
(111) Parker, R.; Sheth, U. *Mol. Cell* **2007**, *25*, 635.
(112) Baker, K. E.; Parker, R. *Curr. Opin. Cell Biol.* **2004**, *16*, 293.
(113) Holbrook, J. A.; Neu-Yilik, G.; Hentze, M. W.; Kulozik, A. E. *Nat. Genet.* **2004**, *36*, 801.
(114) Rebbapragada, I.; Lykke-Andersen, J. *Curr. Opin. Cell Biol.* **2009**, *21*, 394.
(115) Parker, R.; Song, H. *Nat. Struct. Mol. Biol.* **2004**, *11*, 121.
(116) Dictenberg, J. B.; Swanger, S. A.; Antar, L. N.; Singer, R. H.; Bassell, G. J. *Dev. Cell* **2008**, *14*, 926.
(117) Ascano, M., Jr.; Mukherjee, N.; Bandaru, P.; Miller, J. B.; Nusbaum, J. D.; Corcoran, D. L.; Langlois, C.; Munschauer, M.;

Dewell, S.; Hafner, M.; Williams, Z.; Ohler, U.; Tuschl, T. *Nature* **2012**, *492*, 382.
(118) Vasudevan, S.; Steitz, J. A. *Cell* **2007**, *128*, 1105.
(119) Ghildiyal, M.; Zamore, P. D. *Nat. Rev. Genet.* **2009**, *10*, 94.
(120) Carthew, R. W.; Sontheimer, E. J. *Cell* **2009**, *136*, 642.
(121) Siomi, M. C.; Sato, K.; Pezic, D.; Aravin, A. A. *Nat. Rev. Mol. Cell Biol.* **2011**, *12*, 246.
(122) Moazed, D. *Cell* **2011**, *146*, 510.
(123) Francia, S.; Michelini, F.; Saxena, A.; Tang, D.; de Hoon, M.; Anelli, V.; Mione, M.; Carninci, P.; d'Adda di Fagagna, F. *Nature* **2012**, *488*, 231.
(124) Chowdhury, D.; Choi, Y. E.; Brault, M. E. *Nat. Rev. Mol. Cell Biol.* **2013**, *14*, 181.
(125) Lee, R. C.; Feinbaum, R. L.; Ambros, V. *Cell* **1993**, *75*, 843.
(126) Fire, A.; Xu, S.; Montgomery, M. K.; Kostas, S. A.; Driver, S. E.; Mello, C. C. *Nature* **1998**, *391*, 806.
(127) Storz, G.; Vogel, J.; Wassarman, K. M. *Mol. Cell* **2011**, *43*, 880.
(128) Castel, S. E.; Martienssen, R. A. *Nat. Rev. Genet.* **2013**, *14*, 100.
(129) Zisoulis, D. G.; Kai, Z. S.; Chang, R. K.; Pasquinelli, A. E. *Nature* **2012**, *486*, 541.
(130) Friedman, R. C.; Farh, K. K.; Burge, C. B.; Bartel, D. P. *Genome Res.* **2009**, *19*, 92.
(131) Jackson, A. L.; Linsley, P. S. *Nat. Rev. Drug Discovery* **2010**, *9*, 57.
(132) Aalto, A. P.; Pasquinelli, A. E. *Curr. Opin. Cell Biol.* **2012**, *24*, 333.
(133) Ohrt, T.; Merkle, D.; Birkenfeld, K.; Echeverri, C. J.; Schwille, P. *Nucleic Acids Res.* **2006**, *34*, 1369.
(134) Ohrt, T.; Staroske, W.; Mutze, J.; Crell, K.; Landthaler, M.; Schwille, P. *Biophys. J.* **2011**, *100*, 2981.
(135) Pitchiaya, S.; Androsavich, J. R.; Walter, N. G. *EMBO Rep.* **2012**, *13*, 709.
(136) Koh, H. R.; Kidwell, M. A.; Ragunathan, K.; Doudna, J. A.; Myong, S. *Proc. Natl. Acad. Sci. U.S.A.* **2013**, *110*, 151.
(137) Bartel, D. P. *Cell* **2004**, *116*, 281.
(138) Bartel, D. P. *Cell* **2009**, *136*, 215.
(139) Krol, J.; Loedige, I.; Filipowicz, W. *Nat. Rev. Genet.* **2010**, *11*, 597.
(140) Dieci, G.; Fiorino, G.; Castelnuovo, M.; Teichmann, M.; Pagano, A. *Trends Genet.* **2007**, *23*, 614.
(141) Saini, H. K.; Griffiths-Jones, S.; Enright, A. J. *Proc. Natl. Acad. Sci. U.S.A.* **2007**, *104*, 17719.
(142) Han, J.; Lee, Y.; Yeom, K. H.; Nam, J. W.; Heo, I.; Rhee, J. K.; Sohn, S. Y.; Cho, Y.; Zhang, B. T.; Kim, V. N. *Cell* **2006**, *125*, 887.
(143) Czech, B.; Hannon, G. J. *Nat. Rev. Genet.* **2011**, *12*, 19.
(144) Noland, C. L.; Doudna, J. A. *RNA* **2013**, *19*, 639.
(145) Finnegan, E. F.; Pasquinelli, A. E. *Crit. Rev. Biochem. Mol. Biol.* **2013**, *48*, 51.
(146) Okamura, K.; Hagen, J. W.; Duan, H.; Tyler, D. M.; Lai, E. C. *Cell* **2007**, *130*, 89.
(147) Flynt, A. S.; Greimann, J. C.; Chung, W. J.; Lima, C. D.; Lai, E. C. *Mol. Cell* **2010**, *38*, 900.
(148) Huntzinger, E.; Izaurralde, E. *Nat. Rev. Genet.* **2011**, *12*, 99.
(149) Fabian, M. R.; Sonenberg, N. *Nat. Struct. Mol. Biol.* **2012**, *19*, 586.
(150) Fabian, M. R.; Sonenberg, N.; Filipowicz, W. *Annu. Rev. Biochem.* **2010**, *79*, 351.
(151) Meijer, H. A.; Kong, Y. W.; Lu, W. T.; Wilczynska, A.; Spriggs, R. V.; Robinson, S. W.; Godfrey, J. D.; Willis, A. E.; Bushell, M. *Science* **2013**, *340*, 82.
(152) Sioud, M.; Cekaite, L. *Methods Mol. Biol.* **2010**, *629*, 257.
(153) Xia, W.; Cao, G.; Shao, N. *Sci. China, Ser. C: Life Sci.* **2009**, *52*, 1123.
(154) Long, D.; Lee, R.; Williams, P.; Chan, C. Y.; Ambros, V.; Ding, Y. *Nat. Struct. Mol. Biol.* **2007**, *14*, 287.
(155) Helwak, A.; Kudla, G.; Dudnakova, T.; Tollervey, D. *Cell* **2013**, *153*, 654.
(156) Zekri, L.; Kuzuoglu-Ozturk, D.; Izaurralde, E. *EMBO J.* **2013**, *32*, 1052.
(157) Li, S.; Liu, L.; Zhuang, X.; Yu, Y.; Liu, X.; Cui, X.; Ji, L.; Pan, Z.; Cao, X.; Mo, B.; Zhang, F.; Raikhel, N.; Jiang, L.; Chen, X. *Cell* **2013**, *153*, 562.
(158) Stalder, L.; Heusermann, W.; Sokol, L.; Trojer, D.; Wirz, J.; Hean, J.; Fritzsche, A.; Aeschimann, F.; Pfanzagl, V.; Basselet, P.; Weiler, J.; Hintersteiner, M.; Morrissey, D. V.; Meisner-Kober, N. C. *EMBO J.* **2013**, *32*, 1115.
(159) Memczak, S.; Jens, M.; Elefsinioti, A.; Torti, F.; Krueger, J.; Rybak, A.; Maier, L.; Mackowiak, S. D.; Gregersen, L. H.; Munschauer, M.; Loewer, A.; Ziebold, U.; Landthaler, M.; Kocks, C.; le Noble, F.; Rajewsky, N. *Nature* **2013**, *495*, 333.
(160) Hansen, T. B.; Jensen, T. I.; Clausen, B. H.; Bramsen, J. B.; Finsen, B.; Damgaard, C. K.; Kjems, J. *Nature* **2013**, *495*, 384.
(161) Ebert, M. S.; Sharp, P. A. *Curr. Biol.* **2010**, *20*, R858.
(162) Hwang, H. W.; Wentzel, E. A.; Mendell, J. T. *Science* **2007**, *315*, 97.
(163) Weinmann, L.; Hock, J.; Ivacevic, T.; Ohrt, T.; Mutze, J.; Schwille, P.; Kremmer, E.; Benes, V.; Urlaub, H.; Meister, G. *Cell* **2009**, *136*, 496.
(164) Nishi, K.; Nishi, A.; Nagasawa, T.; Ui-Tei, K. *RNA* **2013**, *19*, 17.
(165) Truesdell, S. S.; Mortensen, R. D.; Seo, M.; Schroeder, J. C.; Lee, J. H.; LeTonqueze, O.; Vasudevan, S. *Sci. Rep.* **2012**, *2*, 842.
(166) Grewal, S. I. *Curr. Opin. Genet. Dev.* **2010**, *20*, 134.
(167) Law, J. A.; Jacobsen, S. E. *Nat. Rev. Genet.* **2010**, *11*, 204.
(168) Burton, N. O.; Burkhart, K. B.; Kennedy, S. *Proc. Natl. Acad. Sci. U.S.A.* **2011**, *108*, 19683.
(169) Wu, L.; Zhou, H.; Zhang, Q.; Zhang, J.; Ni, F.; Liu, C.; Qi, Y. *Mol. Cell* **2010**, *38*, 465.
(170) Claycomb, J. M.; Batista, P. J.; Pang, K. M.; Gu, W.; Vasale, J. J.; van Wolfswinkel, J. C.; Chaves, D. A.; Shirayama, M.; Mitani, S.; Ketting, R. F.; Conte, D., Jr.; Mello, C. C. *Cell* **2009**, *139*, 123.
(171) Ruby, J. G.; Jan, C.; Player, C.; Axtell, M. J.; Lee, W.; Nusbaum, C.; Ge, H.; Bartel, D. P. *Cell* **2006**, *127*, 1193.
(172) Batista, P. J.; Ruby, J. G.; Claycomb, J. M.; Chiang, R.; Fahlgren, N.; Kasschau, K. D.; Chaves, D. A.; Gu, W.; Vasale, J. J.; Duan, S.; Conte, D., Jr.; Luo, S.; Schroth, G. P.; Carrington, J. C.; Bartel, D. P.; Mello, C. C. *Mol. Cell* **2008**, *31*, 67.
(173) Das, P. P.; Bagijn, M. P.; Goldstein, L. D.; Woolford, J. R.; Lehrbach, N. J.; Sapetschnig, A.; Buhecha, H. R.; Gilchrist, M. J.; Howe, K. L.; Stark, R.; Matthews, N.; Berezikov, E.; Ketting, R. F.; Tavare, S.; Miska, E. A. *Mol. Cell* **2008**, *31*, 79.
(174) Halic, M.; Moazed, D. *Cell* **2010**, *140*, 504.
(175) Guang, S.; Bochner, A. F.; Burkhart, K. B.; Burton, N.; Pavelec, D. M.; Kennedy, S. *Nature* **2010**, *465*, 1097.
(176) Ameyar-Zazoua, M.; Rachez, C.; Souidi, M.; Robin, P.; Fritsch, L.; Young, R.; Morozova, N.; Fenouil, R.; Descostes, N.; Andrau, J. C.; Mathieu, J.; Hamiche, A.; Ait-Si-Ali, S.; Muchardt, C.; Batsche, E.; Harel-Bellan, A. *Nat. Struct. Mol. Biol.* **2012**, *19*, 998.
(177) Wei, W.; Ba, Z.; Gao, M.; Wu, Y.; Ma, Y.; Amiard, S.; White, C. I.; Rendtlew Danielsen, J. M.; Yang, Y. G.; Qi, Y. *Cell* **2012**, *149*, 101.
(178) Qureshi, I. A.; Mehler, M. F. *Nat. Rev. Neurosci.* **2012**, *13*, 528.
(179) Mercer, T. R.; Mattick, J. S. *Nat. Struct. Mol. Biol.* **2013**, *20*, 300.
(180) Kaikkonen, M. U.; Lam, M. T. Y.; Glass, C. K. *Cardiovasc. Res.* **2011**, *90*, 430.
(181) Guttman, M.; Rinn, J. L. *Nature* **2012**, *482*, 339.
(182) Bartolomei, M. S.; Zemel, S.; Tilghman, S. M. *Nature* **1991**, *351*, 153.
(183) Brown, C. J.; Ballabio, A.; Rupert, J. L.; Lafreniere, R. G.; Grompe, M.; Tonlorenzi, R.; Willard, H. F. *Nature* **1991**, *349*, 38.
(184) Barlow, D. P.; Stoger, R.; Herrmann, B. G.; Saito, K.; Schweifer, N. *Nature* **1991**, *349*, 84.
(185) Wapinski, O.; Chang, H. Y. *Trends Cell Biol.* **2011**, *21*, 354.
(186) Kim, E. D.; Sung, S. *Trends Plant Sci.* **2012**, *17*, 16.
(187) Taft, R. J.; Kaplan, C. D.; Simons, C.; Mattick, J. S. *Cell Cycle* **2009**, *8*, 2332.
(188) Khalil, A. M.; Guttman, M.; Huarte, M.; Garber, M.; Raj, A.; Rivea Morales, D.; Thomas, K.; Presser, A.; Bernstein, B. E.; van

Oudenaarden, A.; Regev, A.; Lander, E. S.; Rinn, J. L. *Proc. Natl. Acad. Sci. U.S.A.* **2009**, *106*, 11667.
(189) Li, W.; Notani, D.; Ma, Q.; Tanasa, B.; Nunez, E.; Chen, A. Y.; Merkurjev, D.; Zhang, J.; Ohgi, K.; Song, X.; Oh, S.; Kim, H. S.; Glass, C. K.; Rosenfeld, M. G. *Nature* **2013**, *498*, 516.
(190) Dinger, M. E.; Gascoigne, D. K.; Mattick, J. S. *Biochimie* **2011**, *93*, 2013.
(191) Nallagatla, S. R.; Jones, C. N.; Ghosh, S. K.; Sharma, S. D.; Cameron, C. E.; Spremulli, L. L.; Bevilacqua, P. C. *PLoS ONE* **2013**, *8*, e57905.
(192) Yin, Q. F.; Yang, L.; Zhang, Y.; Xiang, J. F.; Wu, Y. W.; Carmichael, G. G.; Chen, L. L. *Mol. Cell* **2012**, *48*, 219.
(193) Koziol, M. J.; Rinn, J. L. *Curr. Opin. Genet. Dev.* **2010**, *20*, 142.
(194) Guttman, M.; Donaghey, J.; Carey, B. W.; Garber, M.; Grenier, J. K.; Munson, G.; Young, G.; Lucas, A. B.; Ach, R.; Bruhn, L.; Yang, X.; Amit, I.; Meissner, A.; Regev, A.; Rinn, J. L.; Root, D. E.; Lander, E. S. *Nature* **2011**, *477*, 295.
(195) Willingham, A. T.; Orth, A. P.; Batalov, S.; Peters, E. C.; Wen, B. G.; Aza-Blanc, P.; Hogenesch, J. B.; Schultz, P. G. *Science* **2005**, *309*, 1570.
(196) Carrieri, C.; Cimatti, L.; Biagioli, M.; Beugnet, A.; Zucchelli, S.; Fedele, S.; Pesce, E.; Ferrer, I.; Collavin, L.; Santoro, C.; Forrest, A. R.; Carninci, P.; Biffo, S.; Stupka, E.; Gustincich, S. *Nature* **2012**, *491*, 454.
(197) Gong, C.; Maquat, L. E. *Nature* **2011**, *470*, 284.
(198) Poliseno, L.; Salmena, L.; Zhang, J.; Carver, B.; Haveman, W. J.; Pandolfi, P. P. *Nature* **2010**, *465*, 1033.
(199) Theimer, C. A.; Feigon, J. *Curr. Opin. Struct. Biol.* **2006**, *16*, 307.
(200) O'Sullivan, R. J.; Karlseder, J. *Nat. Rev. Mol. Cell Biol.* **2010**, *11*, 171.
(201) Gilley, D.; Tanaka, H.; Herbert, B. S. *Int. J. Biochem. Cell Biol.* **2005**, *37*, 1000.
(202) Gunes, C.; Rudolph, K. L. *Cell* **2013**, *152*, 390.
(203) Rotman, B. *Proc. Natl. Acad. Sci. U.S.A.* **1961**, *47*, 1981.
(204) Gelles, J.; Schnapp, B. J.; Sheetz, M. P. *Nature* **1988**, *331*, 450.
(205) Thompson, R. E.; Larson, D. R.; Webb, W. W. *Biophys. J.* **2002**, *82*, 2775.
(206) Hua, W.; Chung, J.; Gelles, J. *Science* **2002**, *295*, 844.
(207) Yildiz, A.; Forkey, J. N.; McKinney, S. A.; Ha, T.; Goldman, Y. E.; Selvin, P. R. *Science* **2003**, *300*, 2061.
(208) Kural, C.; Kim, H.; Syed, S.; Goshima, G.; Gelfand, V. I.; Selvin, P. R. *Science* **2005**, *308*, 1469.
(209) Moerner, W. E.; Kador, L. *Phys. Rev. Lett.* **1989**, *62*, 2535.
(210) Orrit, M.; Bernard, J. *Phys. Rev. Lett.* **1990**, *65*, 2716.
(211) Lu, H. P.; Xun, L.; Xie, X. S. *Science* **1998**, *282*, 1877.
(212) Walter, N. G.; Huang, C. Y.; Manzo, A. J.; Sobhy, M. A. *Nat. Methods* **2008**, *5*, 475.
(213) Yoshimura, H.; Inaguma, A.; Yamada, T.; Ozawa, T. *ACS Chem. Biol.* **2012**, *7*, 999.
(214) Ando, R.; Flors, C.; Mizuno, H.; Hofkens, J.; Miyawaki, A. *Biophys. J.* **2007**, *92*, L97.
(215) Sahl, S. J.; Moerner, W. *Curr. Opin. Struct. Biol.* **2013**, *23*, 778.
(216) Gossen, M.; Bujard, H. *Proc. Natl. Acad. Sci. U.S.A.* **1992**, *89*, 5547.
(217) Santangelo, P. J.; Lifland, A. W.; Curt, P.; Sasaki, Y.; Bassell, G. J.; Lindquist, M. E.; Crowe, J. E., Jr. *Nat. Methods* **2009**, *6*, 347.
(218) Sakon, J. J.; Weninger, K. R. *Nat. Methods* **2010**, *7*, 203.
(219) Huang, B.; Bates, M.; Zhuang, X. *Annu. Rev. Biochem.* **2009**, *78*, 993.
(220) Newby Lambert, M.; Vocker, E.; Blumberg, S.; Redemann, S.; Gajraj, A.; Meiners, J. C.; Walter, N. G. *Biophys. J.* **2006**, *90*, 3672.
(221) Shimomura, O.; Johnson, F. H.; Saiga, Y. *J. Cell Comp. Physiol.* **1962**, *59*, 223.
(222) Prasher, D. C.; Eckenrode, V. K.; Ward, W. W.; Prendergast, F. G.; Cormier, M. J. *Gene* **1992**, *111*, 229.
(223) Tsien, R. Y. *Annu. Rev. Biochem.* **1998**, *67*, 509.
(224) Day, R. N.; Davidson, M. W. *Chem. Soc. Rev.* **2009**, *38*, 2887.
(225) Mor, A.; Suliman, S.; Ben-Yishay, R.; Yunger, S.; Brody, Y.; Shav-Tal, Y. *Nat. Cell Biol.* **2010**, *12*, 543.
(226) Lionnet, T.; Czaplinski, K.; Darzacq, X.; Shav-Tal, Y.; Wells, A. L.; Chao, J. A.; Park, H. Y.; de Turris, V.; Lopez-Jones, M.; Singer, R. H. *Nat. Methods* **2011**, *8*, 165.
(227) Farzadfard, F.; Perli, S. D.; Lu, T. K. *ACS Synth. Biol.* **2013**, *2*, 604.
(228) Ha, T.; Tinnefeld, P. *Annu. Rev. Phys. Chem.* **2012**, *63*, 595.
(229) Biteen, J. S.; Thompson, M. A.; Tselentis, N. K.; Bowman, G. R.; Shapiro, L.; Moerner, W. E. *Nat. Methods* **2008**, *5*, 947.
(230) Lew, M. D.; Lee, S. F.; Ptacin, J. L.; Lee, M. K.; Twieg, R. J.; Shapiro, L.; Moerner, W. E. *Proc. Natl. Acad. Sci. U.S.A.* **2011**, *108*, E1102.
(231) Wu, B.; Piatkevich, K. D.; Lionnet, T.; Singer, R. H.; Verkhusha, V. V. *Curr. Opin. Cell Biol.* **2011**, *23*, 310.
(232) Subach, F. V.; Subach, O. M.; Gundorov, I. S.; Morozova, K. S.; Piatkevich, K. D.; Cuervo, A. M.; Verkhusha, V. V. *Nat. Chem. Biol.* **2009**, *5*, 118.
(233) Fusco, D.; Accornero, N.; Lavoie, B.; Shenoy, S. M.; Blanchard, J. M.; Singer, R. H.; Bertrand, E. *Curr. Biol.* **2003**, *13*, 161.
(234) Kapanidis, A. N.; Weiss, S. *J. Chem. Phys.* **2002**, *117*, 10953.
(235) Goncalves, M. S. *Chem. Rev.* **2009**, *109*, 190.
(236) Walter, N. G.; Burke, J. M. *Methods Enzymol.* **2000**, *317*, 409.
(237) Rinaldi, A. J.; Suddala, K. C.; Walter, N. G. *Methods Mol. Biol.* **2014**, in press.
(238) Prescher, J. A.; Bertozzi, C. R. *Nat. Chem. Biol.* **2005**, *1*, 13.
(239) Shi, X.; Jung, Y.; Lin, L. J.; Liu, C.; Wu, C.; Cann, I. K.; Ha, T. *Nat. Methods* **2012**, *9*, 499.
(240) Lord, S. J.; Conley, N. R.; Lee, H. L.; Samuel, R.; Liu, N.; Twieg, R. J.; Moerner, W. E. *J. Am. Chem. Soc.* **2008**, *130*, 9204.
(241) Lord, S. J.; Conley, N. R.; Lee, H. L.; Nishimura, S. Y.; Pomerantz, A. K.; Willets, K. A.; Lu, Z.; Wang, H.; Liu, N.; Samuel, R.; Weber, R.; Semyonov, A.; He, M.; Twieg, R. J.; Moerner, W. E. *ChemPhysChem* **2009**, *10*, 55.
(242) Michalet, X.; Pinaud, F. F.; Bentolila, L. A.; Tsay, J. M.; Doose, S.; Li, J. J.; Sundaresan, G.; Wu, A. M.; Gambhir, S. S.; Weiss, S. *Science* **2005**, *307*, 538.
(243) Sugisaki, M.; Ren, H. W.; Nishi, K.; Masumoto, Y. *Phys. Rev. Lett.* **2001**, *86*, 4883.
(244) Bogdanov, A. M.; Bogdanova, E. A.; Chudakov, D. M.; Gorodnicheva, T. V.; Lukyanov, S.; Lukyanov, K. A. *Nat. Methods* **2009**, *6*, 859.
(245) Billinton, N.; Knight, A. W. *Anal. Biochem.* **2001**, *291*, 175.
(246) Kredel, S.; Nienhaus, K.; Oswald, F.; Wolff, M.; Ivanchenko, S.; Cymer, F.; Jeromin, A.; Michel, F. J.; Spindler, K. D.; Heilker, R.; Nienhaus, G. U.; Wiedenmann, J. *Chem. Biol.* **2008**, *15*, 224.
(247) Aitken, C. E.; Marshall, R. A.; Puglisi, J. D. *Biophys. J.* **2008**, *94*, 1826.
(248) Dave, R.; Terry, D. S.; Munro, J. B.; Blanchard, S. C. *Biophys. J.* **2009**, *96*, 2371.
(249) Altman, R. B.; Terry, D. S.; Zhou, Z.; Zheng, Q.; Geggier, P.; Kolster, R. A.; Zhao, Y.; Javitch, J. A.; Warren, J. D.; Blanchard, S. C. *Nat. Methods* **2012**, *9*, 68.
(250) Widengren, J.; Chmyrov, A.; Eggeling, C.; Lofdahl, P. A.; Seidel, C. A. *J. Phys. Chem. A* **2007**, *111*, 429.
(251) Olenych, S. G.; Claxton, N. S.; Ottenberg, G. K.; Davidson, M. W. *Curr. Protoc. Cell Biol.* **2007**, *Chapter 21*, Unit 21 5.
(252) Roy, R.; Hohng, S.; Ha, T. *Nat. Methods* **2008**, *5*, 507.
(253) Waterman-Storer, C. M.; Sanger, J. W.; Sanger, J. M. *Cell Motil. Cytoskel* **1993**, *26*, 19.
(254) Koritzinsky, M.; Magagnin, M. G.; van den Beucken, T.; Seigneuric, R.; Savelkouls, K.; Dostie, J.; Pyronnet, S.; Kaufman, R. J.; Weppler, S. A.; Voncken, J. W.; Lambin, P.; Koumenis, C.; Sonenberg, N.; Wouters, B. G. *EMBO J.* **2006**, *25*, 1114.
(255) Shi, X.; Lim, J.; Ha, T. *Anal. Chem.* **2010**, *82*, 6132.
(256) Steinhauer, C.; Forthmann, C.; Vogelsang, J.; Tinnefeld, P. *J. Am. Chem. Soc.* **2008**, *130*, 16840.
(257) Elowitz, M. B.; Levine, A. J.; Siggia, E. D.; Swain, P. S. *Science* **2002**, *297*, 1183.
(258) Ozbudak, E. M.; Thattai, M.; Kurtser, I.; Grossman, A. D.; van Oudenaarden, A. *Nat. Genet.* **2002**, *31*, 69.

(259) Hanahan, D.; Weinberg, R. A. *Cell* **2011**, *144*, 646.
(260) Oleynikov, Y.; Singer, R. H. *Curr. Biol.* **2003**, *13*, 199.
(261) Lecuyer, E.; Yoshida, H.; Parthasarathy, N.; Alm, C.; Babak, T.; Cerovina, T.; Hughes, T. R.; Tomancak, P.; Krause, H. M. *Cell* **2007**, *131*, 174.
(262) Montero Llopis, P.; Jackson, A. F.; Sliusarenko, O.; Surovtsev, I.; Heinritz, J.; Emonet, T.; Jacobs-Wagner, C. *Nature* **2010**, *466*, 77.
(263) Xue, Z.; Huang, K.; Cai, C.; Cai, L.; Jiang, C. Y.; Feng, Y.; Liu, Z.; Zeng, Q.; Cheng, L.; Sun, Y. E.; Liu, J. Y.; Horvath, S.; Fan, G. *Nature* **2013**, *500*, 593.
(264) Tischler, J.; Surani, M. A. *Curr. Opin. Biotechnol.* **2013**, *24*, 69.
(265) Levsky, J. M.; Singer, R. H. *J. Cell. Sci.* **2003**, *116*, 2833.
(266) Femino, A. M.; Fay, F. S.; Fogarty, K.; Singer, R. H. *Science* **1998**, *280*, 585.
(267) Raj, A.; van den Bogaard, P.; Rifkin, S. A.; van Oudenaarden, A.; Tyagi, S. *Nat. Methods* **2008**, *5*, 877.
(268) Siebrasse, J. P.; Veith, R.; Dobay, A.; Leonhardt, H.; Daneholt, B.; Kubitscheck, U. *Proc. Natl. Acad. Sci. U.S.A.* **2008**, *105*, 20291.
(269) Vargas, D. Y.; Raj, A.; Marras, S. A.; Kramer, F. R.; Tyagi, S. *Proc. Natl. Acad. Sci. U.S.A.* **2005**, *102*, 17008.
(270) Vargas, D. Y.; Shah, K.; Batish, M.; Levandoski, M.; Sinha, S.; Marras, S. A.; Schedl, P.; Tyagi, S. *Cell* **2011**, *147*, 1054.
(271) Lansdorp, P. M.; Verwoerd, N. P.; van de Rijke, F. M.; Dragowska, V.; Little, M. T.; Dirks, R. W.; Raap, A. K.; Tanke, H. J. *Hum. Mol. Genet.* **1996**, *5*, 685.
(272) Lu, J.; Tsourkas, A. *Nucleic Acids Res.* **2009**, *37*, e100.
(273) Larsson, C.; Grundberg, I.; Soderberg, O.; Nilsson, M. *Nat. Methods* **2010**, *7*, 395.
(274) Player, A. N.; Shen, L. P.; Kenny, D.; Antao, V. P.; Kolberg, J. A. *J. Histochem. Cytochem.* **2001**, *49*, 603.
(275) Femino, A. M.; Fogarty, K.; Lifshitz, L. M.; Carrington, W.; Singer, R. H. *Methods Enzymol.* **2003**, *361*, 245.
(276) Hess, S. T.; Girirajan, T. P. K.; Mason, M. D. *Biophys. J.* **2006**, *91*, 4258.
(277) Maamar, H.; Raj, A.; Dubnau, D. *Science* **2007**, *317*, 526.
(278) Zenklusen, D.; Larson, D. R.; Singer, R. H. *Nat. Struct. Mol. Biol.* **2008**, *15*, 1263.
(279) Tan, R. Z.; van Oudenaarden, A. *Mol. Syst. Biol.* **2010**, *6*, 358.
(280) Raj, A.; Rifkin, S. A.; Andersen, E.; van Oudenaarden, A. *Nature* **2010**, *463*, 913.
(281) Harland, R. M. *Methods Cell Biol.* **1991**, *36*, 685.
(282) Shih, J. D.; Waks, Z.; Kedersha, N.; Silver, P. A. *Nucleic Acids Res.* **2011**, *39*, 7740.
(283) Raj, A.; Tyagi, S. *Methods Enzymol.* **2010**, *472*, 365.
(284) Morrison, L. E.; Halder, T. C.; Stols, L. M. *Anal. Biochem.* **1989**, *183*, 231.
(285) Li, Q.; Luan, G.; Guo, Q.; Liang, J. *Nucleic Acids Res.* **2002**, *30*, E5.
(286) Shepherd, D. P.; Li, N.; Micheva-Viteva, S. N.; Munsky, B.; Hong-Geller, E.; Werner, J. H. *Anal. Chem.* **2013**, *85*, 4938.
(287) Taniguchi, Y.; Choi, P. J.; Li, G. W.; Chen, H.; Babu, M.; Hearn, J.; Emili, A.; Xie, X. S. *Science* **2010**, *329*, 533.
(288) Larsson, C.; Koch, J.; Nygren, A.; Janssen, G.; Raap, A. K.; Landegren, U.; Nilsson, M. *Nat. Methods* **2004**, *1*, 227.
(289) Battich, N.; Stoeger, T.; Pelkmans, L. *Nat. Methods* **2013**, *10*, 1127.
(290) Choi, H. M.; Chang, J. Y.; Trinh le, A.; Padilla, J. E.; Fraser, S. E.; Pierce, N. A. *Nat. Biotechnol.* **2010**, *28*, 1208.
(291) Levsky, J. M.; Shenoy, S. M.; Pezo, R. C.; Singer, R. H. *Science* **2002**, *297*, 836.
(292) Levesque, M. J.; Raj, A. *Nat. Methods* **2013**, *10*, 246.
(293) Ishihama, Y.; Funatsu, T. *Biochem. Biophys. Res. Commun.* **2009**, *381*, 33.
(294) Lifland, A. W.; Zurla, C.; Santangelo, P. J. *Bioconj. Chem.* **2010**, *21*, 483.
(295) Luebke, K. J.; Balog, R. P.; Garner, H. R. *Nucleic Acids Res.* **2003**, *31*, 750.
(296) Coulon, A.; Chow, C. C.; Singer, R. H.; Larson, D. R. *Nat. Rev. Genet.* **2013**, *14*, 572.
(297) Xie, X. S.; Choi, P. J.; Li, G. W.; Lee, N. K.; Lia, G. *Annu. Rev. Biophys.* **2008**, *37*, 417.
(298) Kerppola, T. K. *Nat. Rev. Mol. Cell Biol.* **2006**, *7*, 449.
(299) Keryer-Bibens, C.; Barreau, C.; Osborne, H. B. *Biol. Cell* **2008**, *100*, 125.
(300) Chao, J. A.; Patskovsky, Y.; Almo, S. C.; Singer, R. H. *Nat. Struct. Mol. Biol.* **2008**, *15*, 103.
(301) Larson, D. R.; Zenklusen, D.; Wu, B.; Chao, J. A.; Singer, R. H. *Science* **2011**, *332*, 475.
(302) Daigle, N.; Ellenberg, J. *Nat. Methods* **2007**, *4*, 633.
(303) Lange, S.; Katayama, Y.; Schmid, M.; Burkacky, O.; Brauchle, C.; Lamb, D. C.; Jansen, R. P. *Traffic* **2008**, *9*, 1256.
(304) Haim, L.; Zipor, G.; Aronov, S.; Gerst, J. E. *Nat. Methods* **2007**, *4*, 409.
(305) Golding, I.; Cox, E. C. *Proc. Natl. Acad. Sci. U.S.A.* **2004**, *101*, 11310.
(306) Golding, I.; Paulsson, J.; Zawilski, S. M.; Cox, E. C. *Cell* **2005**, *123*, 1025.
(307) Grunwald, D.; Singer, R. H. *Nature* **2010**, *467*, 604.
(308) Wu, B.; Chao, J. A.; Singer, R. H. *Biophys. J.* **2012**, *102*, 2936.
(309) Ozawa, T.; Natori, Y.; Sato, M.; Umezawa, Y. *Nat. Methods* **2007**, *4*, 413.
(310) Yamada, T.; Yoshimura, H.; Inaguma, A.; Ozawa, T. *Anal. Chem.* **2011**, *83*, 5708.
(311) Quenault, T.; Lithgow, T.; Traven, A. *Trends Cell Biol.* **2011**, *21*, 104.
(312) Wang, X.; McLachlan, J.; Zamore, P. D.; Hall, T. M. *Cell* **2002**, *110*, 501.
(313) Cheong, C. G.; Hall, T. M. *Proc. Natl. Acad. Sci. U.S.A.* **2006**, *103*, 13635.
(314) Katahira, J. *Biochim. Biophys. Acta* **2012**, *1819*, 507.
(315) Siebrasse, J. P.; Kaminski, T.; Kubitscheck, U. *Proc. Natl. Acad. Sci. U.S.A.* **2012**, *109*, 9426.
(316) Calapez, A.; Pereira, H. M.; Calado, A.; Braga, J.; Rino, J.; Carvalho, C.; Tavanez, J. P.; Wahle, E.; Rosa, A. C.; Carmo-Fonseca, M. *J. Cell Biol.* **2002**, *159*, 795.
(317) Valencia-Burton, M.; McCullough, R. M.; Cantor, C. R.; Broude, N. E. *Nat. Methods* **2007**, *4*, 421.
(318) Rackham, O.; Brown, C. M. *EMBO J.* **2004**, *23*, 3346.
(319) Nguyen, D. H.; DeFina, S. C.; Fink, W. H.; Dieckmann, T. *J. Am. Chem. Soc.* **2002**, *124*, 15081.
(320) Babendure, J. R.; Adams, S. R.; Tsien, R. Y. *J. Am. Chem. Soc.* **2003**, *125*, 14716.
(321) Paige, J. S.; Wu, K. Y.; Jaffrey, S. R. *Science* **2011**, *333*, 642.
(322) Song, W.; Strack, R. L.; Jaffrey, S. R. *Nat. Methods* **2013**, *10*, 873.
(323) Martin, G.; Keller, W. *RNA* **1998**, *4*, 226.
(324) Kinoshita, Y.; Nishigaki, K.; Husimi, Y. *Nucleic Acids Res.* **1997**, *25*, 3747.
(325) Huang, Z.; Szostak, J. W. *Nucleic Acids Res.* **1996**, *24*, 4360.
(326) Rosemeyer, V.; Laubrock, A.; Seibl, R. *Anal. Biochem.* **1995**, *224*, 446.
(327) Qin, P. Z.; Pyle, A. M. *Methods* **1999**, *18*, 60.
(328) Walter, N. G. *Curr. Prot. Nucleic Acid Chem.* 2003, *Chapter 11*, Unit 11 10.
(329) Motorin, Y.; Burhenne, J.; Teimer, R.; Koynov, K.; Willnow, S.; Weinhold, E.; Helm, M. *Nucleic Acids Res.* **2011**, *39*, 1943.
(330) Rao, H.; Tanpure, A. A.; Sawant, A. A.; Srivatsan, S. G. *Nat. Protoc.* **2012**, *7*, 1097.
(331) Winz, M. L.; Samanta, A.; Benzinger, D.; Jaschke, A. *Nucleic Acids Res.* **2012**, *40*, e78.
(332) Pillai, R. S.; Bhattacharyya, S. N.; Artus, C. G.; Zoller, T.; Cougot, N.; Basyuk, E.; Bertrand, E.; Filipowicz, W. *Science* **2005**, *309*, 1573.
(333) Tadakuma, H.; Ishihama, Y.; Shibuya, T.; Tani, T.; Funatsu, T. *Biochem. Biophys. Res. Commun.* **2006**, *344*, 772.
(334) Leake, M. C.; Chandler, J. H.; Wadhams, G. H.; Bai, F.; Berry, R. M.; Armitage, J. P. *Nature* **2006**, *443*, 355.
(335) Coffman, V. C.; Wu, J. Q. *Trends Biochem. Sci.* **2012**, *37*, 499.

(336) Mutch, S. A.; Fujimoto, B. S.; Kuyper, C. L.; Kuo, J. S.; Bajjalieh, S. M.; Chiu, D. T. *Biophys. J.* **2007**, *92*, 2926.
(337) de Turris, V.; Nicholson, P.; Orozco, R. Z.; Singer, R. H.; Muhlemann, O. *RNA* **2011**, *17*, 2094.
(338) Valencia-Burton, M.; Shah, A.; Sutin, J.; Borogovac, A.; McCullough, R. M.; Cantor, C. R.; Meller, A.; Broude, N. E. *Proc. Natl. Acad. Sci. U.S.A.* **2009**, *106*, 16399.
(339) Zipor, G.; Haim-Vilmovsky, L.; Gelin-Licht, R.; Gadir, N.; Brocard, C.; Gerst, J. E. *Proc. Natl. Acad. Sci. U.S.A.* **2009**, *106*, 19848.
(340) So, L. H.; Ghosh, A.; Zong, C.; Sepulveda, L. A.; Segev, R.; Golding, I. *Nat. Genet.* **2011**, *43*, 554.
(341) Geerts, H.; De Brabander, M.; Nuydens, R.; Geuens, S.; Moeremans, M.; De Mey, J.; Hollenbeck, P. *Biophys. J.* **1987**, *52*, 775.
(342) Babcock, H. P.; Chen, C.; Zhuang, X. *Biophys. J.* **2004**, *87*, 2749.
(343) Grunwald, D.; Spottke, B.; Buschmann, V.; Kubitscheck, U. *Mol. Biol. Cell* **2006**, *17*, 5017.
(344) Ohrt, T.; Mutze, J.; Staroske, W.; Weinmann, L.; Hock, J.; Crell, K.; Meister, G.; Schwille, P. *Nucleic Acids Res.* **2008**, *36*, 6439.
(345) Tatavarty, V.; Ifrim, M. F.; Levin, M.; Korza, G.; Barbarese, E.; Yu, J.; Carson, J. H. *Mol. Biol. Cell* **2012**, *23*, 918.
(346) Lifland, A. W.; Zurla, C.; Yu, J.; Santangelo, P. J. *Traffic* **2011**, *12*, 1000.
(347) Zurla, C.; Lifland, A. W.; Santangelo, P. J. *PLoS One* **2011**, *6*, e19727.
(348) Trcek, T.; Chao, J. A.; Larson, D. R.; Park, H. Y.; Zenklusen, D.; Shenoy, S. M.; Singer, R. H. *Nat. Protoc.* **2012**, *7*, 408.
(349) Gerlach, D.; Kohler, W.; Gunther, E.; Mann, K. *Infect. Immun.* **1993**, *61*, 2727.
(350) Palmer, M.; Harris, R.; Freytag, C.; Kehoe, M.; Tranum-Jensen, J.; Bhakdi, S. *EMBO J.* **1998**, *17*, 1598.
(351) Dange, T.; Grunwald, D.; Grunwald, A.; Peters, R.; Kubitscheck, U. *J. Cell Biol.* **2008**, *183*, 77.
(352) Nitin, N.; Santangelo, P. J.; Kim, G.; Nie, S.; Bao, G. *Nucleic Acids Res.* **2004**, *32*, e58.
(353) Grunwald, D.; Shenoy, S. M.; Burke, S.; Singer, R. H. *Nat. Protoc.* **2008**, *3*, 1809.
(354) Gebhardt, J. C.; Suter, D. M.; Roy, R.; Zhao, Z. W.; Chapman, A. R.; Basu, S.; Maniatis, T.; Xie, X. S. *Nat. Methods* **2013**, *10*, 421.
(355) Rehemtulla, A.; Hamilton, C. A.; Chinnaiyan, A. M.; Dixit, V. M. *J. Biol. Chem.* **1997**, *272*, 25783.
(356) Kao, H. P.; Verkman, A. S. *Biophys. J.* **1994**, *67*, 1291.
(357) Huang, B.; Wang, W.; Bates, M.; Zhuang, X. *Science* **2008**, *319*, 810.
(358) Thompson, M. A.; Lew, M. D.; Badieirostami, M.; Moerner, W. E. *Nano Lett.* **2010**, *10*, 211.
(359) Thompson, M. A.; Casolari, J. M.; Badieirostami, M.; Brown, P. O.; Moerner, W. E. *Proc. Natl. Acad. Sci. U.S.A.* **2010**, *107*, 17864.
(360) Toprak, E.; Balci, H.; Blehm, B. H.; Selvin, P. R. *Nano Lett.* **2007**, *7*, 2043.
(361) Sun, Y.; McKenna, J. D.; Murray, J. M.; Ostap, E. M.; Goldman, Y. E. *Nano Lett.* **2009**, *9*, 2676.
(362) Axelrod, D. *J. Cell Biol.* **1981**, *89*, 141.
(363) Konopka, C. A.; Bednarek, S. Y. *Plant J.* **2008**, *53*, 186.
(364) Tokunaga, M.; Imamoto, N.; Sakata-Sogawa, K. *Nat. Methods* **2008**, *5*, 159.
(365) Ritter, J. G.; Veith, R.; Siebrasse, J. P.; Kubitscheck, U. *Opt. Express* **2008**, *16*, 7142.
(366) Ritter, J. G.; Veith, R.; Veenendaal, A.; Siebrasse, J. P.; Kubitscheck, U. *PLoS One* **2010**, *5*, e11639.
(367) Spille, J. H.; Kaminski, T.; Konigshoven, H. P.; Kubitscheck, U. *Opt. Express* **2012**, *20*, 19697.
(368) Lang, M. C.; Engelhardt, J.; Hell, S. W. *Opt. Lett.* **2007**, *32*, 259.
(369) Hell, S. W. *Science* **2007**, *316*, 1153.
(370) Nakano, A. *Cell Struct. Funct.* **2002**, *27*, 349.
(371) Ma, J.; Yang, W. *Proc. Natl. Acad. Sci. U.S.A.* **2010**, *107*, 7305.
(372) Michalet, X.; Weiss, S.; Jager, M. *Chem. Rev.* **2006**, *106*, 1785.
(373) Elf, J.; Li, G. W.; Xie, X. S. *Science* **2007**, *316*, 1191.
(374) Poo, M.; Cone, R. A. *Nature* **1974**, *247*, 438.
(375) Magde, D.; Elson, E.; Webb, W. W. *Phys. Rev. Lett.* **1972**, *29*, 705.
(376) Cheezum, M. K.; Walker, W. F.; Guilford, W. H. *Biophys. J.* **2001**, *81*, 2378.
(377) Sbalzarini, I. F.; Koumoutsakos, P. *J. Struct. Biol.* **2005**, *151*, 182.
(378) Jaqaman, K.; Loerke, D.; Mettlen, M.; Kuwata, H.; Grinstein, S.; Schmid, S. L.; Danuser, G. *Nat. Methods* **2008**, *5*, 695.
(379) Serge, A.; Bertaux, N.; Rigneault, H.; Marguet, D. *Nat. Methods* **2008**, *5*, 687.
(380) Reck-Peterson, S. L.; Yildiz, A.; Carter, A. P.; Gennerich, A.; Zhang, N.; Vale, R. D. *Cell* **2006**, *126*, 335.
(381) Saxton, M. J. *Biophys. J.* **1997**, *72*, 1744.
(382) Saxton, M. J.; Jacobson, K. *Annu. Rev. Biophys. Biomol. Struct.* **1997**, *26*, 373.
(383) Itzkovitz, S.; van Oudenaarden, A. *Nat. Methods* **2011**, *8*, S12.
(384) Itzkovitz, S.; Lyubimova, A.; Blat, I. C.; Maynard, M.; van Es, J.; Lees, J.; Jacks, T.; Clevers, H.; van Oudenaarden, A. *Nat. Cell Biol.* **2012**, *14*, 106.
(385) Kwon, S. *BMB Rep.* **2013**, *46*, 65.
(386) Shestakova, E. A.; Singer, R. H.; Condeelis, J. *Proc. Natl. Acad. Sci. U.S.A.* **2001**, *98*, 7045.
(387) Shandilya, J.; Roberts, S. G. *Biochim. Biophys. Acta* **2012**, *1819*, 391.
(388) Papantonis, A.; Cook, P. R. *Chem. Rev.* **2013**, *113*, 8683.
(389) Holstege, F. C.; Jennings, E. G.; Wyrick, J. J.; Lee, T. I.; Hengartner, C. J.; Green, M. R.; Golub, T. R.; Lander, E. S.; Young, R. A. *Cell* **1998**, *95*, 717.
(390) Raser, J. M.; O'Shea, E. K. *Science* **2004**, *304*, 1811.
(391) Rosenfeld, N.; Young, J. W.; Alon, U.; Swain, P. S.; Elowitz, M. B. *Science* **2005**, *307*, 1962.
(392) Thomas, M. C.; Chiang, C. M. *Crit. Rev. Biochem. Mol. Biol.* **2006**, *41*, 105.
(393) Li, B.; Carey, M.; Workman, J. L. *Cell* **2007**, *128*, 707.
(394) Saunders, A.; Core, L. J.; Lis, J. T. *Nat. Rev. Mol. Cell Biol.* **2006**, *7*, 557.
(395) Lionnet, T.; Singer, R. H. *EMBO Rep.* **2012**, *13*, 313.
(396) Thattai, M.; van Oudenaarden, A. *Proc. Natl. Acad. Sci. U.S.A.* **2001**, *98*, 8614.
(397) Munsky, B.; Neuert, G.; van Oudenaarden, A. *Science* **2012**, *336*, 183.
(398) Cai, L.; Friedman, N.; Xie, X. S. *Nature* **2006**, *440*, 358.
(399) Li, G. W.; Xie, X. S. *Nature* **2011**, *475*, 308.
(400) Raj, A.; Peskin, C. S.; Tranchina, D.; Vargas, D. Y.; Tyagi, S. *PLoS Biol.* **2006**, *4*, e309.
(401) Muthukrishnan, A. B.; Kandhavelu, M.; Lloyd-Price, J.; Kudasov, F.; Chowdhury, S.; Yli-Harja, O.; Ribeiro, A. S. *Nucleic Acids Res.* **2012**, *40*, 8472.
(402) Muramoto, T.; Cannon, D.; Gierlinski, M.; Corrigan, A.; Barton, G. J.; Chubb, J. R. *Proc. Natl. Acad. Sci. U.S.A.* **2012**, *109*, 7350.
(403) Dar, R. D.; Razooky, B. S.; Singh, A.; Trimeloni, T. V.; McCollum, J. M.; Cox, C. D.; Simpson, M. L.; Weinberger, L. S. *Proc. Natl. Acad. Sci. U.S.A.* **2012**, *109*, 17454.
(404) Chubb, J. R.; Trcek, T.; Shenoy, S. M.; Singer, R. H. *Curr. Biol.* **2006**, *16*, 1018.
(405) Ben-Ari, Y.; Brody, Y.; Kinor, N.; Mor, A.; Tsukamoto, T.; Spector, D. L.; Singer, R. H.; Shav-Tal, Y. *J. Cell Sci.* **2010**, *123*, 1761.
(406) Kandhavelu, M.; Mannerstrom, H.; Gupta, A.; Hakkinen, A.; Lloyd-Price, J.; Yli-Harja, O.; Ribeiro, A. S. *BMC Syst. Biol.* **2011**, *5*, 149.
(407) Newman, J. R.; Ghaemmaghami, S.; Ihmels, J.; Breslow, D. K.; Noble, M.; DeRisi, J. L.; Weissman, J. S. *Nature* **2006**, *441*, 840.
(408) Buganim, Y.; Faddah, D. A.; Cheng, A. W.; Itskovich, E.; Markoulaki, S.; Ganz, K.; Klemm, S. L.; van Oudenaarden, A.; Jaenisch, R. *Cell* **2012**, *150*, 1209.
(409) Makela, J.; Kandhavelu, M.; Oliveira, S. M.; Chandraseelan, J. G.; Lloyd-Price, J.; Peltonen, J.; Yli-Harja, O.; Ribeiro, A. S. *Nucleic Acids Res.* **2013**, *41*, 6544.

(410) Larson, D. R.; Singer, R. H.; Zenklusen, D. *Trends Cell Biol.* **2009**, *19*, 630.
(411) Coppey, M.; Benichou, O.; Voituriez, R.; Moreau, M. *Biophys. J.* **2004**, *87*, 1640.
(412) Shahrezaei, V.; Swain, P. S. *Proc. Natl. Acad. Sci. U.S.A.* **2008**, *105*, 17256.
(413) Iyer-Biswas, S.; Hayot, F.; Jayaprakash, C. *Phys. Rev. E* **2009**, *79*, 031911.
(414) Maamar, H.; Cabili, M. N.; Rinn, J.; Raj, A. *Genes Dev.* **2013**, *27*, 1260.
(415) Goodrich, J. A.; Kugel, J. F. *Nat. Rev. Mol. Cell Biol.* **2006**, *7*, 612.
(416) van Werven, F. J.; Neuert, G.; Hendrick, N.; Lardenois, A.; Buratowski, S.; van Oudenaarden, A.; Primig, M.; Amon, A. *Cell* **2012**, *150*, 1170.
(417) Bumgarner, S. L.; Neuert, G.; Voight, B. F.; Symbor-Nagrabska, A.; Grisafi, P.; van Oudenaarden, A.; Fink, G. R. *Mol. Cell* **2012**, *45*, 470.
(418) Ng, K.; Daigle, N.; Bancaud, A.; Ohhata, T.; Humphreys, P.; Walker, R.; Ellenberg, J.; Wutz, A. *Mol. Biol. Cell* **2011**, *22*, 2634.
(419) Neil, H.; Malabat, C.; d'Aubenton-Carafa, Y.; Xu, Z.; Steinmetz, L. M.; Jacquier, A. *Nature* **2009**, *457*, 1038.
(420) Camblong, J.; Iglesias, N.; Fickentscher, C.; Dieppois, G.; Stutz, F. *Cell* **2007**, *131*, 706.
(421) Castelnuovo, M.; Rahman, S.; Guffanti, E.; Infantino, V.; Stutz, F.; Zenklusen, D. *Nat. Struct. Mol. Biol.* **2013**, *20*, 851.
(422) Martin, R. M.; Rino, J.; Carvalho, C.; Kirchhausen, T.; Carmo-Fonseca, M. *Cell Rep.* **2013**, *4*, 1144.
(423) Waks, Z.; Klein, A. M.; Silver, P. A. *Mol. Syst. Biol.* **2011**, *7*, 506.
(424) Gibcus, J. H.; Dekker, J. *Mol. Cell* **2013**, *49*, 773.
(425) Bickmore, W. A.; van Steensel, B. *Cell* **2013**, *152*, 1270.
(426) Huang, S.; Deerinck, T. J.; Ellisman, M. H.; Spector, D. L. *J. Cell Biol.* **1994**, *126*, 877.
(427) Singh, O. P.; Bjorkroth, B.; Masich, S.; Wieslander, L.; Daneholt, B. *Exp. Cell Res.* **1999**, *251*, 135.
(428) Veith, R.; Sorkalla, T.; Baumgart, E.; Anzt, J.; Haberlein, H.; Tyagi, S.; Siebrasse, J. P.; Kubitscheck, U. *Biophys. J.* **2010**, *99*, 2676.
(429) Politz, J. C.; Tuft, R. A.; Pederson, T.; Singer, R. H. *Curr. Biol.* **1999**, *9*, 285.
(430) Shav-Tal, Y.; Darzacq, X.; Shenoy, S. M.; Fusco, D.; Janicki, S. M.; Spector, D. L.; Singer, R. H. *Science* **2004**, *304*, 1797.
(431) Rino, J.; Carvalho, T.; Braga, J.; Desterro, J. M.; Luhrmann, R.; Carmo-Fonseca, M. *PLoS Comput. Biol.* **2007**, *3*, 2019.
(432) Fiserova, J.; Richards, S. A.; Wente, S. R.; Goldberg, M. W. *J. Cell Sci.* **2010**, *123*, 2773.
(433) Holt, C. E.; Bullock, S. L. *Science* **2009**, *326*, 1212.
(434) Bertrand, E.; Chartrand, P.; Schaefer, M.; Shenoy, S. M.; Singer, R. H.; Long, R. M. *Mol. Cell* **1998**, *2*, 437.
(435) Casolari, J. M.; Thompson, M. A.; Salzman, J.; Champion, L. M.; Moerner, W. E.; Brown, P. O. *PLoS One* **2012**, *7*, e31912.
(436) Bratu, D. P.; Cha, B. J.; Mhlanga, M. M.; Kramer, F. R.; Tyagi, S. *Proc. Natl. Acad. Sci. U.S.A.* **2003**, *100*, 13308.
(437) Weil, T. T.; Parton, R.; Davis, I.; Gavis, E. R. *Curr. Biol.* **2008**, *18*, 1055.
(438) Weil, T. T.; Forrest, K. M.; Gavis, E. R. *Dev. Cell* **2006**, *11*, 251.
(439) Wilkie, G. S.; Davis, I. *Cell* **2001**, *105*, 209.
(440) Middelkoop, T. C.; Williams, L.; Yang, P. T.; Luchtenberg, J.; Betist, M. C.; Ji, N.; van Oudenaarden, A.; Kenyon, C.; Korswagen, H. C. *Dev. Biol.* **2012**, *361*, 338.
(441) Tyagi, S.; Alsmadi, O. *Biophys. J.* **2004**, *87*, 4153.
(442) Batish, M.; van den Bogaard, P.; Kramer, F. R.; Tyagi, S. *Proc. Natl. Acad. Sci. U.S.A.* **2012**, *109*, 4645.
(443) Mikl, M.; Vendra, G.; Kiebler, M. A. *EMBO Rep.* **2011**, *12*, 1077.
(444) Tubing, F.; Vendra, G.; Mikl, M.; Macchi, P.; Thomas, S.; Kiebler, M. A. *J. Neurosci.* **2010**, *30*, 4160.
(445) Mingle, L. A.; Okuhama, N. N.; Shi, J.; Singer, R. H.; Condeelis, J.; Liu, G. *J. Cell Sci.* **2005**, *118*, 2425.
(446) Rook, M. S.; Lu, M.; Kosik, K. S. *J. Neurosci.* **2000**, *20*, 6385.
(447) Yamagishi, M.; Ishihama, Y.; Shirasaki, Y.; Kurama, H.; Funatsu, T. *Exp. Cell Res.* **2009**, *315*, 1142.
(448) Forrest, K. M.; Gavis, E. R. *Curr. Biol.* **2003**, *13*, 1159.
(449) Rodriguez, A. J.; Shenoy, S. M.; Singer, R. H.; Condeelis, J. *J. Cell Biol.* **2006**, *175*, 67.
(450) English, B. P.; Hauryliuk, V.; Sanamrad, A.; Tankov, S.; Dekker, N. H.; Elf, J. *Proc. Natl. Acad. Sci. U.S.A.* **2011**, *108*, E365.
(451) Korzelius, J.; The, I.; Ruijtenberg, S.; Prinsen, M. B.; Portegijs, V.; Middelkoop, T. C.; Groot Koerkamp, M. J.; Holstege, F. C.; Boxem, M.; van den Heuvel, S. *PLoS Genet.* **2011**, *7*, e1002362.
(452) Harris, D. T.; Horvitz, H. R. *Development* **2011**, *138*, 4051.
(453) Saffer, A. M.; Kim, D. H.; van Oudenaarden, A.; Horvitz, H. R. *PLoS Genet.* **2011**, *7*, e1002418.
(454) Neely, L. A.; Patel, S.; Garver, J.; Gallo, M.; Hackett, M.; McLaughlin, S.; Nadel, M.; Harris, J.; Gullans, S.; Rooke, J. *Nat. Methods* **2006**, *3*, 41.
(455) Li, J.; Li, X.; Li, Y.; Yang, H.; Wang, L.; Qin, Y.; Liu, H.; Fu, L.; Guan, X. Y. *PLoS One* **2013**, *8*, e53582.
(456) Trcek, T.; Larson, D. R.; Moldon, A.; Query, C. C.; Singer, R. H. *Cell* **2011**, *147*, 1484.
(457) Anderson, P.; Kedersha, N. *J. Cell Biol.* **2006**, *172*, 803.
(458) Goff, S. P. *Nat. Rev. Microbiol.* **2007**, *5*, 253.
(459) Chou, Y. Y.; Heaton, N. S.; Gao, Q.; Palese, P.; Singer, R.; Lionnet, T. *PLoS Pathog.* **2013**, *9*, e1003358.
(460) Ni, N.; Nikolaitchik, O. A.; Dilley, K. A.; Chen, J.; Galli, A.; Fu, W.; Prasad, V. V.; Ptak, R. G.; Pathak, V. K.; Hu, W. S. *J. Virol.* **2011**, *85*, 7603.
(461) Boireau, S.; Maiuri, P.; Basyuk, E.; de la Mata, M.; Knezevich, A.; Pradet-Balade, B.; Backer, V.; Kornblihtt, A.; Marcello, A.; Bertrand, E. *J. Cell Biol.* **2007**, *179*, 291.
(462) Basyuk, E.; Galli, T.; Mougel, M.; Blanchard, J. M.; Sitbon, M.; Bertrand, E. *Dev. Cell* **2003**, *5*, 161.
(463) Kemler, I.; Meehan, A.; Poeschla, E. M. *J. Virol.* **2010**, *84*, 6352.
(464) Jouvenet, N.; Simon, S. M.; Bieniasz, P. D. *Proc. Natl. Acad. Sci. U.S.A.* **2009**, *106*, 19114.
(465) Jouvenet, N.; Bieniasz, P. D.; Simon, S. M. *Nature* **2008**, *454*, 236.
(466) Ivanchenko, S.; Godinez, W. J.; Lampe, M.; Krausslich, H. G.; Eils, R.; Rohr, K.; Brauchle, C.; Muller, B.; Lamb, D. C. *PLoS Pathog.* **2009**, *5*, e1000652.
(467) Chen, J.; Nikolaitchik, O.; Singh, J.; Wright, A.; Bencsics, C. E.; Coffin, J. M.; Ni, N.; Lockett, S.; Pathak, V. K.; Hu, W. S. *Proc. Natl. Acad. Sci. U.S.A.* **2009**, *106*, 13535.
(468) Dilley, K. A.; Ni, N.; Nikolaitchik, O. A.; Chen, J.; Galli, A.; Hu, W. S. *J. Virol.* **2011**, *85*, 10499.
(469) Gallardo, F.; Laterreur, N.; Cusanelli, E.; Ouenzar, F.; Querido, E.; Wellinger, R. J.; Chartrand, P. *Mol. Cell* **2011**, *44*, 819.
(470) Pruitt, K. D.; Harrow, J.; Harte, R. A.; Wallin, C.; Diekhans, M.; Maglott, D. R.; Searle, S.; Farrell, C. M.; Loveland, J. E.; Ruef, B. J.; Hart, E.; Suner, M. M.; Landrum, M. J.; Aken, B.; Ayling, S.; Baertsch, R.; Fernandez-Banet, J.; Cherry, J. L.; Curwen, V.; Dicuccio, M.; Kellis, M.; Lee, J.; Lin, M. F.; Schuster, M.; Shkeda, A.; Amid, C.; Brown, G.; Dukhanina, O.; Frankish, A.; Hart, J.; Maidak, B. L.; Mudge, J.; Murphy, M. R.; Murphy, T.; Rajan, J.; Rajput, B.; Riddick, L. D.; Snow, C.; Steward, C.; Webb, D.; Weber, J. A.; Wilming, L.; Wu, W.; Birney, E.; Haussler, D.; Hubbard, T.; Ostell, J.; Durbin, R.; Lipman, D. *Genome Res.* **2009**, *19*, 1316.
(471) Pruitt, K. D.; Tatusova, T.; Brown, G. R.; Maglott, D. R. *Nucleic Acids Res.* **2012**, *40*, D130.
(472) Lempiainen, H.; Shore, D. *Curr. Opin. Cell Biol.* **2009**, *21*, 855.
(473) Henras, A. K.; Soudet, J.; Gerus, M.; Lebaron, S.; Caizergues-Ferrer, M.; Mougin, A.; Henry, Y. *Cell. Mol. Life Sci.* **2008**, *65*, 2334.
(474) Tschochner, H.; Hurt, E. *Trends Cell Biol.* **2003**, *13*, 255.
(475) Cole, J. R.; Wang, Q.; Cardenas, E.; Fish, J.; Chai, B.; Farris, R. J.; Kulam-Syed-Mohideen, A. S.; McGarrell, D. M.; Marsh, T.; Garrity, G. M.; Tiedje, J. M. *Nucleic Acids Res.* **2009**, *37*, D141.
(476) Rosenblad, M. A.; Gorodkin, J.; Knudsen, B.; Zwieb, C.; Samuelsson, T. *Nucleic Acids Res.* **2003**, *31*, 363.
(477) Chan, P. P.; Lowe, T. M. *Nucleic Acids Res.* **2009**, *37*, D93.

(478) Juhling, F.; Morl, M.; Hartmann, R. K.; Sprinzl, M.; Stadler, P. F.; Putz, J. *Nucleic Acids Res.* **2009**, *37*, D159.
(479) Ellis, J. C.; Brown, D. D.; Brown, J. W. *RNA* **2010**, *16*, 664.
(480) Brown, J. W. *Nucleic Acids Res.* **1999**, *27*, 314.
(481) Yang, J. H.; Shao, P.; Zhou, H.; Chen, Y. Q.; Qu, L. H. *Nucleic Acids Res.* **2010**, *38*, D123.
(482) Webb, C. H.; Riccitelli, N. J.; Ruminski, D. J.; Luptak, A. *Science* **2009**, *326*, 953.
(483) Kozomara, A.; Griffiths-Jones, S. *Nucleic Acids Res.* **2011**, *39*, D152.
(484) Paraskevopoulou, M. D.; Georgakilas, G.; Kostoulas, N.; Reczko, M.; Maragkakis, M.; Dalamagas, T. M.; Hatzigeorgiou, A. G. *Nucleic Acids Res.* **2013**, *41*, D239.
(485) Backman, T. W.; Sullivan, C. M.; Cumbie, J. S.; Miller, Z. A.; Chapman, E. J.; Fahlgren, N.; Givan, S. A.; Carrington, J. C.; Kasschau, K. D. *Nucleic Acids Res.* **2008**, *36*, D982.
(486) Ishizu, H.; Siomi, H.; Siomi, M. C. *Genes Dev.* **2012**, *26*, 2361.
(487) Sai Lakshmi, S.; Agrawal, S. *Nucleic Acids Res.* **2008**, *36*, D173.
(488) Amaral, P. P.; Clark, M. B.; Gascoigne, D. K.; Dinger, M. E.; Mattick, J. S. *Nucleic Acids Res.* **2011**, *39*, D146.
(489) Cabili, M. N.; Trapnell, C.; Goff, L.; Koziol, M.; Tazon-Vega, B.; Regev, A.; Rinn, J. L. *Genes Dev.* **2011**, *25*, 1915.
(490) Grillo, G.; Turi, A.; Licciulli, F.; Mignone, F.; Liuni, S.; Banfi, S.; Gennarino, V. A.; Horner, D. S.; Pavesi, G.; Picardi, E.; Pesole, G. *Nucleic Acids Res.* **2010**, *38*, D75.
(491) Roy, S. W.; Gilbert, W. *Nat. Rev. Genet.* **2006**, *7*, 211.
(492) Zhou, Y.; Lu, C.; Wu, Q. J.; Wang, Y.; Sun, Z. T.; Deng, J. C.; Zhang, Y. *Nucleic Acids Res.* **2008**, *36*, D31.
(493) Cardullo, R. A.; Agrawal, S.; Flores, C.; Zamecnik, P. C.; Wolf, D. E. *Proc. Natl. Acad. Sci. U.S.A.* **1988**, *85*, 8790.
(494) Sando, S.; Kool, E. T. *J. Am. Chem. Soc.* **2002**, *124*, 9686.
(495) Abe, H.; Kool, E. T. *Proc. Natl. Acad. Sci. U.S.A.* **2006**, *103*, 263.
(496) Santangelo, P. J.; Nix, B.; Tsourkas, A.; Bao, G. *Nucleic Acids Res.* **2004**, *32*, e57.

NOTE ADDED AFTER ASAP PUBLICATION

This paper was published ASAP on January 8, 2014. Panel (iii) was removed from Figure 3 and replaced by the previous panel (iv). The corrected version was reposted on January 13, 2014.